Characterisation of Earthing Systems and Materials under DC, Variable Frequency and Impulse Conditions

Hasan Ali Hasan

B.Sc., M.Sc. (Electrical Engineering)

A thesis submitted in fulfilment of the requirement for the degree of doctor of philosophy

School of Engineering - Cardiff University

UK, 2017

I

ABSTRACT

This thesis is primarily concerned with experimental tests and computer simulations to evaluate the performance and behaviour of earth electrode systems subjected to DC, AC variable frequency and impulse currents.

The performance of the earth electrode systems at the power frequency is now well understood. However, the response of the system under high frequency and transient conditions still need more clarification. Therefore, simulations and experimental investigations in both laboratory and full-scale field site have been performed and reported in this thesis. The results contribute to better understanding of complex earthing systems under high frequency and transient conditions.

The response of the earthing system of different configurations (vertical and horizontal electrode) was conducted for soil resistivity ranged from 10Ωm to 10kΩm using numerical computational model. The effect of soil resistivity, permittivity, and the electrode length on the performance of the earthing system was investigated. Particular emphasis applied to study the effect of segmentation on the evaluation of earthing electrode response. The investigations result in some recommendations contribute to the better evaluation of the performance and the behaviour of simulated earth electrodes.

New earthing system facilities were prepared. The first stage was soil resistivity survey, which resulted in 2D soil models construction showed both horizontal and vertical soil resistivity variation. In addition, step voltages and touch voltages were computed to ensure the safety of the workers. Then, high frequency and impulse characteristics of vertical test rod and horizontal electrode buried in non-uniform soil at Llanrumney were tested. DC, AC and impulse tests results show that the measured earth impedance is constant over a low-frequency range, while higher impedance values are observed in the high-frequency range due to the inductive effects. To validate the analytical approaches and computational models, a new earthing system facility was prepared at Dinorwig substation at North Wales, UK. High frequency and impulse characteristics of 5m × 5m earth grid electrodes immersed in fresh water (close to uniform medium) were tested. DC, AC and impulse test results show that the resistive behaviour dominates the performance of the earthing grid. In addition, the measured impulse resistance exhibits constant values with the increase of the injected currents.

Experiments were carried out at new high voltage laboratory to investigate the frequency dependence of electrical soil parameters. The soil was prepared and mixed with a different percentage of water contents according to weight. The results showed that both the resistivity and the permittivity decreased with increasing water contents. In addition, the results compared with the developed models available in literature and exhibited close agreements with them.

Moreover, experimental investigations carried out at the laboratory on high resistivity material (gravel and concrete) which are used to increase the contact resistance between the earth and workers. The resistance showed a decrease in its value with increasing the water contents.

PUBLICATIONS

1. **H. Hasan**, H. Griffiths, and A. Haddad, ''Modelling of vertical earth electrodes: a parametric study and investigation into the effect of model segmentation'' eighth Universities High Voltage Network, UHVNet 2015, Colloquium on HVDC Power Transmission Technologies, 14-15 Jan 2015, Staffordshire University 2015.
(Poster)

2. **H. Hasan**, H. Hamzehbahmani, H. Griffiths, N. Harid, D. Clark, S. Robson, and A. Haddad, "Characterisation of earth electrodes subjected to impulse and variable frequency currents," in The 19th International Symposium on High Voltage Engineering, Pilsen, Czech Republic, 2015, pp. 23–28.

3. **H. Hasan**, H. Hamzehbahmani, S. Robson, H. Griffiths, D. Clark and A. Haddad, "Characterization of horizontal earth electrodes: Variable frequency and impulse responses," *2015 50th International Universities Power Engineering Conference (UPEC)*, Stoke on Trent, 2015, pp. 1-5

4. **H. Hasan**, H. Hamzehbahmani, H. Griffiths, N. Harid, D. Clark, S. Robson, and A. Haddad, "Characterisation of earth electrodes subjected to impulse and variable frequency currents," ninth Universities High Voltage Network, UHVNet 2016, Colloquium on electrical networks infrastructure and equipment for 2030, 14-15 Jan. 2016, Cardiff University 2016.

   (Poster)

5. **H. Hasan**, H. Hamzehbahmani, S. Robson, H. Griffiths, D. Clark and A. Haddad, "Characterization of horizontal earth electrodes: Variable frequency and impulse responses," tenth Universities High Voltage Network, UHVNet 2017, Colloquium on Challenges and opportunities in HV future network, 19 Jan. 2017, Glasgow Caledonian University 2017.

   (Poster)

6. **H. Hasan**, H. Hamzehbahmani, H. Griffiths, D. Guo, and A. Haddad, ''Characterization of site soils using variable frequency and impulse voltages,'' *10th Asia-Pacific International Conference on Lightning (APL2017)*, Krabi, Thailand, 2017, pp.1-4

DECLARATION

This work has not been submitted in substance for any other degree or award at this or any other university or place of learning, nor is being submitted concurrently in candidature for any degree or other award.

Signed……………………..…… (Candidate) Date…...................................

STATEMENT 1

This thesis is being submitted in partial fulfilment of the requirements for the degree of Doctor of Philosophy (PhD).

Signed……………………..…… (Candidate) Date…...................................

STATEMENT 2

This thesis is the result of my own independent work/investigation, except where otherwise stated, and the thesis has not been edited by a third party beyond what is permitted by Cardiff University's Policy on the Use of Third Party Editors by Research Degree Students. Other sources are acknowledged by explicit references. The views expressed are my own.

Signed……………………..…… (Candidate) Date…...................................

STATEMENT 3

I hereby give consent for my thesis, if accepted, to be available online in the University's Open Access repository and for inter-library loan, and for the title and summary to be made available to outside organisations.

Signed……………………..…… (Candidate) Date…...................................

ACKNOWLEDGEMENTS

TABLE OF CONTENTS

CHAPTER FOUR: CHARACTERISTICS OF EARTH ELECTRODES UNDER HIGH FREQUENCY AND TRANSIENT CONDITIONS: NUMERICAL MODELLING

CHAPTER FIVE: CHARACTERISATION OF EARTH ELECTRODES SUBJECTED TO IMPULSE AND VARIABLE FREQUENCY CURRENTS

CHAPTER SIX: LABORATORY CHARACTERISATION OF SOIL PARAMETERS UNDER HIGH FREQUENCY AND TRANSIENT CONDITIONS

CHAPTER SEVEN: CHARACTERISATION OF HIGH RESISTIVITY SUBSTATION MATERIAL: LABORATORY INVESTIGATIONS

CHAPTER EIGHT: GENERAL DISCUSSION AND CONCLUSIONS

REFERENCES

LIST OF FIGURES

LIST OF TABLES

CHAPTER ONE: INTRODUCTION

1.1 Introduction

Earthing systems are designed to provide a path for the currents caused by abnormal conditions, such as lightning strikes and faults, with minimum impedance to limit the potential difference between the earthing equipment and any conducting bodies in the vicinity. Therefore, it is important to study the behaviour of the earthing system under different conditions to examine its effectiveness.

The earthing resistance/impedance is usually measured by either switching DC current to the earth rod or injecting low currents with frequencies close to the power frequency. This resistance helps to estimate the behaviour of the earthing system under these frequencies. However, under lightning and transient conditions, the earthing system exhibits different behaviour. Many factors significantly affect the performance of the earthing system, such as the resistivity and permittivity of the soil in which the earthing electrode is installed, the configuration and dimension of the earthing electrode, and the current magnitude and front rise time of the impulse. These aspects pose many challenges in designing an effective earthing system to meet the requirements.

This thesis investigates the characteristics of the earthing system of vertical, horizontal and grid configurations, when subjected to impulses and variable frequency currents, taking into consideration the uniformity of the conducting medium. In addition, experimental work has been undertaken in the high voltage laboratory at Cardiff University to investigate frequency dependence of soil conductivity and permittivity and the effects of these parameters on the characteristics of the earthing system. Further investigations were implemented to highlight the effect of water contents on the resistivity of gravel and concrete, which are used in the substation to increase the contact resistance.

1.2   Earthing System configurations

Earthing electrodes, such as vertical, horizontal, and grid, usually consist of solid copper or aluminium conductors or a combination of both. Electrodes are buried under the equipment so they are protected against abnormal and transient conditions. The protected equipment is connected to the earthing system by a downlead above-ground conductor. At power frequency, the effect of this conductor can usually be neglected, and the characteristics of the currents dissipated through the buried earth electrode are considered in the earth resistance calculations. Under transient conditions, the above–ground leads have a significant impedance that should be taken into consideration. BS 7430 [1] and EA TS 41-24 [2] recommend that the above–ground lead should be as short as possible to minimise the impedance under transient conditions.

A vertical earth rod, called a 'high-frequency earth electrode' is used to improve the performance of the earthing system when the rods are bonded to the main grid. The phrase ''high frequency earth electrode'' proposes that the role of the earth rod is to disperse to earth the high frequency components of the transient. Moreover, it is recommended to apply the rod at the point where high-frequency and surge current will be discharged to the earth [2]. In addition, horizontal electrodes are used in high soil resistivity to enhance the performance of the earthing system by minimising earth impedance in accordance with IEEE Std. 80-2000 [3]. Furthermore, an earthing grid is used in both outdoor transmission substations, which occupy a wide area reaching more than 30,000 m^2 and for indoor substations with a smaller area.

1.3   Earthing System Functions and Requirements

The main function of the earthing system is to provide a means to dissipate the currents generated due to lightning and fault conditions to the earth without generating dangerous earth potential rise and securing the safety of the power system equipment and personnel

and the continuity of the power supply. In order to achieve satisfactory performance, it is important to highlight and understand the effect of many factors on the behaviour and performance of the earthing systems, such as soil type, its chemical composition and moisture content, its grain size and its distribution, geometry of the earthing electrodes, temperature, shape of lightning impulse, and current level.

The integrity of the earthing system is essential, and it must be considered in an electrical power system design for the following reasons:

1. to maintain a reference point of the earth potential for the safety of both equipment and workers.

2. to provide a conductive path for current to flow under transient conditions and to ensure the return path for fault currents.

3. to limit the generation of hazardous overvoltages on the power system.

To achieve satisfactory performance of the earthing system, proper design, installation, and testing of the earthing electrodes is required. The ideal earthing system is one exhibiting a zero-ohm earth resistance. However, in practical systems, this value cannot be achieved. Therefore, different techniques are used to specify the required maximum value of earth resistance to limit the generated voltages to a safe level [4]–[10]. The earth is characterised as a poor conductor, and, therefore, when a high magnitude current is passed to the earth, a large potential gradient will result, and the earthing system will exhibit a potential earth rise [11]. Earth potential rise is defined as the voltage between an earthing system and the reference earth [3]. When the power system is subjected to a direct lightning strike, a high magnitude of current can be injected in the earthing system. The discharge of the higher fault current into the earth will result in a high potential rise. Due to the large magnitude of generated earth potential rise, a potential risk threatens the safety of workers in the immediate vicinity of the power network during abnormal

conditions, as well as possible damage to the equipment for example transformers. Therefore, intensive measurements and investigations should be undertaken to determine the generated earth potential rise and be able or control its value inside and near the substation.

1.4   Measurements of Frequency Dependence Soil Parameters.

Several studies have been conducted to characterise the behaviour of earthing systems. As a result, many computational models based on different approaches have been developed to evaluate earthing system performance with high-frequency currents [12]–[15]. These powerful models play a major role in understanding the earthing system's behaviour and response under transient conditions since they allow investigation of the earthing system performance with respect to some relevant variables, which have a significant impact on the behaviour of the earthing system, including soil resistivity and permittivity and electrode dimensions [16]. Adequate soil modelling is the most important aspect of any earthing system analysis. However, in most investigations, the soil electrical parameters of conductivity and permittivity are assumed to be constant. The soil electrical conductivity is characterised by low-frequency earthing resistance measurements; whilst, the relative soil permittivity varies from 1 to 80 depending on its water content. The assumptions adopted constitute a conservative approach due to the lack of an accurate general formulation to express and characterise the frequency dependence of these parameters.

Several studies based on laboratory and field measurements [17]–[19] have demonstrated the frequency dependence of soil electrical parameters. These investigations show how the frequency affects conductivity and permittivity values, and how applying the conservative model, in which the soil electrical parameters are assumed to be constant, will lead to significant errors in characterising the earthing system performance.

Additionally, computer simulations based on experimental data have focused on studying the behaviour of earthing systems considering the frequency dependence of the soil parameters [20], [21]. According to these studies, the frequency dependence of soil conductivity and permittivity has a significant effect in the performance of earthing systems, particularly, at high resistivity soil.

1.5   Aims and objective

The goals and objective of the thesis are summarised in the following points:

1. To present the published works of earthing system behaviour under normal and transient conditions, focusing on the factors that affect earthing systems' performance, in particular, those related to the soil resistivity, conductivity and permittivity, and their frequency dependence (Chapter 2).

2. To investigate the frequency response of simple earth electrodes (vertical and horizontal) by highlighting the significant influence of the electrode geometry and the soil parameters on the performance of earthing systems. An intensive simulation study has been performed to clarify the effect of electrode segmentation on the behaviour of simulated earthing systems (Chapter 3).

3. To design and prepare the new location of Cardiff University's earthing system facility at Llanrumney. The soil resistivity surveys have been implemented near the test zone over one year. The results have been analysed, and 2D soil resistivity maps have been extracted from the raw data (Chapter 4).

4. To characterise both vertical and horizontal electrodes buried in the non-uniform conducting medium at the Cardiff University earthing system facility when subjected to DC/AC variable frequency and impulse currents. The same scenarios have been repeated with an earthing grid immersed in a uniform conducting

medium (water) at Dinorwig pump storage power station in North Wales (Chapters 5).

5. To present the results obtained from intensive laboratory investigations, which highlight the frequency dependence of soil electrical parameters and the effect of moisture content on the performance of earthing systems (Chapter 6).

6. To investigate the safety conditions in substations, in particular those related to human safety. The properties of gravel and concrete have been tested, and the effects of water content have been clarified (Chapter 7).

1.6 Contribution of the Thesis

The investigation carried out in this work has led to the following contributions:

1. An extensive literature review of characteristics of earthing system behaviour and performance under DC/AC variable frequency and transient conditions was carried out. Relevant publication in the case of earthing resistance/impedance measurements, soil electrical properties and their frequency response were reviewed. The literature review identifying frequency dependence and equivalent circuit work.

2. Preparation of two earthing systems test sites and characterisation of electrical parameters, to carry out high voltage tests on different types of practical earthing electrodes, taking into consideration the safety requirements for the personnel and for people in the vicinity of the test area. One of the test facilities, Dinorwig pumped storage power station, offered exceptional uniform conditions.

3. A comprehensive investigation of different earthing system configurations (vertical, horizontal, and grid) under AC variable frequency and impulse current was performed. These investigations result in characrerisation of installed

electrodes using variable frequency and impulse quantifying the frequency dependance of earth impedance.

4. Verification of the test results using one of the most accurate numerical modelling commercially available. The computer software CDEGS-HIFREQ was used, taking into account the effect of segmentation on the simulated electrodes.

5. Clarify the behaviour of earthing grid immersed in uniform conducting medium using controlled full-scale test facility. The results identify the limitation of the computational model (CDEGS) at high frequency.

6. Laboratory characterisation of site soil with variable frequency and impulse and correlation with the earth electrodes tests. No previous work was found in this area.

7. Characterisation of the gravel and concrete using variable frequency, which was not defined in available literature.

1.7   Thesis Layout

The thesis is divided into seven chapters. References are numbered in square brackets, and each number corresponds to a numbered reference in the full list at the end of the thesis. The contents of each main chapter are summarised as follows.

Chapter 2: Characteristics of the earthing system under AC variable frequency impulse energisation: literature review

An extensive review of the published studies on the performance of the earthing system under AC variable frequency and transient conditions is presented in this chapter. Both theoretical and experimental results are discussed as well as the DC resistance/impedance, and the factors that affect its value are highlighted. The published works on the frequency dependence of the soil electrical parameters are reviewed.

Chapter 3: Development of field test facilities and soil survey at Llanrumeney and Dinorwig power station

An overview of Cardiff University's earthing system facility at Llanrumeny is provided in this chapter. Site location and discretion, as well as the installation and safety conditions and requirements of high voltage experiments, are explained. A large-scale soil resistivity survey was conducted, and so the seasonal effect on soil resistivity values is discussed.

Chapter 4: Characteristics of earth electrodes under high frequency and transient conditions: Numerical modelling.

In this chapter, a detailed computer simulation software (CDEGS-HIFREQ) is utilised to identify the frequency response of earth electrodes. The study involves different arrangements of earth electrodes over a range of frequencies, from DC up to 1 MHz. The effect of soil resistivity and permittivity, as well as the variation of electrode length on the frequency response, is computed. Further investigations were performed to identify the effect of segmentation. These investigations resulted in important recommendations that should be considered when the earth electrode is simulated.

Chapter 5: Characterisation of earth electrodes subjected to impulse and variable frequency currents.

This chapter examines the experimental set up that was developed at Cardiff University earthing system facility's new location at Llanrumeny to perform characterization of practical size earthing systems under AC variable frequency and transient conditions. A course of experiments was designed using a 1.2 m vertical earth electrode installed in the centre of a ring electrode to ensure a uniform current distribution and an industry-standard horizontal earth electrode. The tested electrodes and the test circuits were modelled in the computational software program (HIFREQ/FFTSES-CDEGS) with a uniform equivalent

soil model. The results of the computer simulations are compared with the test results, and good agreement is obtained. The effect of soil resistivity and permittivity is investigated.

Chapter 6: Laboratory characterisation of soil parameters under high frequency and transient conditions.

An intensive laboratory investigation is explored in this chapter to identify the frequency dependence of soil conductivity and permittivity under DC, AC variable frequency and impulse currents. The study clarifies the effect of water content on the resistivity of the soil. The results of the investigations are discussed and compared with the published expressions for soil electrical parameters frequency dependence.

Chapter 7: characterisation of high resistivity substation material: laboratory investigations

This chapter discusses the experimental set up that was developed in the new high voltage laboratory at Cardiff University to investigate the properties of high resistivity materials. The electrical characteristics of different types of loose ballast and concrete is studied. DC and AC variable frequency was energised into the materials under wet and dry conditions. The effect of water contents on the resistivity of each material is identified.

CHAPTER TWO: CHARACTERISTICS OF EARTHING SYSTEM UNDER AC VARIABLE FREQUENCY AND IMPULSE ENERGISATION: LITERATURE REVIEW

2.1 Introduction

Earthing systems of electrical power systems play a very important role regarding human safety and the protection of plant and ancillary equipment. Therefore, highlighting the response of earthing systems to DC/AC and impulse energisations is essential to design effective earthing systems. Three main components are responsible for earthing system performance: first, the connection between the power system and the electrodes; second, the configuration of earthing electrodes; and finally, the conducting medium where the electrodes are installed. Intensive work and investigations on the behaviour and performance of earthing systems started a century ago [2.1], [2.2]. The results of these investigations outlined the design of earthing systems and provided useful guidance for installing the earth electrodes, and for measuring and testing the earthing systems' impedance. In terms of the conducting medium, useful knowledge on soil resistivity was obtained, such as the method of measurement and its effect on the behaviour of earthing systems at power frequency and transient conditions. The most important outcomes of the previous studies [2.1]-[2.18] resulted in good descriptions of the variations in earthing systems' responses under normal and transient conditions, and the factors responsible for such behaviour. In addition, the rapid growth in computer technology has led to the development of very powerful numerical computational models to perform evaluations of the response of complex earthing system configurations.

This chapter provides a review of previously published studies describing the behaviour of earthing systems under variable frequency and their impulse performance. A review of studies performed by previous authors [2.34]-[2.47] is carried out to obtain further

understanding of the characteristics of earthing systems, in particular, the characteristics related to the frequency dependence of soil parameters.

2.2 Characteristics of Earthing Systems Subjected to Impulse Energization

2.2.1 Vertical Earth Electrode

The vertical earth electrodes are the most common type of electrodes in earthing systems, and they are usually placed under the item of the plant to be earthed or bonded to the main earth grid. The first experimental work was published in 1928, when Towne [2.1] carried out experimental field tests on a galvanised iron pipe up to 6.1 m in length and 21.3 mm in diameter buried in loose gravel soil to investigate its behaviour when subjected to impulse current conditions. The test object energised with discharge currents of 20 µs to 30 µs rise-time with peak currents of up to 1500 A. The results showed a reduction in the measured impulse resistance, which is defined as the ratio of the measured voltage to the current at any instant, from 24 Ω at 60 Hz to 17 Ω due to the non-linear behaviour of the conducting medium. This study soon motivated researchers to conduct more investigations to obtain a better understanding of the earthing system behaviour.

In 1941, Bellaschi [2.3] performed experimental field tests on four steel rods of one-inch diameter (25.4mm) and up to 2.7m length, which were installed in natural soil, with earth resistance magnitudes between 30Ω and 40Ω at 60Hz in parallel with deep-driven earth rods as improvements to the performance of earthing systems under power frequency fault conditions. Discharge currents with peak values of 2kA to 8kA were applied to the four rods with rise-time values of 6µs and 13µs. In this study, Bellaschi defined impulse resistance as the ratio between voltage peak value to current peak value, neglecting the inductive and capacitive effect. The measured impulse resistance under these impulse conditions was found to be lower than the 60Hz resistance values, and it decreased over an injected current magnitude, due to the soil ionisation process (Figure 2.1). He defined

a curve as 'characteristic of driven grounds' in which the ratio of the impulse resistance to the measured 60 Hz value is plotted against the peak impulse current (Figure 2.2). His results agreed with those of Towne [2.1].
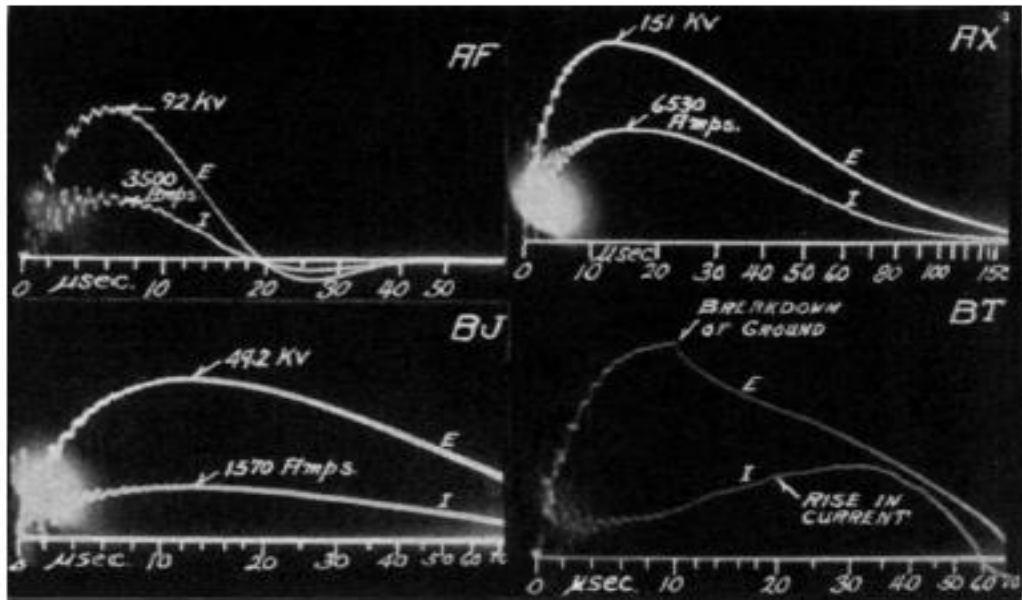
Figure 2.1: V and I waveforms for vertical rod (5 kA, 10/16 μs impulse) (reproduced from reference [2.3])
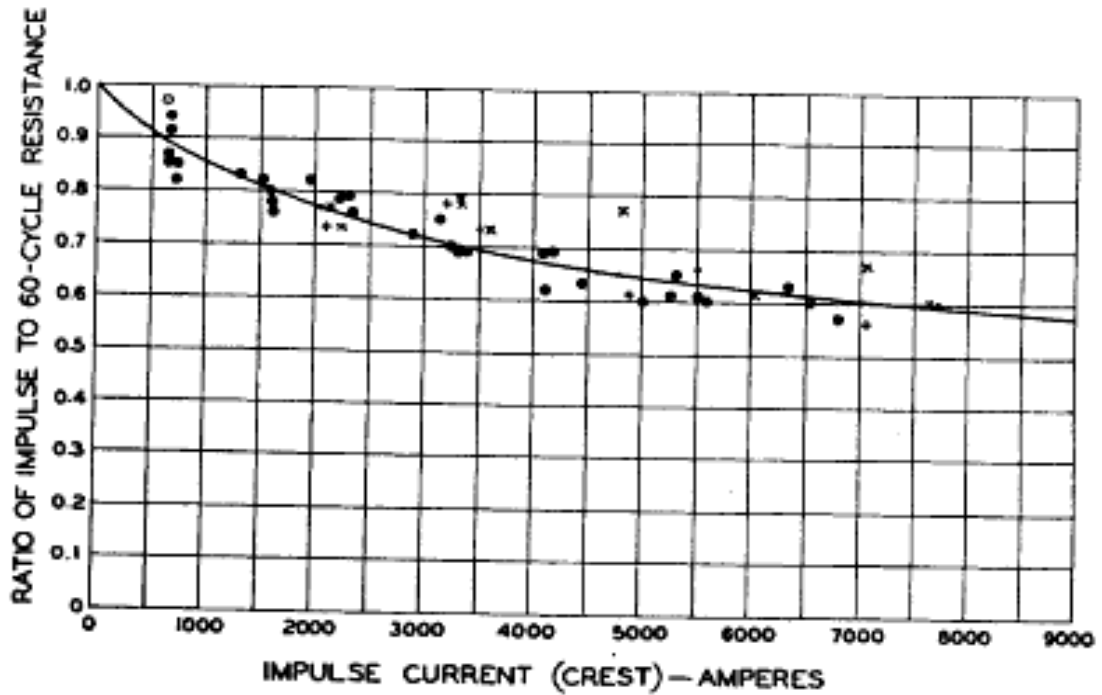
Figure 2.2: Characteristics of driven grounds (reproduced from reference [2.3])

Bellaschi, in his subsequent paper [2.4], extended the experimental work to involve 12 earth-driven electrodes in the field at depths ranging from 2.44 m to 9.14 m. The details of the conducting media are given in Table 2.1.

Table 2.1: The properties of the experimental field for Bellaschi [2.4]

Conducting medium	Earth resistance measured at 60Hz
Clay soil	10Ω - 40Ω
Dry and gravelly soil	60Ω - 220Ω
Sand	60Ω - 220Ω
Mixture of clay and stone	25Ω - 190Ω

The impulse current values, which ranged from 400 to 15,500 A with various rise-times of 20/50 µs, 8/125 µs, and 25/65 µs, were injected into the test object. The results

demonstrated a reduction in the impulse resistance value, which is defined as the ratio of impulse resistance to 60 Hz resistance. In addition, the experiment found that the soil and electrode arrangement has a significant effect on the impulse resistance. However, its value was independent of the current rise-time. Vainer [2.5] confirmed the results when he applied a high impulse voltage of 1.5 and 0.8 MV to vertical rods of 10 m to 140 m in length. Vainer defined the impulse impedance as the ratio of the crest voltage to the corresponding current at crest voltage and found that there is a small reduction of impulse impedance for an electrode of lower AC earth resistance, which is similar to Bellaschi's results [2.4].

Liew and Darvenzia [2.6] developed an analytical model to describe the nonlinear behaviour of earthing electrodes. A discharge current up to 20 kA with different rise-times between 10 µs and 54 µs was injected into 0.61 m (2 ft) long vertical rods with a diameter of 12.7mm that are buried at 25.4mm in soil and electrode of diameter 152.4mm buried under the surface of the soil with resistivities between 5,000 Ωcm and 31,000 Ωcm. The dynamic model is shown in Figure 2.3. they have observed 3 stages: (a) First there is constant soil resistivity in all directions, named the 'no ionisation zone'; and (c) when, the current density exceeds the critical current density value Jc, and the soil resistivity decreases exponentially i.e. ionization zone. (b) if the current density has built up to a value greater than a critical value, then the resistivity will be less than the low current resistivity, and the soil resistivity decays exponentially to recover the initial value;. A reduction in impulse resistance was reported with an increase in the current magnitudes due to soil ionisation. This reduction was found to be dependent on the characteristics of the soil and lower breakdown gradients. It was found from tests that there is a greater reduction in impulse resistance for individual vertical rods compared with multiple rods due to the current density. Moreover, at 100 kA impulse current, the impulse resistance

decreased more than in the case of a 15 kA current. The obtained results revealed that the impulse resistance of the vertical electrodes was dependent on the impulse current rise-time, which contradicted the results found by Bellaschi et al. [2.4], who concluded that the impulse resistance is independent of current rise-time.
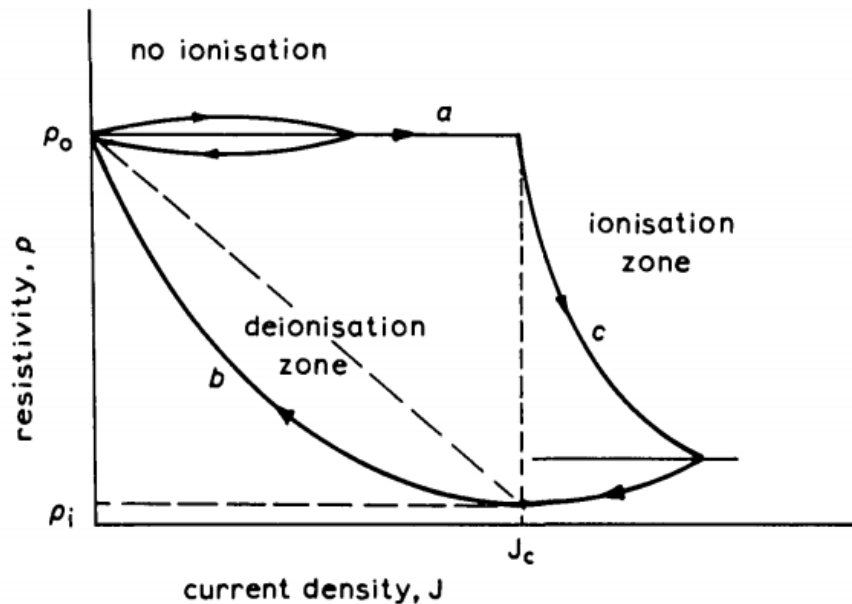
Figure 2.3: Dynamic model for soil ionisation (reproduced from reference [2.6])

In addition, a number of impulse investigations on soils, performed in the Cardiff University earthing system facility located at Llanrumney, Wales, UK, were performed and reported in [2.7]-[2.9]. The results of the previous investigations on the characteristics of vertical electrodes under transient conditions can be summarised as follows:

1. The discharge current magnitude has a significant effect on the impulse resistance of the earthing electrode, which is decreased to values less than the 60 Hz earth resistance value.

2. The reduction in the impulse resistance, which is expressed by the ratio of impulse resistance to 60 Hz resistance, is dependent on soil properties and electrode

configurations. However, the current rise time makes no contribution to this reduction.

3. The various investigations reported that there is a small reduction in impulse impedance for an electrode of lower AC earth resistances.

2.2.2 Horizontal and grid earth electrodes

In 1934, an impulse test was carried out by Bewley [2.2]. Long horizontal earth electrodes (counterpoises) of different lengths (281 m and 465 m) were buried to a depth of 1 ft in earth of soil resistivity 100 Ωm. Impulse currents of 2 µs rise times with peak currents of 900 A were injected. In his analysis, which was based on travelling wave methods using a model with distributed inductance, leakage conductance, and capacitance, he found that the transient impedance of the counterpoises fell rapidly to values less than for the 60 Hz power frequency. The transient impedance is expressed as the ratio of instantaneous voltage to current. In addition, it was noticed that increasing the length of the counterpoise over 91.4 m has no major effect on the impedance value. In his study, no ionisation occurred due to the low magnitude of the discharge current. To verify his calculation model, Bewley carried out more experiments on counterpoises [2.10]. Different lengths of counterpoises (61 m, 152 m and 282 m) were subjected to impulse voltages of 15 kV and 90 kV with a rise time of 0.5 µs. It was observed that the impulse impedance started at a magnitude equal to the surge impedance and decreased quickly to a value less than the 60 Hz resistance (Figure 2.4).

An empirical formula to characterise the impulse impedance of substation earth grids was provided by Gupta et al. [2.11]. The tests were carried out on 16 mesh square grids of copper wire. It was found that the measured impulse impedance of the earth grid was significantly affected by the location of the injection point, the shape of the earth grid, the distance between the electrodes, the magnitude and wave shape of the injected impulse

current, and the characteristics of the soil. Here, the impulse impedance is defined as the ratio of the voltage peak measured at the injection point to the peak value of the current injection. However, it is well known that due to the inductive and capacitive effects, the peak value of the voltage and of the current do not always occur at the same time. It was concluded that the effect of soil ionisation was very small when using an earthing grid and so could be ignored. In a subsequent paper, Gupta et al. [2.12] performed additional work to investigate the effect of the earth grid shape on the impulse impedance. It was observed that the square earth grid exhibited a lower impedance value compared to the rectangular grid for the same area.
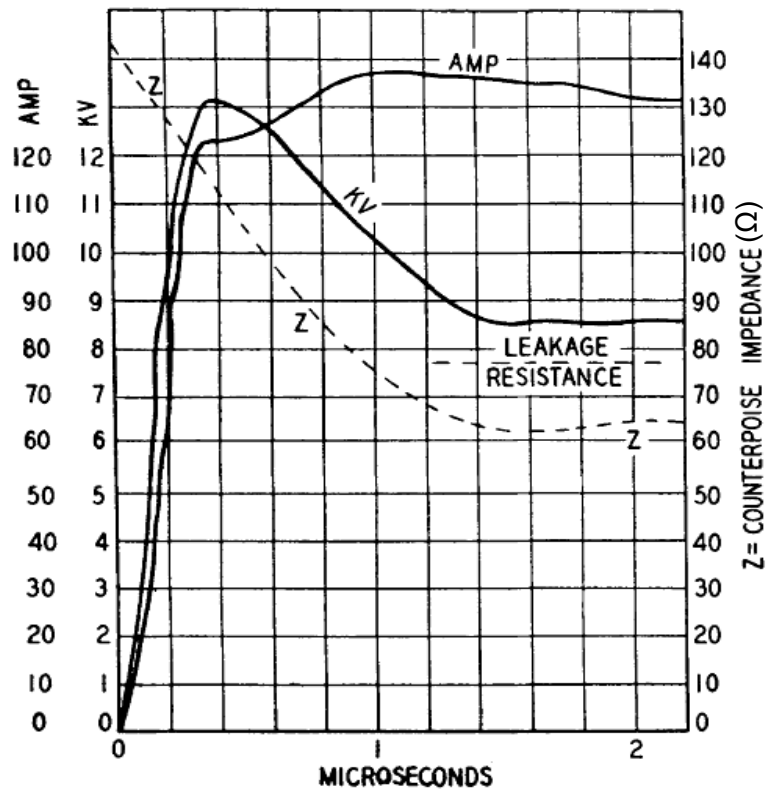
Figure 2.4: Experimental results on a 61 m horizontal electrode (counterpoise)

(Reproduced from reference [2.10])

Toshio et al. [2.13] carried out measurements in the field to investigate the soil characteristics of horizontal electrodes. The tests were implemented with two-

17

dimensional square grids, which measured (i) 10m^2 and (ii) 20m^2, and two horizontal earth electrodes of lengths 5 m and 20 m. The test objects were energised with impulse currents up to 30 kA and impulse voltages up to 3MV. The measured values of the impulse resistance of the horizontal electrodes were found to be strongly dependent on the injected currents; this is attributed to the soil ionisation process, as shown in Figure 2.5a. However, the impulse resistance was found to be a constant for almost all current values the grid (ii) (see Figure 2.5b).

Yanqing et al. [2.14] investigated the characteristics of earthing grids under transient conditions. An earthing grid of 20 x 20 m^2 buried at 0.8 m depth in soil with a resistivity value of 500 Ωm and permittivity of $\varepsilon_r = 9$ was injected into the corner and centre with impulse currents up to 10 kA with a 2.6/50 µs wave shape. It was found that there is a many-parameters effect on the characteristics of the impulse resistance, such as the waveform and the magnitude of the energised current and the location of the injection point. The results showed that the impulse resistance exhibited a higher value for current injection at the corner of the grid than for injection at the grid centre, which is in agreement with Gupta [2.11].
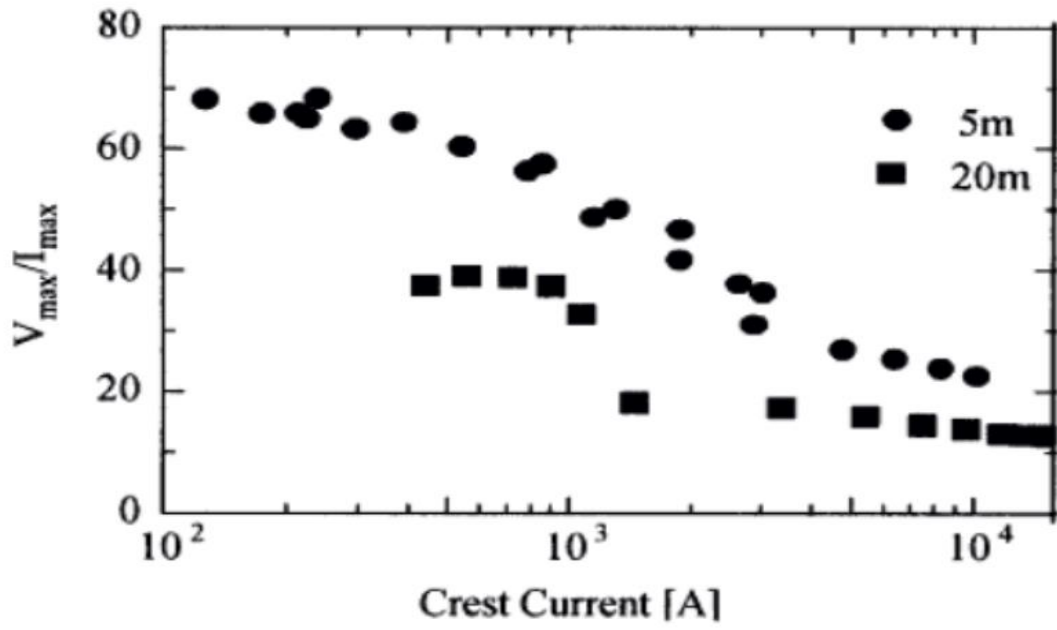
(a) Horizontal electrodes
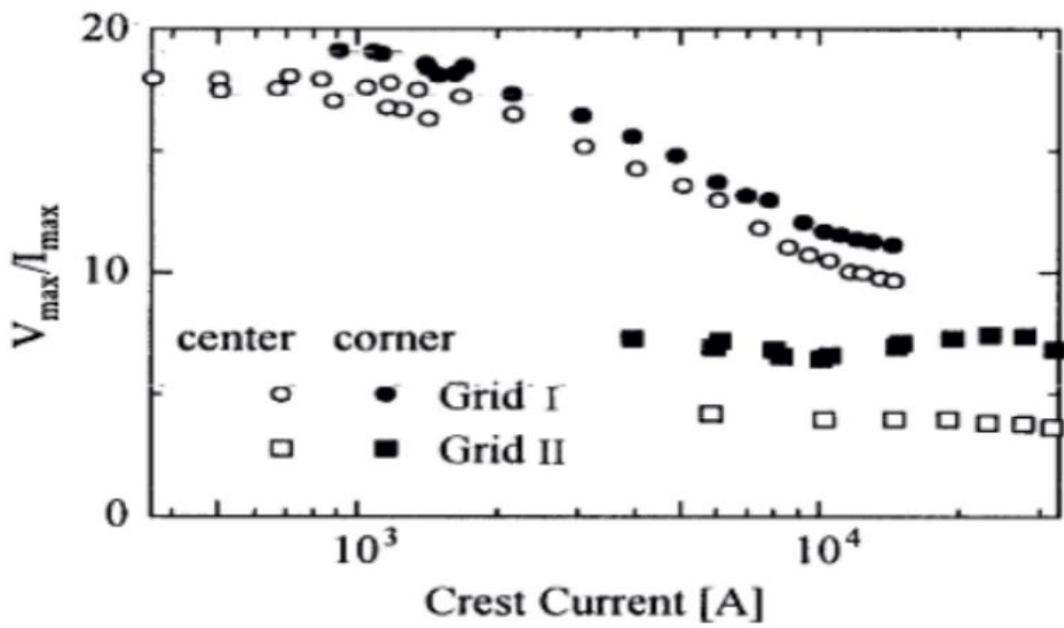
(b) Earthing grid

Figure 2.5: Current dependency of earthing resistance (reproduced from reference [2.13])

The results of the previous investigations on the characteristics of horizontal and grid electrodes under transient conditions can be summarised as follows:

1. The earth impedance of the horizontal earth electrode under transient conditions, which is strongly current-dependent, can be reduced even at low currents.

2. The investigations confirmed that the impulse resistance of the earthing grid buried in a low resistivity medium exhibits lower current-dependent characteristics than those buried in a high resistivity medium, which agrees with the results conducted with vertical electrodes. The earth resistance current-dependence under impulse currents was found to be related to the DC earth resistance (R_{DC}) value.

3. The earthing impedance magnitude is dependent on many parameters, such as the waveform, the magnitude of the energised current, and the location of the injection point.

2.3 Characteristics of earthing system under high frequency

Brourg et al. [2.15] conducted an experimental work on short electrodes (<4 m) to characterise the frequency response of vertical electrodes buried in high resistivity soil. The earth impedance was measured over frequencies up to 1 MHz. It was found that there was a reduction in the earth impedance magnitude with a frequency of up to 1 MHz. The same scenario was repeated with a vertical rod 32 m long; the earth impedance exhibited a constant value over frequencies up to a threshold frequency, after which the earthing impedance increased sharply.

Choi et al. [2.16] carried out tests on a medium-sized grid (20×9 m^2) buried in a high resistivity medium. A reduction in impedance was observed over the range DC to 200 kHz, which was attributed to capacitive effects.

Llovera et al. [2.17] carried out laboratory investigations on a hemispherical electrode and short vertical rods buried in soils with a range of resistivities. The earth impedance was measured over frequencies from DC up to 10 MHz; the measurement results showed capacitive behaviour for both low soil resistivity (281 Ωm) and high soil resistivity (1900 Ωm) up to 1 MHz. After that frequency, the earth impedance increased, and the inductive effect was dominant for high soil resistivity.

Choi et al. [2.18] carried out tests on a 40 m horizontal electrode with a radius of 0.28 cm buried in ground with two-layered soil resistivity. A low resistivity material was mixed with the soil at one end of the counterpoise to study the earthing impedance. It was found from the test that when the electrode was energised at both ends, the end immersed in the low resistivity material exhibited a high rate of current dissipation compared with the other. In addition, the measured impedance at the low resistivity material end showed a lower value compared to the other end for both the low and the high frequency ranges. Recently, Musa [2.7] presented the variation of impedance magnitude at various frequencies for the vertical electrode of lengths up to 6 m and a 100 m horizontal earth electrode buried in soil with a resistivity of 150 Ωm. The impedance magnitude of both the vertical and the horizontal electrodes was measured over a range of frequencies from DC up to 10 MHz and showed a constant value at low frequency up to the characteristic frequency. Then, the measured impedance either increased or decreased due to inductive or capacitive effects. The author investigated the effect of length on the measured impedance.

The characteristics of earthing electrodes under high frequency can be summarised as follows:

1. The impedance of earth rods is purely resistive up to a particular frequency; after this frequency, they become either inductive or capacitive depending on the length and the resistivity values.

2. The impedance magnitude of horizontal and grid electrodes exhibited an increase in value above a particular frequency for low soil resistivities. However, for high soil resistivity, the resonance in the response for frequencies occurred above 1 MHz, and the impedance decreased above a particular frequency.

3. The characteristic frequency depends on the electrode length and the soil resistivity.

2.4   Development on numerical and computational models

Different approaches have been developed to simulate the behaviour of earthing systems under variable frequency and impulse conditions. Bellaschi and Armington [2.19] developed equivalent circuit models to investigate the behaviour of vertical earth electrodes. All the models considered the effect of the down lead. The behaviour of short rods (up to 6.1 m) and long rods are represented by models (a) and (d) in Table 2.2(I) respectively. In these models, the equivalent circuit is represented by lumped down lead and rods inductances in series with earth resistance. However, for high soil resistivity, medium 1000 Ωm and above, models (c) and (b) were used. The models were applied to ten different configurations and variable down lead lengths and a discharge current of 40 kA with front rise times from 1 µs to 8 µs. Model (b) exhibited a significant rise in voltage magnitude with short rise times of 1 µs and 2 µs due to down lead inductance. However, the effect of soil ionisation is not taken into consideration with these models. In 1941, Davis and Johnston [2.20] suggested an equivalent model similar to Bellaschi's model (e) to determine the impedance of a transmission tower line under transient conditions.

Simple cylindrical and hemispherical electrodes were tested, and it was found that the resistance exhibited a decrease in its value over the injected currents magnitude range due to the ionisation process. The impedance was expressed as earth resistance in series with the tower inductance. Four equivalent circuit models were developed in 1945 by Rundenberg [2.21] according to the energised frequency and earth electrode arrangements (see Table 2.2 (II)). This work was updated and published in 1968 in textbook [2.22]. In these models, at low frequency, the earth electrodes behaved as a pure resistors (model a). However, at high frequency, the inductive reactance of the down lead becomes higher (model b), causing a significant rise in voltage, which might lead to soil ionisation. Model (c) was used in case of fast transient conditions; however, (model d) was suggested in case of surge conditions when the inductance of the earth rods becomes significant. Devgan and Whitehead [2.23] developed a transmission model to investigate the frequency dependence of soil parameters. See Table 2.2 (III).

Table 2.2 (IV) shows the equivalent circuit model developed by Verma and Mukhedkar [2.24]. In this model, the distributed parameter transmission line equation is used to express the impulse impedance of horizontal electrodes. Mazzetti and Veca [2.25] to model buried earth wire developed a simple transmission line model. In their model, both longitudinal resistance and transverse capacitance were neglected. The capacitive effect was shown to be more significant with an increase in the energised frequency, and the soil parameters (resistivity and permittivity). A 5kA impulse current was applied to the test object with front rise times varying from 1 µs to 25 µs. The results showed that there was a significant voltage drop along the electrode up to a specific length, which was expressed as (effective length). An empirical formula to calculate the effective length was developed by Gupta and Thapar [2.11] Equation (2.1).

$$l_e = K \, \rho^{0.5} r^{0.2} \tag{2.1}$$

Where K is constant, ρ is the soil resistivity (Ωm), and r is the radius of the electrode (m).

Velazquez and Mukhedkar [2.26] developed a uniform distributed parameter (see Table 2.2(V)), which is used to analyse earth electrodes of different lengths ranging from 30 m to 150 m in different soil resistivities (1000 to 5000 Ωm). The results reported that the transient behaviour of earth electrodes depends on the soil resistivity and permittivity, the length of the electrode and the impulse shape. A simple model was developed by Verma and Mukhedkar [2.27] to model the behaviour of an earth grid, in which the equivalent circuit is described by a lumped inductance in series with a parallel resistance and capacitance branch (see Table 2.2 (VI)).

The Electromagnetic Transient Program (EMTP) was used by Lorentzou and Hatziargyriou [2.28] to model the behaviour of two types of earth electrodes: a vertical electrode (1 m long) and a horizontal electrode (100 m long). The results compared two models, that is, the lumped pi-model and the frequency dependent transmission line model, and exhibited good agreement up to 1MHz. Grcev et al. [2.29] made a comparison between simple equivalent circuits and electromagnetic field theory (EMF), which was used to simulate vertical earth electrodes with lengths of 3 m and 30 m buried in 30 Ωm and 300Ωm soil resistivity. The behaviour of the earth electrodes was computed by the lumped circuit model, distributed parameter circuit model and EMF. The results showed that both the RLC circuit and lumped circuit model overestimated the earth rod impedance, in particular at high frequencies, compared to the EMF model, which gave much better results (see Figure 2.6).

Table 2.2: The developed equivalent circuit models to characterise the behaviour of earthing electrodes
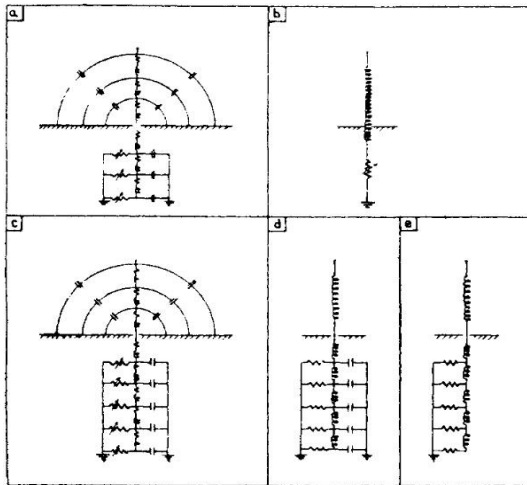
(I) Reproduced from Ballaschi [2.19]	**(II) Reproduced from Rudenberg [2.22]**
(III) Reproduced from Devgan [2.23]	**(IV) Reproduced from Verma [2.24]**
(V) Reproduced from Velazquez [2.26]	**(VI) Reproduced from Verma [2.27]**
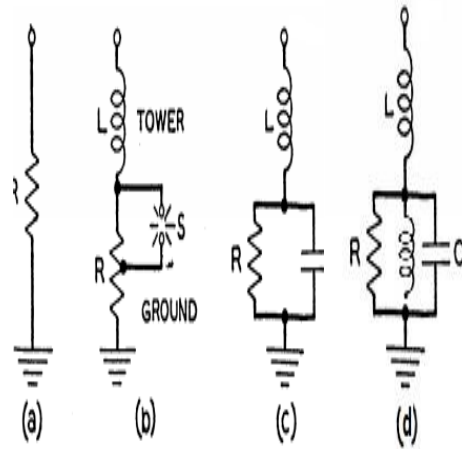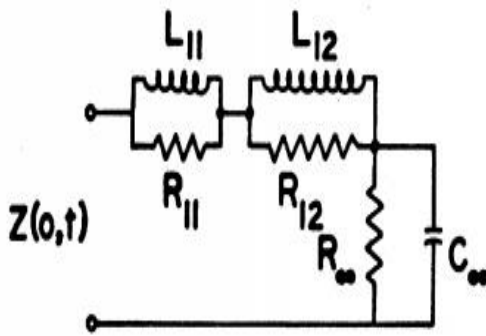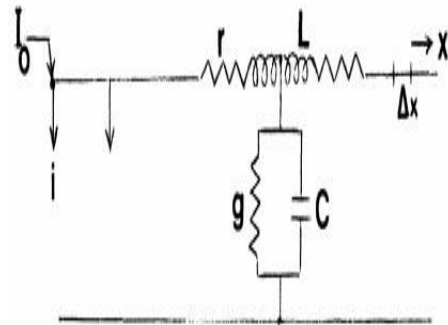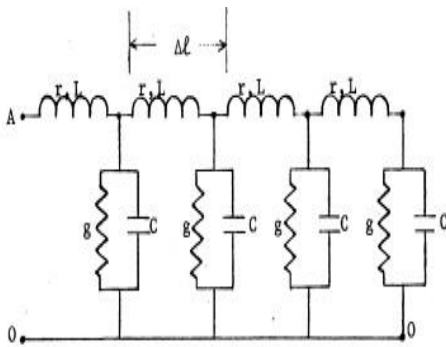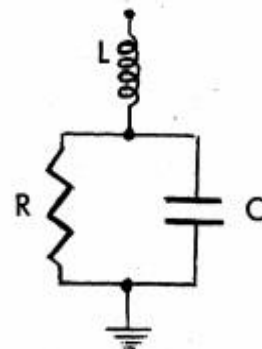
25
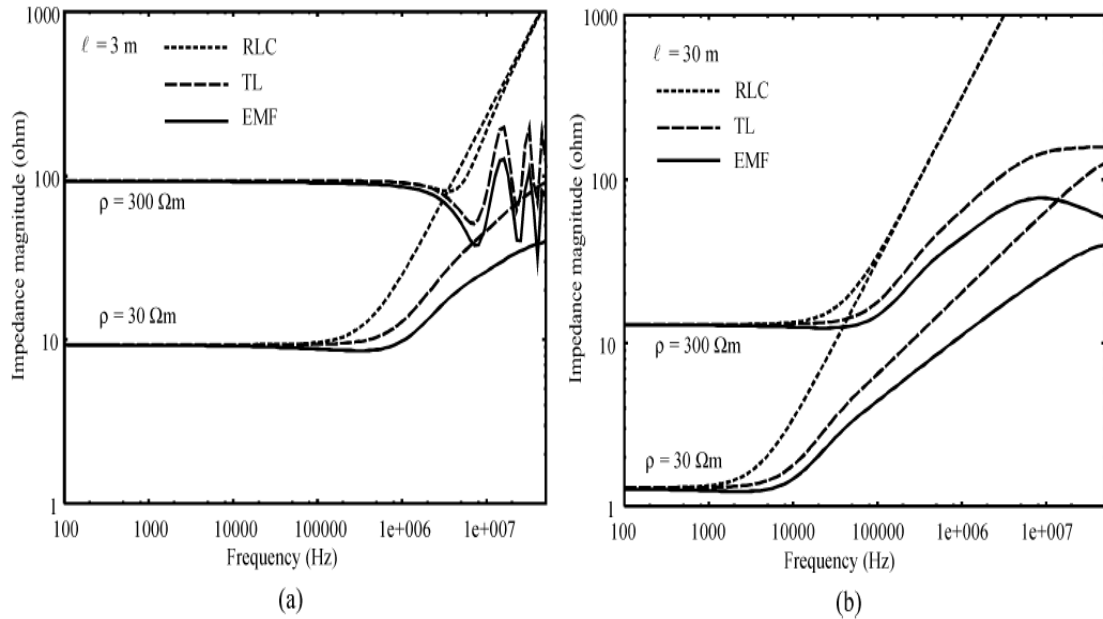
Figure 2.6: High frequency response of vertical electrodes: (a) l=3 m, (b) l=30 m

(reproduced from reference [2.29])

A computer simulation program based on quasi-static field theory was developed in 1986 by Dawalibi [2.30] and became commercially available as 'MALT'. This code modelled the earth resistance as a number of cylindrical conductors and was able to deal with multi-layered soil. However, the code did not take account of the longitudinal impedance of the conductor; therefore, it is valid only at low frequencies. The work was then extended to take account of the longitudinal impedance of the earth electrodes and the mutual impedance between different parts of the electrodes due to circuit theory expression; see Dawalibi [2.31]. The software was known commercially as 'MALZ', and the author states that it is valid up to 1 MHz. In 1990, Grcev and Dawalibi [2.32] developed a simulation code based on exact field theory, which became known as 'HIFREQ'. The quasi-static approach used in 'MALZ' was replaced with a developed methodology using the method of moments. The simulation becomes able to calculate the impedance of any arrangement of electrodes and the associated scalar potential, and of the electric and magnetic field at

any point in space at any frequency. However, the soil ionisation was not taken into account in any of these computational models.

Alipio et al. [2.33] proposed a new methodology based on the Hybrid Electromagnetic Model (HEM). This approach was used to simulate the behaviour of horizontal earth electrodes with lengths ranging from 5 m to 90 m buried at a depth of 0.5 m in soils of low and high resistivity (300 Ωm and 3 kΩm) over frequencies ranging from low and high frequencies up to 1 MHz. It was found that, at low frequencies, the earthing impedance was frequency-independent and equal to the low frequency resistance for both low and high resistivity. However, at high frequencies, the results showed that for both low and high soil resistivity, the frequency dependence of the soil parameters caused a reduction in the earthing impedance due to capacitive effects.

2.5   Frequency Dependence of Soil Parameters

According to Sunde [2.34], permittivity is more important with lightning phenomena and varies within limits from 1 to 80, depending on the nature of the soil, and its relative value is not greatly affected by frequency. In contrast, the soil resistivity varies over an extremely wide range and has an effect on lightning protection. The response of an earthing system subjected to transient and variable frequency energisation is a complex phenomenon and can significantly affect the performance of the electrical power system. In 1934, Smith-Rose [2.35] carried out his laboratory and field experiments on the electrical parameters of the soil (conductivity and permittivity). Five types of soil with different moisture levels and subjected to an AC with frequencies ranging from 1 kHz up to 10 MHz were used in these investigations. The results showed that the moisture level in the soil has a significant effect on both its electrical conductivity and dielectric constant. In addition, the frequency effect on the conductivity was more pronounced for dry soil compared to the soil with different moisture levels, which showed an increase in

conductivity value at high frequencies. However, the dielectric constant exhibited small variations in its value over the frequency range for dry soil. Then, a reduction in permittivity values was observed as the frequency and moisture level increased. In the 1960s, Scott [2.36]-[2.38] conducted laboratory experiments on a variety of rock and soil samples containing various amounts of water to determine the electrical conductivity and permittivity over frequencies from 1 kHz up to 10 MHz. These investigations resulted in curve-fit expressions for the electrical soil parameters as a function of frequency and water content.

An analytical model was developed by Longmire and Longley [2.39], based on Scott's experimental data, to represent the frequency dependence of soil conductivity and permittivity. Their curve-fit expressions were presented for the frequency range 100 Hz to 1 MHz. In 1975, Smith and Longmire [2.40] derived what they called the universal soil model, which depended on the measured conductivity and permittivity of samples of concrete and grout. Their model was able to present the frequency of soil parameters over frequencies ranging from 1Hz up to 200MHz. Visacro and Portela et al. [2.41] conducted laboratory measurements on different soil samples. The measurements resulted in empirical expressions to represent the variations in soil conductivity and permittivity with respect to frequency in the range 40 Hz to 2MHz. Portela [2.42] carried out laboratory measurements on 68 samples representing five types of soil with frequencies of 100 Hz up to 2MHz. Based on these measurements, he proposed new expressions for the conductivity and permittivity of these specific soil types. Recently, Visacro and Alipio [2.43] developed an experimental methodology to determine the variation in electrical soil parameters with respect to frequency. They applied their methodology to 31 soil samples with a wide range of resistivity, from 60 to 9,100 Ωm. It was found that both soil resistivity and permittivity exhibited strong variations in their values for the frequency

interval in the range 100 Hz to 4 MHz. A significant decrease was observed in soil parameters with an increase in frequency. Based on their obtained data, they proposed a new curve-fit expression for the frequency dependence of the soil's relative permittivity and conductivity. Akbari et al. [2.44] applied Visacro and Alipio's empirical expressions in their approach, which was based on the finite element method (FEM) to analyse the behaviour of different earthing electrodes, such as simple vertical and horizontal earthing electrodes, and earthing grids. It was found that the frequency dependence of soil parameters had a significant effect on the behaviour of earthing systems. This effect was more marked for long electrodes buried in a high resistivity medium. They confirmed also that there was no marked change in the effective length of earthing electrodes while considering the frequency dependence. Visacro et al. [2.45] also conducted experimental investigations; peak voltages of 0.5–2 kV were used to inject a very short front time current into hemispherical, vertical, and horizontal electrodes buried in soil with a resistivity value of 1400 Ωm and frequencies ranging from 100 – 4 MHz. In this study, a fast Fourier transform (FFT) was applied to both the acquired voltage and current signals. The results showed that considering constant values of soil resistivity and permittivity led to significant errors in earth potrential rise (EPR) for the simulated electrodes when they were subjected to the impulse current; these errors ranged from 30% to more than 100%. Guimaraes et al. [2.46] applied Visacro's expressions to simulate an earthing grid of 20 m with 4 m × 4 m meshes buried at 0.5 m depth in 160 Ωm soil. The earthing grid was simulated to take account of both the conservative approach and the frequency-dependent soil parameters model, and the results were compared with those obtained by experiment. It was observed that the measured and simulated earth potential rises were quite close in magnitude. In addition, due to the low value of soil resistivity, the earthing potential rises considering both approaches were probably close. Silveira et al. [2.47] applied the Hybrid

Electromagnetic Model (HEM) to explore the impact of the frequency-dependent soil parameters on lightning-induced voltages. The expressions were applied with resistivity variations from 100 to 10,000 Ωm subjected to lightning current with first and subsequent strikes. It was found that considering frequency dependence resulted in a significant reduction in induced voltage, in particular at high soil resistivity.

2.6   Conclusions

In this chapter, an extensive review of the published work on the behaviour of earthing systems under high frequency and surge conditions has been undertaken. Published field tests, laboratory tests and computational work for different earthing electrodes, such as vertical, horizontal, and grid earth electrodes, have been investigated.

Two earthing system facilities were prepared in accordance with all the recommendations and information available in standards and published work (see Chapter 3).

The majority of the work reviewed presents the results of simulating high frequency and transient conditions using computational models. The CDEGS (HIFREQ-FFTES) software program is one of the most commonly used computational tools to characterise the behaviour of earthing systems. This program divides the earth electrode into a number of segments to calculate the total resistance. These numbers of segments should satisfy certain conditions. Within these conditions, the number of segments remains reliable and choices depending on the experience. Therefore, the frequency responses of different earthing systems have been investigated using CDEGS numerical software, and the effective number of segments for different scenarios has been proposed (see Chapter 4).

The results and recommendations concluded in Chapter 4 should be compared with those obtained from practical earthing systems. Therefore, the characteristics of different arrangements of practical earthing electrodes under low and high frequency and transient conditions were investigated. In addition, many researchers have either investigated the

performance of earthing electrodes under different energisation conditions experimentally, including laboratory measurements or field tests measurements, or theoretically, by applying different computational models. The results obtained from these investigations are highly dependent on the assumptions adopted for the behaviour of the conducting medium. Therefore, further experimental investigations are required to check the quality of the results conducted by both experimental investigations and numerical models. This leads to a need to develop experimental tests used for calibrating earthing meters, validating the computational models, and identifying the influence of soil parameters on the behaviour of earthing systems under power frequency and transient conditions (see Chapter 5).

The satisfactory performance of earthing systems under both low and high frequencies is important to ensure protection for electrical equipment and for workers. Although the frequency responses of earthing systems have been studied extensively, both theoretically and experimentally, a common underlying assumption is that the soil parameters (σ, μ and ε) are constant. There has been recent interest in investigating the frequency response of the conductivity σ and permittivity μ; however, no accurate general formulation is provided in the literature for expressing soil parameter frequency dependence, and there appears to be a need to clarify both the range limits and the frequency response of these parameters (see Chapter 6).

Several authors have investigated the effect of moisture levels on the behaviour of earthing systems, and their results have shown that the resistance decreases when the water content in the soil increases. However, since no available research work investigated the effect of moisture on the resistance and impedance of different high resistivity materials used to increase the contact resistance at substation to ensure the safety of personnel, laboratory tests were set up (see Chapter 7).

CHAPTER THREE: DEVELOPMENT OF FIELD TEST FACILITIES AND SOIL SURVEY AT LLANRUMNEY AND DINORWIG POWERSTATION

3.1 Description of Test Site

The majority of the earthing system investigations in this work were implemented at the Cardiff University earthing test facility at Llanrumney and at the Dinorwig pumped storage substation in North Wales. Much work was carried out to prepare both test sites with regard to safety requirements and risk assessment. This chapter will provide an overview of these facilities, test sites and the electrode installations.

Moreover, the earthing resistivity survey measurements, which were taken at different times at Llanrumney facility, are presented and discussed.

3.2 Llanrumney Fields Test Site

Much work and extensive numerical computer simulations were carried out to prepare the new field test site at Llanrumney in advance of the high current impulse testing of earthing electrodes. Figure 3.1 presents an aerial view of the test facility. The test equipment was arranged in the cabin positioned in the north - east of the working zone. Vertical, ring, and horizontal electrodes were installed at different locations around the site.
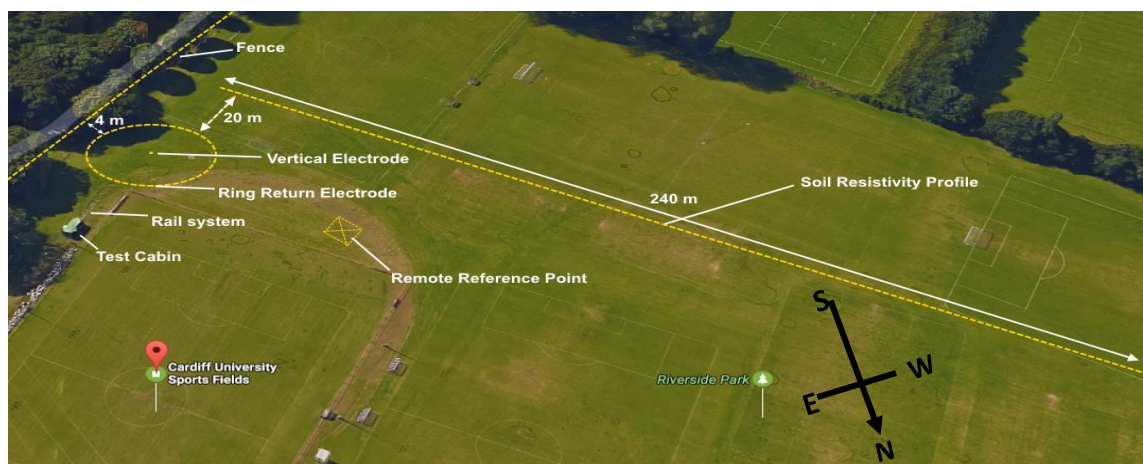
Figure 3.1: Aerial view of Llanrumney test facility

3.2.1   Numerical Model

To ensure the safety of test personnel, site employees and members of the public in the vicinity of the test location as well as the integrity of test equipment, extensive computational studies were employed for high current tests using a 30m diameter ring electrode as a current return. A suite of computations were performed using CDEGS [3.1] in advance of high voltage tests to assess the suitability of the field test arrangements, in the particular interest of safety. From the computations, it is possible to estimate the following:

1. The generated earth potential rise and step voltages in the vicinity of the return electrode which might endanger people safety in the working zone, as well as the touch voltages generated at fences

    a. The maximum current magnitude that can be injected into the test electrodes from the 200kV impulse generator

    b. The proportion of the source voltage dropped across the injection leads return electrode

The computer simulations helped to estimate the generated earth potential rise and to identify the hazardous touch potentials developed by exposed metalwork at the site perimeter. A 3D view of the CDEGS model employed is depicted in Figure 3.2. A 50mm² single core conductor of length 15 m and elevated to a height of 1.7 m was used for the current injection circuit. The remote ground reference potential was taken from a point 60 m away from the test electrode, in a direction perpendicular to the current injection line. The ring return electrode was modelled as a bare copper conductor of CSA 35 mm², buried to a depth of 30 cm. Peak EPR and step voltages were calculated over an area of 100 x 100 m, with profiles at 1 m intervals in the x- and y- directions. Peak touch voltages

were also calculated along linear profiles running parallel to the perimeter fence, at a distance of 1 m on both sides.
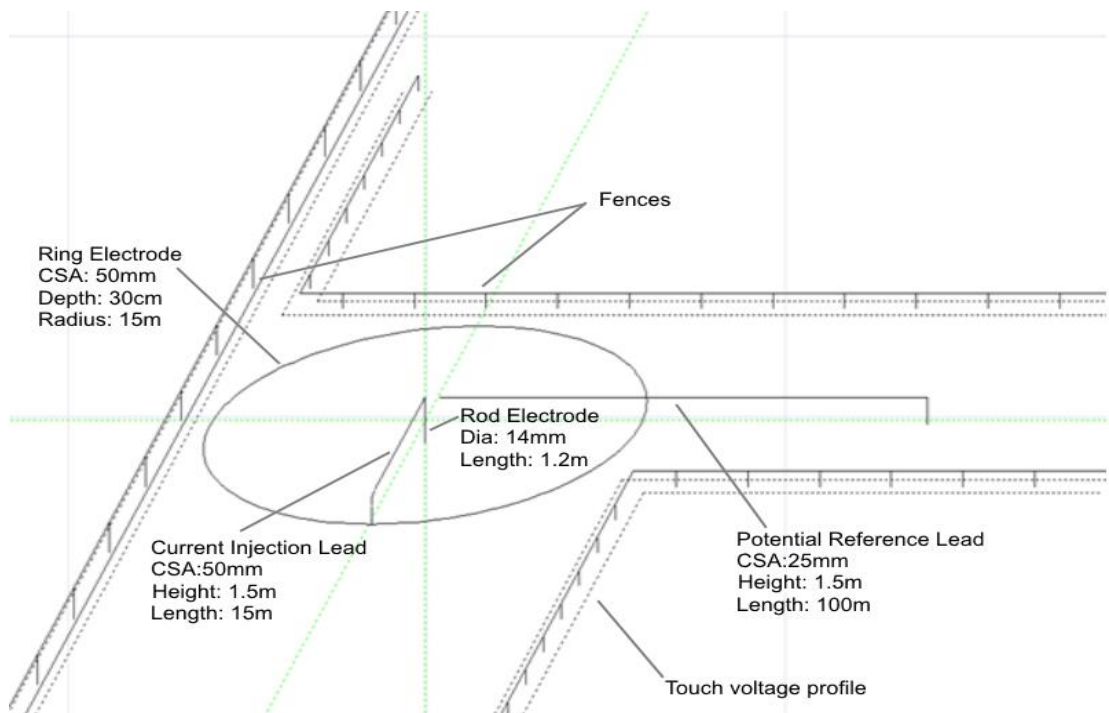
Figure 3.2: Simulation model configuration using ring current return electrode

The expected step voltage contour map for the circuit is given in Figure 3.3. It can be seen from the figure that the maximum generated transient step voltages over $50m \times 50m$ area in both the x- and y-direction were limited to a peak value of less than 100 V. This means there were no safety concerns for the people in the working area.

However, Figure 3.4 shows the simulated earth potential rise (EPR) with respect to a remote reference point for the test configuration. The figure indicates that the generated EPR decreased rapidly outside the ring electrode, which helped to minimise the transferred touch voltage on the fence.

Transient peak touch voltages for a 200 kV, 1.2/50 impulse were computed, using the actual measured soil resistivity range. Figure 3.5 illustrates that the peak touch voltage was limited to a maximum values of 325V and 324V for persons standing 1 m away from

the perimeter fence inside and outside the field respectively. According to BS EN 50522-2010 [3.2], the results were acceptable (see Figure 3.6).
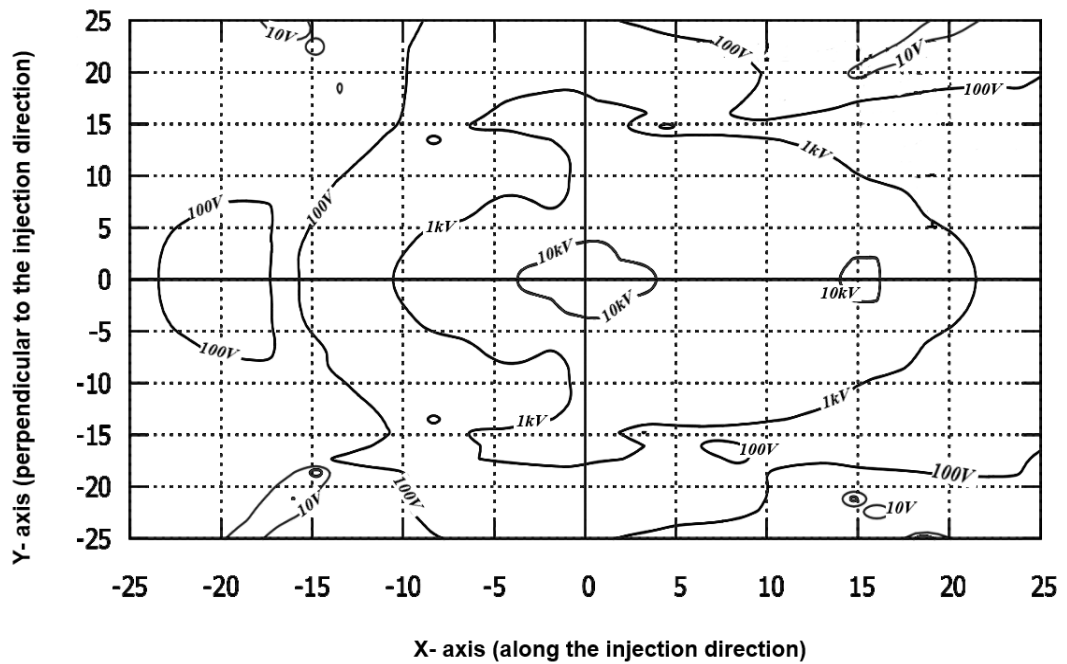
Figure 3.3: Peak step voltage contour plot using ring current return electrode (200 kV ‹ 1.2/50 µs wave shape)
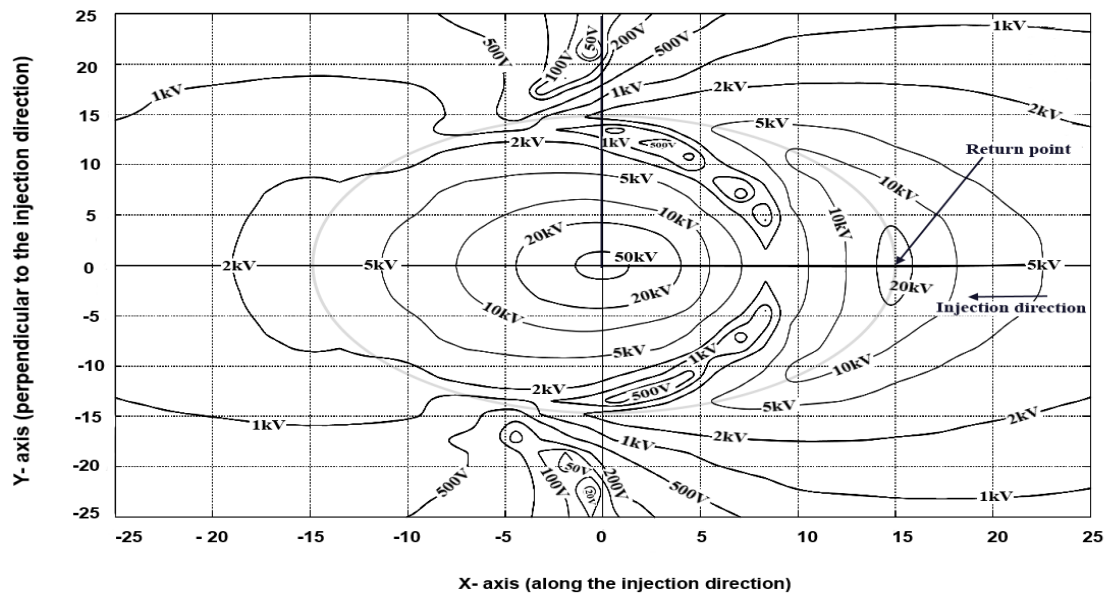
Figure 3.4: Peak EPR contour plot using ring current return electrode (200 kV, 1.2/50 µs Waveshape)
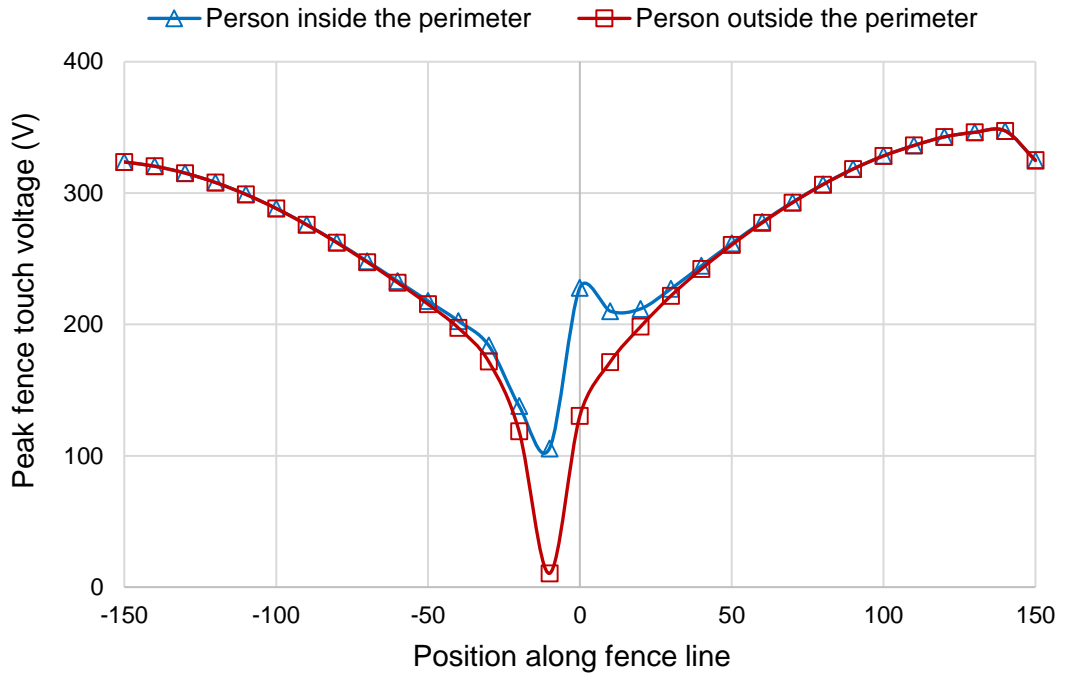
Figure 3.5: Perimeter fence peak touch voltage using ring current return electrode

(200kV, 1.2/50 µs wave shape)
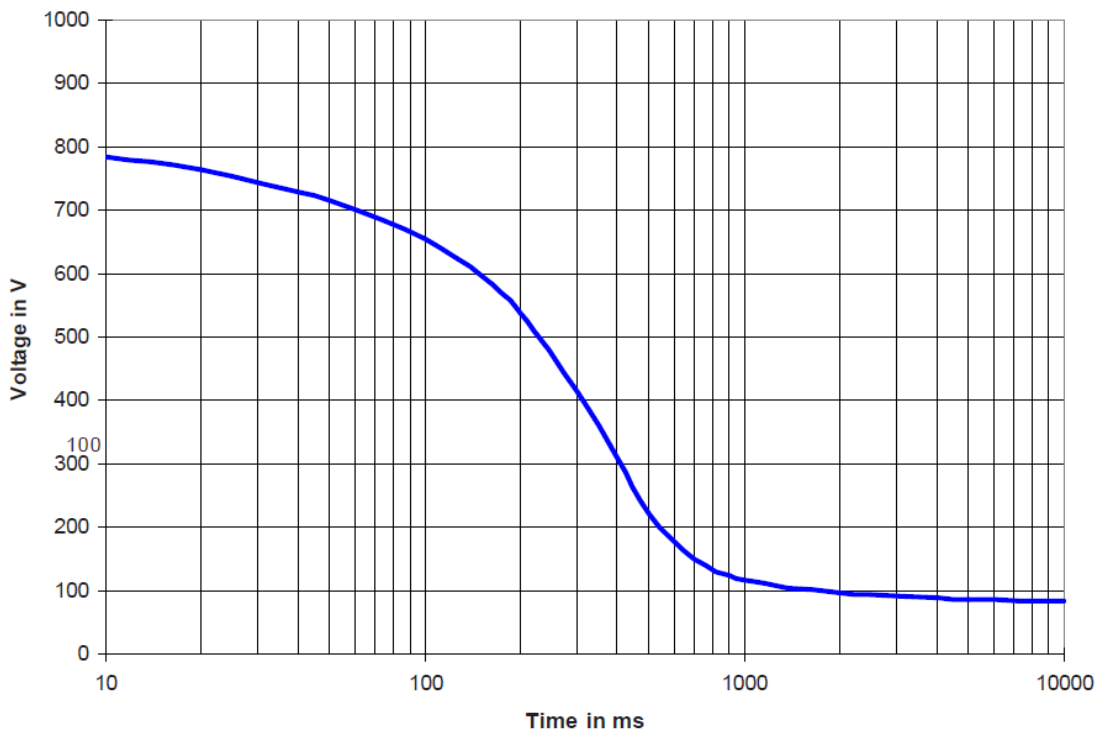
Figure 3.6: Tolerable touch voltages (Reproduced from BS EN 50522-2010 [3.2])

3.2.2 Earthing System Installation

A vertical copper test electrode with a length of 1.2 m and radius of 7 mm was placed at the centre of a concentric ring earth return conductor with 15 m radius. The ring was made of a 7-strand, 35 mm^2 cross-sectional area copper conductor buried 0.3 m beneath the ground surface and comprised eight equal-length sections with connection and measurement access points provided by eight corresponding inspection points. The ring current return arrangement was utilised to produce a uniform current distribution around the test electrode. Low voltage tests could be carried out with test sources located in a 6m × 3m metal cabin which housed the test and measurement equipment, while for the high voltage tests, a rail system was installed to transport the high voltage impulse generator to a position at the edge of the concentric current return electrode. For all low voltage and high voltage tests, current was injected into the central electrode using a current injection lead (transmission line) suspended from wooden poles 1.7 m above ground. A reference 'remote' ground potential for earth potential rise (EPR) measurements was imported from a distance of 35 m via a conductor arranged perpendicularly to the current injection circuit and also suspended by a wood pole line.

The horizontal electrode used in the tests is an industry standard arrangement for the 'LV earthing system' of an 11 kV/415 V pole-mounted transformer. The electrode system comprised a 24 m length 3-stranded copper conductor with an overall cross-section area of 35 mm^2 buried horizontally at a depth of 1.5 m. A set of vertical rods were connected along the length of the buried horizontal conductor. The first three rods were positioned 1.5 m apart and starting 6 m from the pole base. The remaining 6 rods were separated at a distance of 3 m.

Based on the schematic diagram of the fall of potential method (FOP) shown in Figure 3.7, an auxiliary current probe (CP) with a diameter of 10 mm and a length of 500 mm

was installed at a distance of 100 m from the grounding electrode under test. Another electrode, with a diameter of 10 mm and a length of 300 mm, was implemented as the potential probe (PP) or remote point. In the DC test, the PP was installed at a distance of 62 m (X=0.62 D) from the grounding electrode under test, in line with the current return lead. In the AC variable frequency test, however, will be described in chapter 5, in order to eliminate the influence of inductive coupling between the current and voltage leads, the PP was installed at an angle of 90° to the current return lead [3.3].
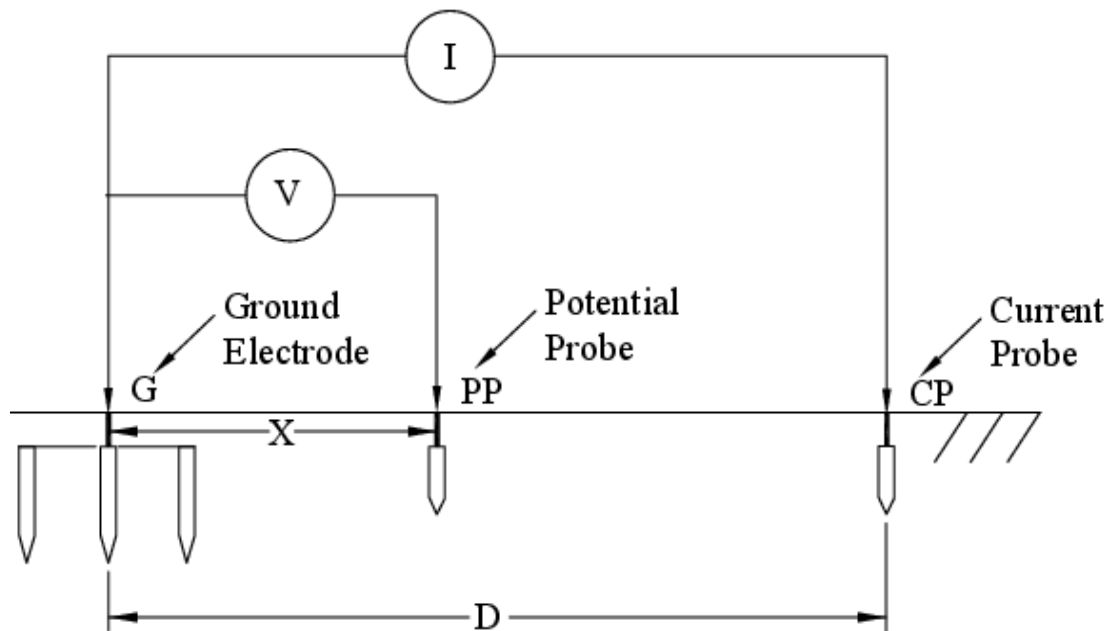
Figure 3.7: Test electrodes arrangement in Fall of Potential method [3.4]

3.3 Dinorwig earthing facility

3.3.1 Introduction

Several laboratory and full-scale experimental tests on the site have been performed on earthing systems to measure the earth resistance/ impedance of the earth electrodes. These tests provided valuable knowledge to investigate the behaviour of the earthing systems for different energisation conditions. In these full-scale studies, the behaviour of the

earhing systems were computed ignoring the fact that the soil is nonhomogeneous with significant variations both laterally and with depth. However, laboratory tests were undertaken at specific conditions, trying to scale up these test might be not valid. Furthermore, in simulation studies, soil is modelled as a simple uniform single layer, uniform multi-layer, or hemispherical symmetric soil structure, and again, the horizontal and vertical variation in soil resistivity was ignored. A uniform medium is required to validate these studies and models. Therefore, the lower reservoir of Dinorwig power station was chosen as the location to conduct experiments on test earth electrodes. The Dinorwig pumped-storage hydroelectric power station, located in North Wales, UK offered a large test area and uniformity of the test medium. The water resistivity is almost constant, and there is little variation in the resistivity for all locations within the reservoir, thanks to the daily pumping cycle. Hence, the facility is considered as close to a perfect test environment to conduct accurate experimental results for practical earthing electrodes. Figure 3.8, shows a plan view of the lower reservoir at the power station.

Figure 3.8: Arial view of the lower reservoir at the Dinorwig power station and test area.

The reservoir is approximately 1.8km long and 400m wide, and it is characterized by steep sides and a relatively flat bed. The water level of the reservoir usually varies over a range of about 15 m according to power station records, and it is ascertainable accurately at any time.

A test control and measurement cabin was set up on the shore 50 m from the reservoir edge. A motorboat was used to install the test grounding systems in the reservoir and for carrying out the experiments. To make immersion of the test electrodes possible at a fixed location, a 72-m pontoon was built from the shore to the specified electrode test position. The pontoon was anchored at intervals along its length, and a typical cross arrangement was constructed to fix a 5m × 5m test grid, which was immersed in the water at 0.8 m depth as shown in Figure 3.9. Plastic chain of constant length used to suspend the grid and to ensure a constant depth at any point of grid surface.
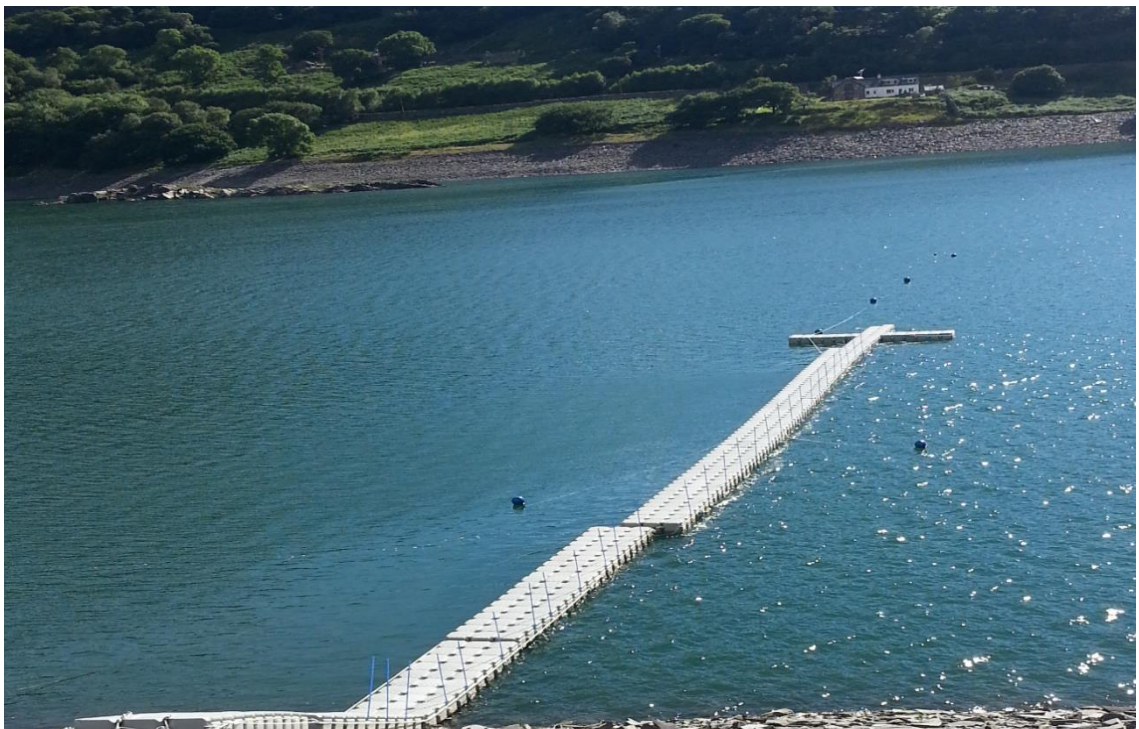
Figure 3.9: Pontoon construction and view of the test area from the shore side cabin

3.3.2 Numerical Model

Preparatory simulations were performed to evaluate the safety requirements at the Dinorwig power station test area [3.5]. The maximum EPR and step voltages were calculated over a zone measuring 200 x 200 m. The injected current magnitude was selected to give a resulting peak source voltage of 200 kV, since the experimental test has been carried out using a voltage source of this magnitude.

The EPR contour map is shown in Figure 3.10. Figure 3.11 shows the step voltage maps produced from computational analysis, which indicate no safety concerns for personnel working at the test cabin.
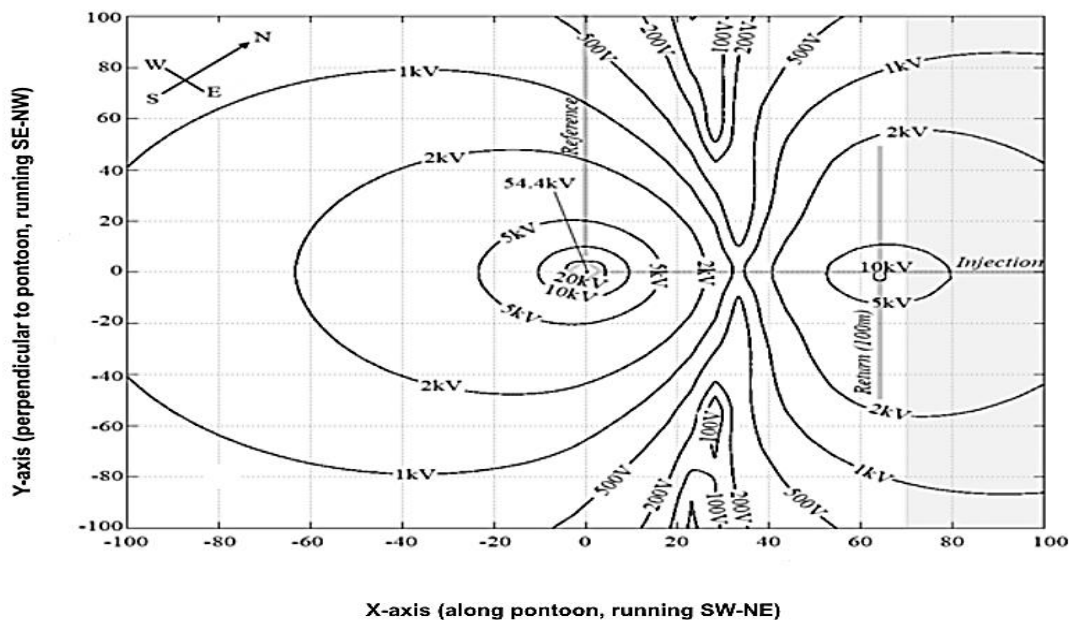
Figure 3.10:Peak EPR Contour Plot for a zone measuring 200 x 200 m ‹centred on the test electrode (5 x 5 grid) [3.5].
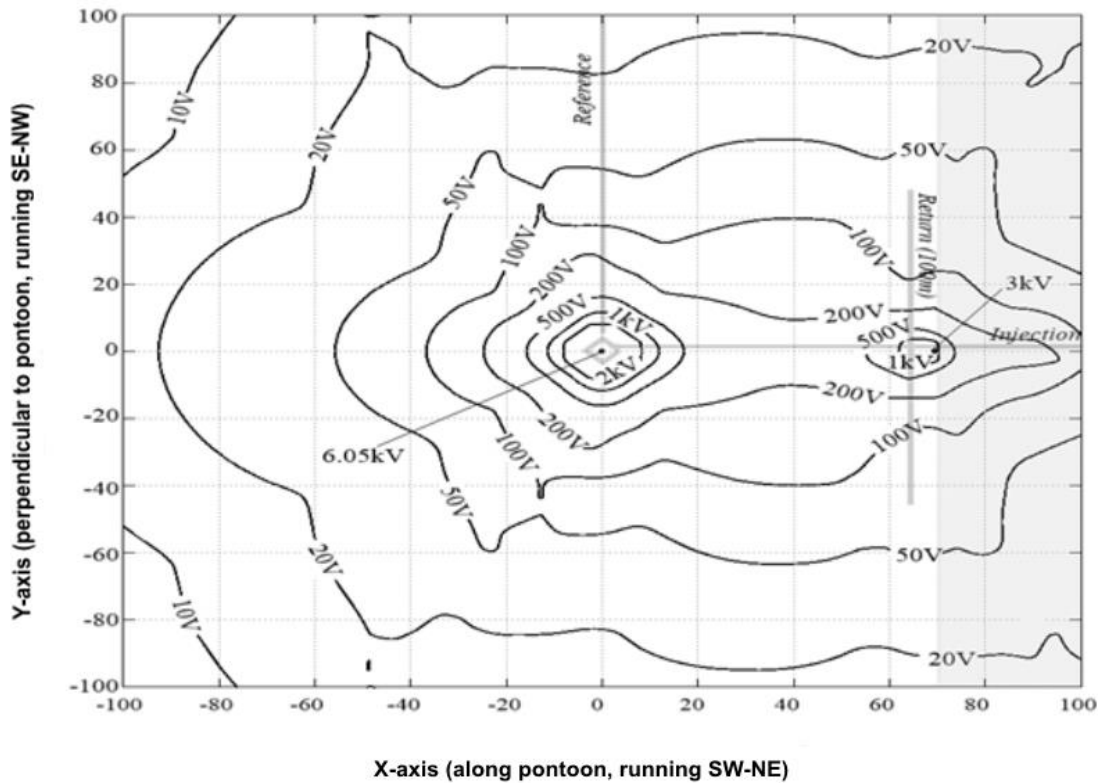
Figure 3.11: Step Voltage Contour Plot for a zone measuring 200 x 200 m, centred on the test electrode (5 x 5 grid) [3.5].

3.4 Resistivity Measurements at Llanrumney fields

The first stage of the earthing system design involves taking the soil resistivity measurements. An understanding of soil resistivity and its variations vertically and horizontally (position in the field and depth) and the factors that affect its value, such as moisture level and temperature, is very important to produce an efficient earthing system design. In addition, good knowledge about the behaviour of soil resistivity enables the electrical engineers to achieve and maintain the desired earth resistance value over the life of the installation with minimum cost and effort.

The resistivity of the soil varies from one location to another because it is highly affected by many factors, such as temperature, grain size distribution and packing of soil, and concentration of dissolved salts in the contained water, and this has a significant effect on

an earthing system's performance [3.6]. Table 3.1 shows examples of typical soil resistivity ranges for different soil types [3.7]. The values are given for normal to high rainfall conditions (500 mm per year to greater values).

Measuring the resistivity of the soil gives details about its physical structure, which may be used in the model. The simplest soil model assumes a single homogenous layer of infinite depth. This single layer representation is usually considered to be overly simplistic, as per standard [3.7], and a more realistic representation is suggested by increasing the number of layers, as shown in Figure 3.12.

Table 3.1: Examples of soil resistivity (Ωm) [3.7]

Type of soil	Typical resistivity range (Ωm)
Clay	5-20
Marls	10-30
Porous limestone	30-100
Porous sandstone	30-300
Quartzites, compact and crystalline limestone	100-1000
Clay slates, salty shales and granite	300-3000
Igneous rock	1000 upwards
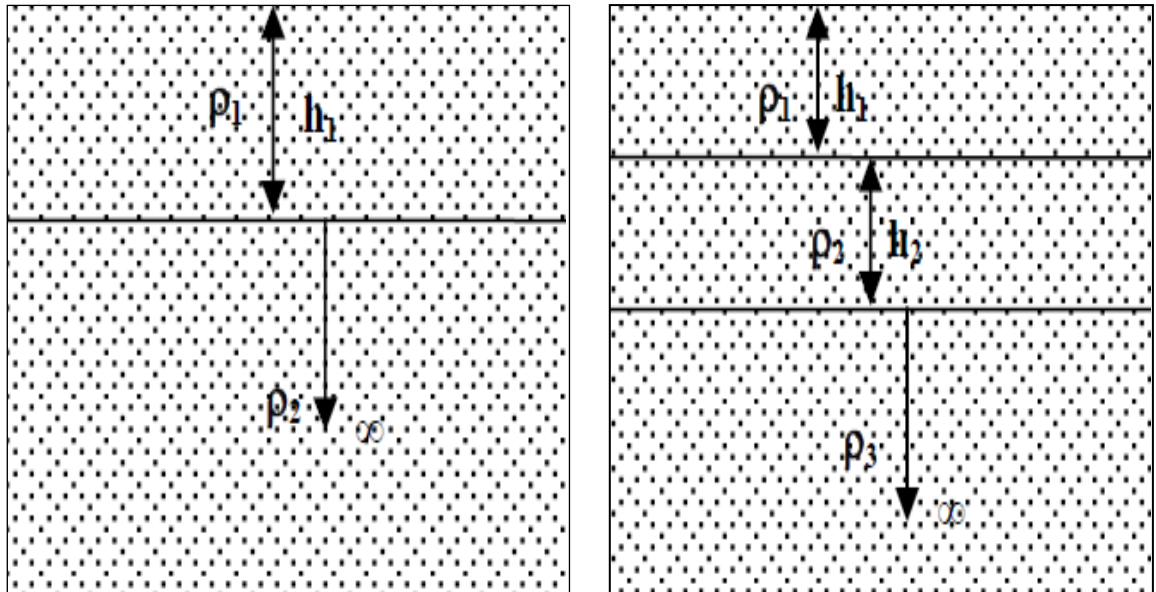
Figure 3.12: Two and three layers soil model representations [3.8]

3.4.1 Resistivity Measurement Set up

A multi-electrode, multi-channel array using the Wenner configuration was utilised in soil resistivity mapping with the cabability of automatic roll-along with coordinate updating in x-direction as shown in Figure 3.13 or y-direction. Soil resistivity measurements were taken along a 240 m profile located about 20 m away from the earthing electrode under test. The ABEM Terrameter SAS 1000/4000 Lund imaging system [3.9] were used to carry out the resistivity measurements by injecting a controlled current (I) between two driven electrodes and measuring the potential difference (V) between two intermediate electrodes. Ohm's law R=V/I is used to calculate the apparent resistance (R). With the Wenner configuration, the four electrodes are equally spaced with distance 'a' used to obtain data. The survey progresses from left to right as shown in Figure 3.14, stepping by one electrode spacing at a time. On completion of the first step, the spacing is increased by an integer multiplier 'N' and the procces is repeated for n=2, 3, 4, … . In this manner, the effective depth of the survey is increased and a 2-D profile of resistivity can be computed.

Soil resistivity measurements were carried out two times. The first survey in February 2015, and the second in October 2015. Figure 3.15 shows the Lund imaging system that was set up and used to carry out the resistivity measurements.
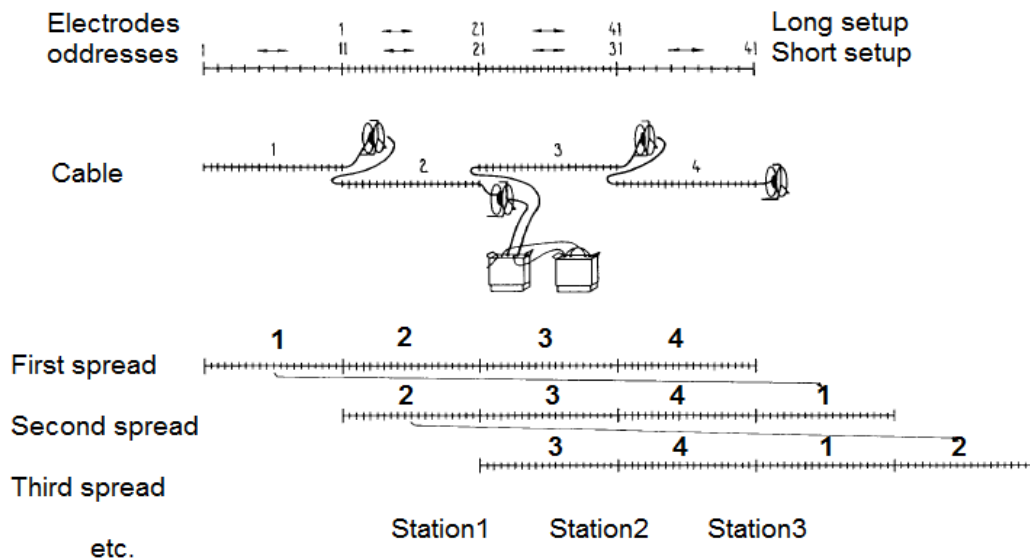
Figure 3.13: Soil resistivity measurements set up using LUND imaging system explain automatic roll-along with coordinate with x-direction [3.9].
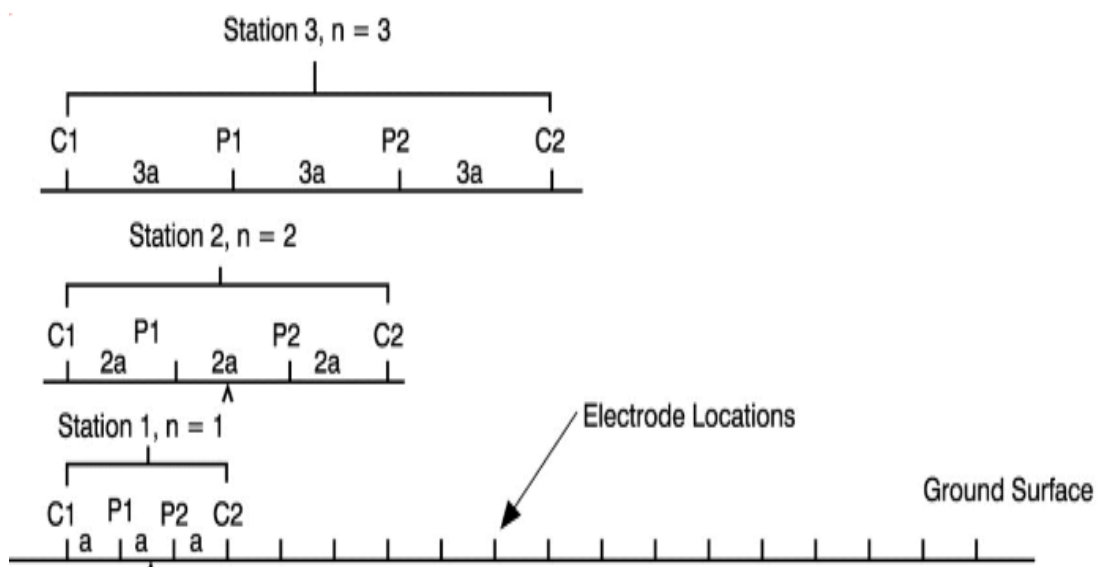
Figure 3.14: Array layout of electrodes for measurements using Wenner configuration.

Figure 3.15: The soil resistivity set up at the earthing system facility at Llanrumney site.

3.4.2 Resistivity measurement survey on 02/02/2015

The configuration shown in Figure 3.15 was used to carry out a soil resistivity survey in February 2015 using a multi-electrode multi-channel array. Figure 3.16 shows the initial pseudo section produced in RES2DINV [3.10], based on the measured apparent resistivity values. By taking the average resistivity of the raw data according to the distance or spacing between the driven electrodes, the average resistivity was obtained, as described in Figure 3.17. Figure 3.18 shows the '2D' inversion soil model [3.11].
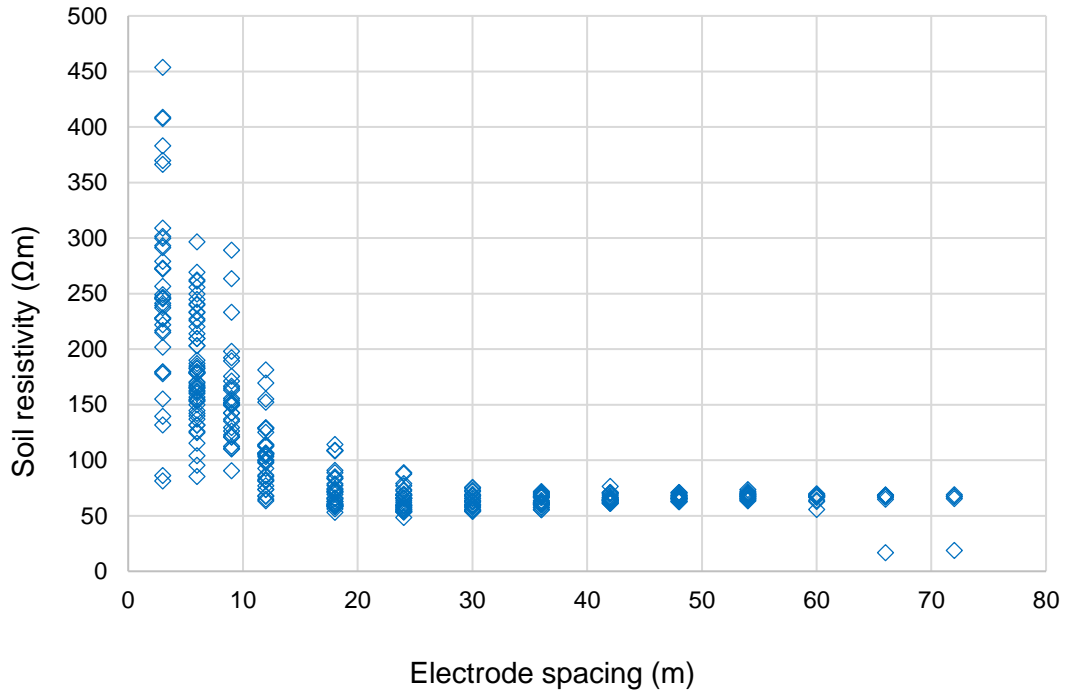
Figure 3.16: Apparent resistivity variation with spacing (02/02/2015)
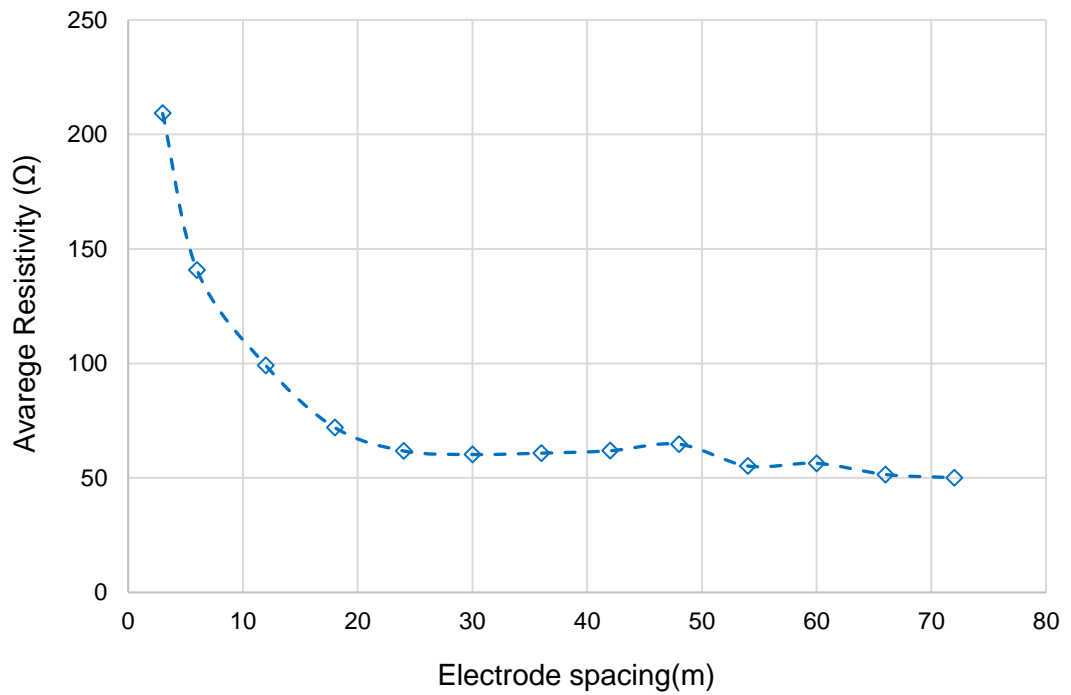
Figure 3.17: Variation of average of apparent soil resistivity with electrodes spacing

(02/02/2015).
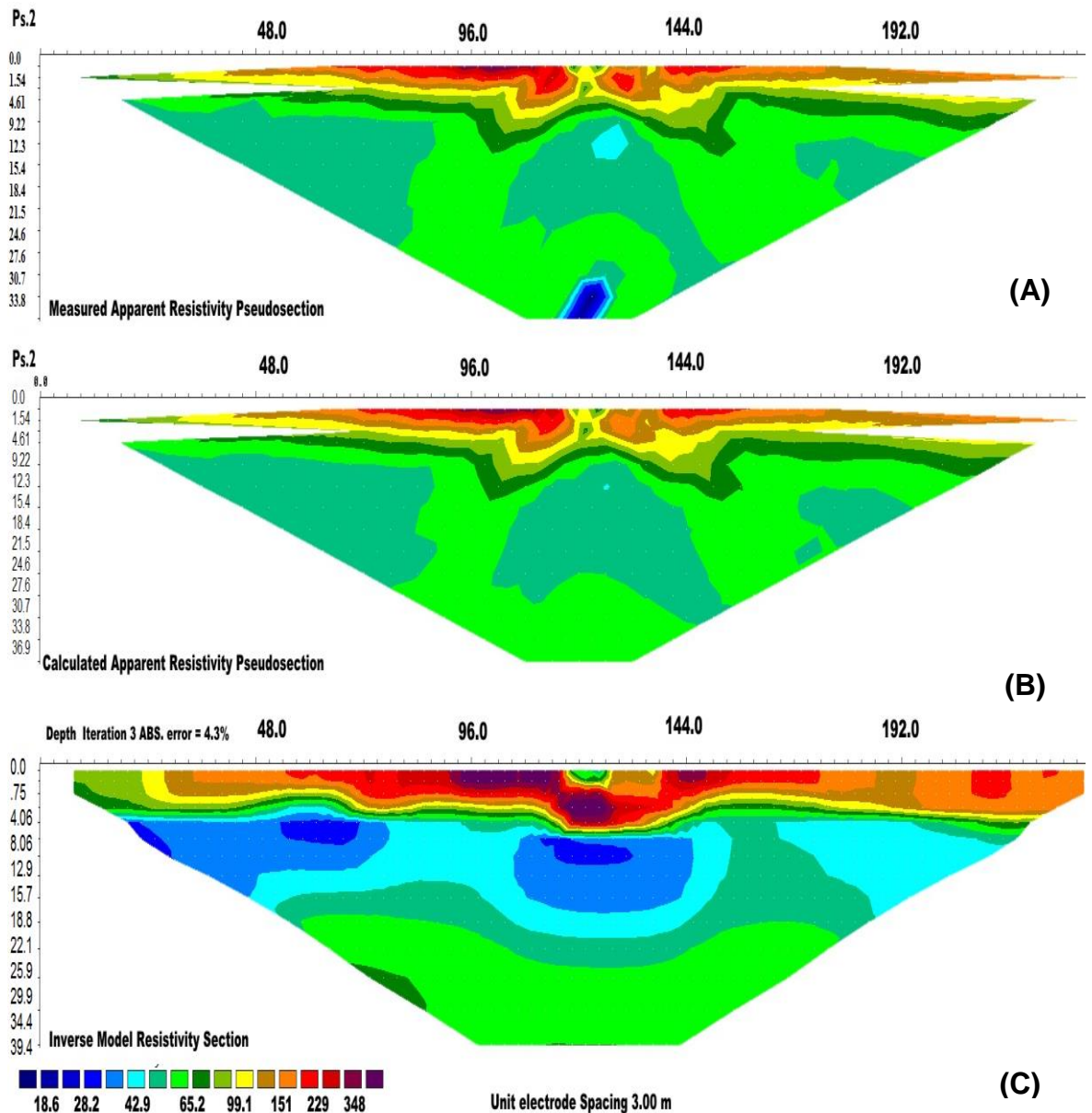
Figure 3.18: 2-D resistivity model for profile near to the test location (02/02/2015).

From Figure 3.18, the results show that, for the 240 m length Wenner array, it is possible to obtain a depth of investigation up to about 40 m. The results indicate that the soil is nonhomogeneous with significant lateral and vertical variations in resistivity. Ignoring the values at the boundary points of the model, it can be seen that there are three main layers, the top layer of higher resistivity in the region of 150 Ωm-450 Ωm of about 10 m thickness (estimated average 200 Ωm). A second lower layer region exhibits a much

lower resistivity (18 Ωm-56 Ωm) where the boundary between this layer and the top layer likely correspond to the local water table (estimated average 30 Ωm). The results indicate that this second layer may be 15 m thick. A further third layer, the lower region, extending to the depth of the investigation limit, indicates a slightly higher resistivity (~50Ωm). Figure 3.18 (C) also indicates regions of very low resistivity at the centre of the resistivity test profile. During the tests, it was noted that this position corresponded to water saturated ground surface conditions. These initial results would suggest a possible 3-layer soil model, as shown in Table 3.2, but for preliminary model simulations, a simplified 2-layer and uniform resistivity model was adopted for simplicity.

Table 3.2: Approximate soil models (02/02/2015)

3-layer model	Top		Middle		Lower	
	Resistivity (Ωm)	Depth (m)	Resistivity (Ωm)	Depth (m)	Resistivity (Ωm)	Depth (m)
	200	10	30	15	50	∞
2-layer model	Upper			Lower		
	Resistivity (Ωm)	Depth (m)		Resistivity (Ωm)	Depth (m)	
	150	10		65	∞	
Uniform model	Resistivity (Ωm)					
	150					

3.4.3   Resistivity measurement survey on 02/10/2015

The second test was carried out in October 2015; using the same configuration presented in the first survey. Figure 3.19 show the apparent soil resistivity values. The average resistivity of the raw data according to the distance or spacing between the driven electrodes is as shown in Figure 3.20.
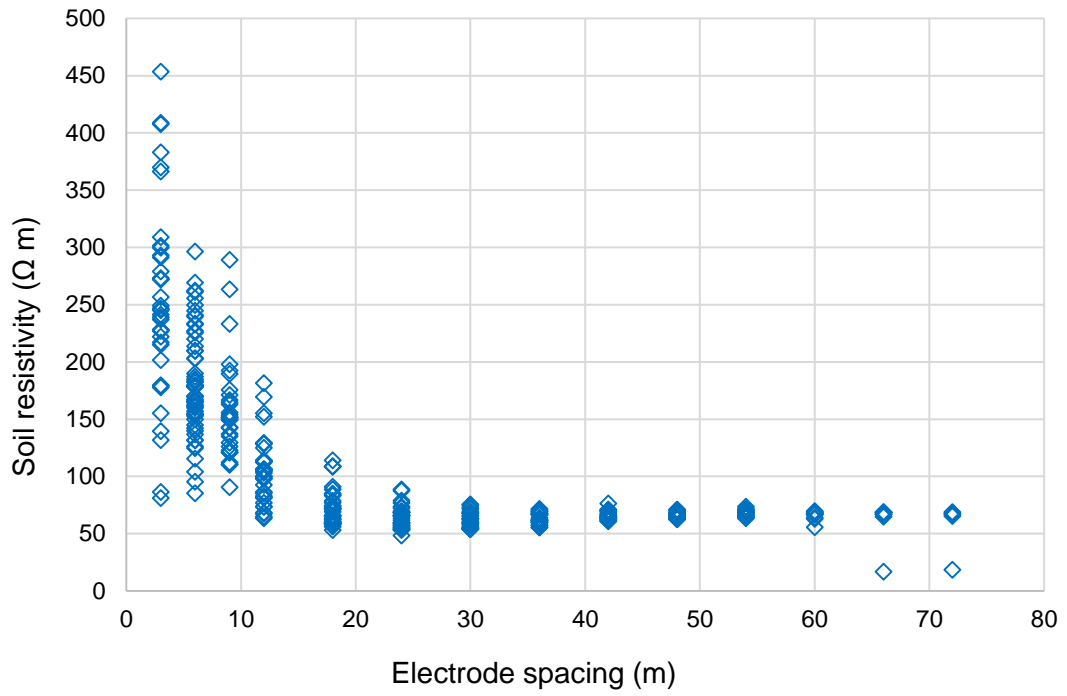
Figure 3.19: Apparent resistivity variation with spacing (02/10/2015).
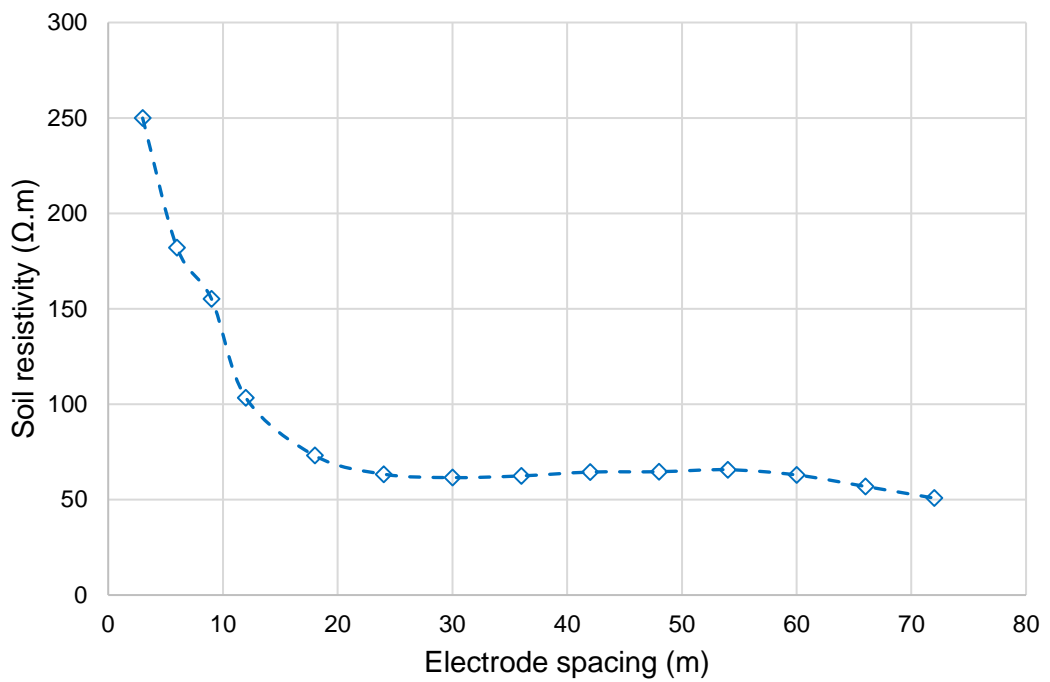
Figure 3.20: Variation of average of apparent soil resistivity with electrodes spacing

(02/10/2015).

The raw data were used to produce 2-D inversion soil resistivity model as shown in Figure 3.21. The results indicate that the soil resistivity values are changeable with depth and field location, as described in the previous test. However, in this test, the seasonal effect can be observed. The test was carried out after a period with little rainfall, and consequently, the position of the water table is less clearly defined. In addition, the soil resistivity value is slightly higher. A 3-layer soil model is suggested according to the results, as shown in Table 3.3.
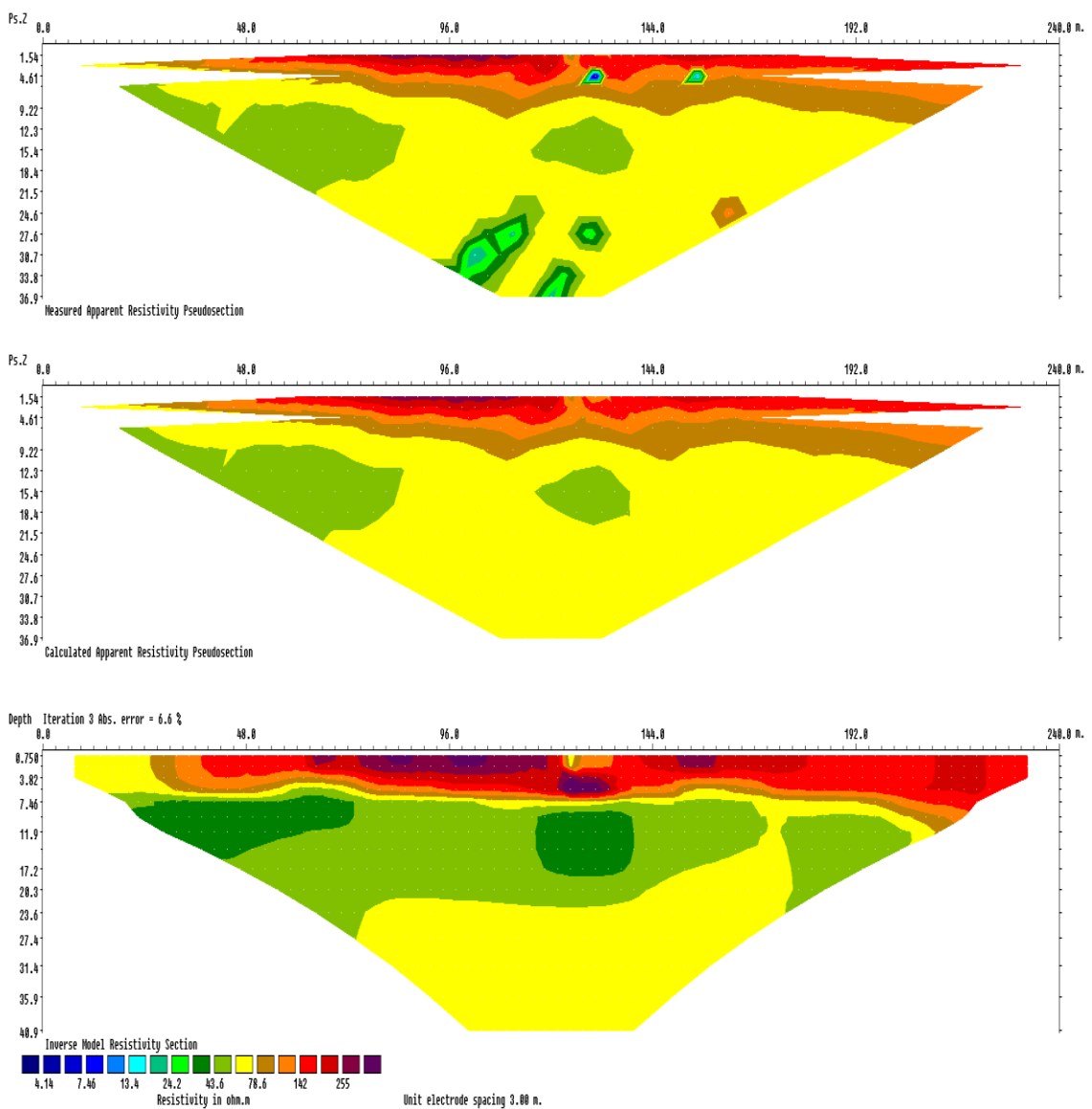
Figure 3.21: 2-D Resistivity model performed on 2 October 2015.

51

Table 3.3: Approximate soil models (02/10/2015)

3-layer model	Top		Middle		Lower	
	Resistivity (Ωm)	Depth (m)	Resistivity (Ωm)	Depth (m)	Resistivity (Ωm)	Depth (m)
	250	10	40	15	70	∞
2-layer model	Upper			Lower		
	Resistivity (Ωm)	Depth (m)		Resistivity (Ωm)	Depth (m)	
	200	10		70	∞	
Uniform model	Resistivity (Ωm)					
	200					

3.5 Conclusion

As described in this chapter, the new location of Cardiff University's earthing test facility at Llanrumney was prepared to carry out high voltage tests on practical earthing electrodes. Different types of practical earthing systems, such as single rod, horizontal electrode and ring earthing systems were installed at Llanrumney test site. Soil resistivity measurements were performed in the approximate earth electrode locations, and inversion software was applied to produce the 2D resistivity survey images, which helped to estimate the value of soil resistivity as a function of depth. A considerable variation in soil resistivity according to both the position in the field and with depth was observed from the results. The soil resistivity values obtained are used in numerical simulation models in Chapters 4 and 5 of this thesis.

Extensive computer simulations using CDEGS were undertaken in advance of high voltage tests to assess the safety requirements for the personnel and for people in the vicinity of the test area. According to the British standard BS EN 50522 [3.2], the results showed that both step and touch voltages in the vicinity of the test electrode area were at a safe level.

In addition, the Dinorwig test site was prepared for high voltage measurements by constructing a floating pontoon with a 5 m x 5 m earthing grid immersed in the water at a depth of 0.8 m suspended in cross section at the end of the pontoon. Earlier preparatory simulations had been performed in 2014 to achieve the safety requirements. Contour maps for EPR and step voltages were generated. The results indicate that there were no safety concerns for the personnel in the test cabin.

CHAPTER FOUR: CHARACTERISTICS OF EARTH ELECTRODES UNDER HIGH FREQUENCY AND TRANSIENT CONDITIONS: NUMERICAL MODELLING

4.1 Introduction

The earthing systems of electrical power system plays a crucial role in human safety and the protection of plant and ancillary equipment. Lightning current has a variable frequency spectrum; this leads to different characteristics of the earthing impedance. Such impedance can be resistive, inductive or capacitive depending on the frequency and geometry of earth electrode. Earthing DC resistance is an important factor in understanding the behaviour of the earthing system and is defined as the ratio of the voltage to the current Equation (4.1):

$$R = V/I \tag{4.1}$$

Where I is the current at the injection point of the test object, and V is the potential difference between the injection point and the remote or reference point, which is positioned in a perpendicular direction to the injection point.

In the case of frequency spectrum, both voltage and current are phasor quantities. Therefore, Equation (4.1) can be rewritten as Equation (4.2):

$$Z(j\omega) = V(j\omega)/I(j\omega) \tag{4.2}$$

where Z (jω), is the earthing impedance or the complex harmonic impedance [4.1]. In general, two intervals can be seen in the behaviour of the earthing system under variable frequency energization.

> 1. Low frequency (LF): the earthing impedance is frequency independent and its value is equal to the DC resistance.

2. High frequency (HF): the earthing impedance is frequency dependent and its value is either higher or lower than DC resistance.

High-frequency characteristics rely on the phase angle between voltage and current. Therefore, an inductive or a capacitive effect or both will dominate the behaviour of the earthing system at high frequency. The transition point from the low-frequency characteristics to the high-frequency characteristics is named "characteristic frequency" or "cut-off frequency", and it depends on the geometry of the electrode and the soil resistivity [4.2] and [4.3].

In this work, detailed numerical simulations of vertical and horizontal earth electrodes are reported. The results describe the frequency response of the simulated earthing electrodes in different soil resistivity media (10, 100, 1k, and 10k) Ωm and relative permittivity was considered (1-50), and the effect of electrodes length on harmonic impedance over a range of frequencies from (DC up to 10 MHz). In addition, details are provided of the earth potential rise in the electrode itself and on the earthing surface in its vicinity. Finally, the influence of conductor segmentation in the model is quantified.

4.2 Frequency Response of a Vertical Electrode

4.2.1 Development a Computer Model, with Variable Rod and Soil Medium Parameters

Computer models were set up in CDEGS-HIFREQ [4.4] to obtain the frequency responses of vertical earth rods buried in homogeneous soil. A range of rod lengths was considered using multiples of 1.2 m to represent the standard available lengths in practice. The dimensions and properties of the simulated rods are shown in Table 4.1 together with the assumed electrical properties of the soil. The simulations were carried out by injecting 1A AC current at the top of 0.5m downlead as shown in Figure 4.1. Earthing impedance magnitude, phase angle at the injection point and surface ground potential are calculated.

Table 4.1: Dimensions and properties of simulated vertical rod and soil medium.

Earth rod properties		Down lead	Medium properties
Material:	Copper	Copper	Resistivity: 10^1, 10^2, 10^3, and 10^4 Ωm
Resistivity:	1.7×10^{-8} Ωm	1.7×10^{-8} Ωm	
Length (m):	1.2, 2.4, 3.6, 4.8, and 6	0.5	
Diameter(mm):	14	35	Relative permittivity and permeability =1
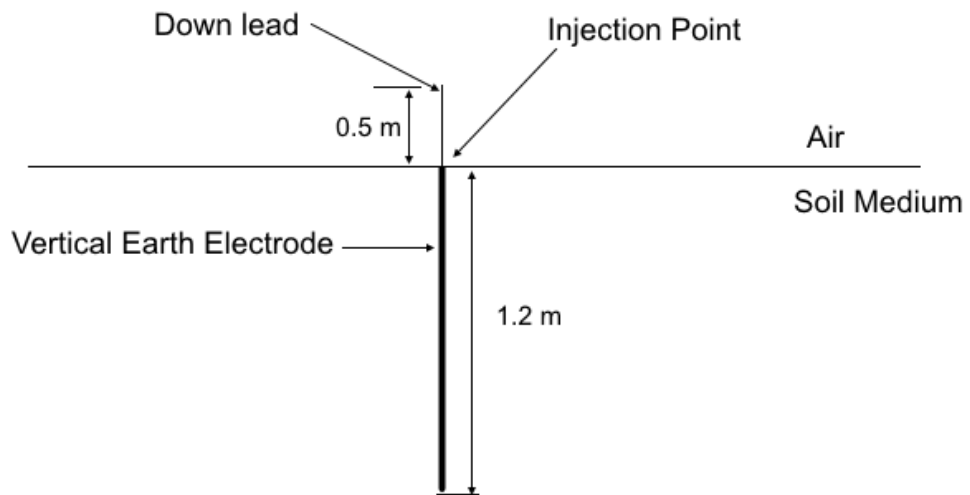
Figure 4.1: Simulated vertical rod configuration.

4.2.2 Effect of Soil Resistivity

Figure 4.2(a) shows the frequency response of a 1.2 m vertical earth rod. For a low soil resistivity of 10 Ωm the earthing impedance exhibited approximately a constant value of 7.4 Ω with DC frequency and the rise begins with a frequency increase to reach about 40Ω at 10MHz. A similar response is obtained with 100 Ωm soil resistivity. However, the earthing impedance magnitude was ten times that with 10 Ωm soil resistivity. Such a response is explained by the inductive effect. Although the earth rod shows a similar response with low and with high frequency, the characteristic frequencies are different and are related to soil resistivity value. With high soil resistivity (1 and 10 kΩm), the simulated earth rod exhibited a capacitive behaviour. Therefore, a reduction in the impedance value was observed. The earthing impedance for 1kΩm varied from 743 Ω with DC frequency to 533 Ω at 10MHz. At 10 kΩm soil resistivity, the capacitive effect was evident, and the impedance magnitude decreased exponentially with frequency. The reduction in the impedance magnitude of 10 kΩm compared with that of 1k Ωm was much greater. The frequency response of the simulated rod showed good agreement with the published work [4.5] and [4.6].

In addition, the impedance angle had the same variation of earthing impedance over the frequency and was greatly affected by the soil resistivity value, as shown in Figure 4.2(b). At low frequency range and low soil resistivity (10, 100 Ωm), the impedance angle is positive and almost constant. The angle starts to increase remarkably after the characteristic frequency, which, as explained, depends on the soil resistivity value to reach 66° and 25° with 10, and 100 Ωm respectively. However, with high soil resistivity and low-frequency current lead voltage by a small and almost constant angle up to the cut-off frequency. Above this frequency, the angle starts to increase with the increase in frequency to reach 36° and 80° with 1 and 10kΩm) respectively.
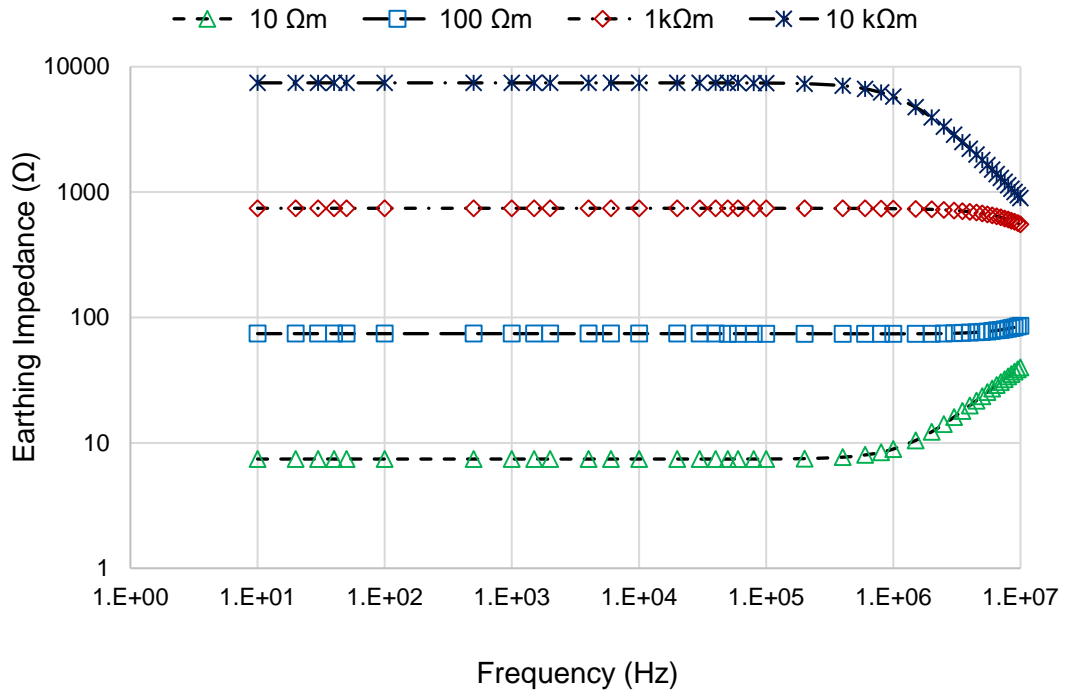
(a) Impedance of simulated earth rod.
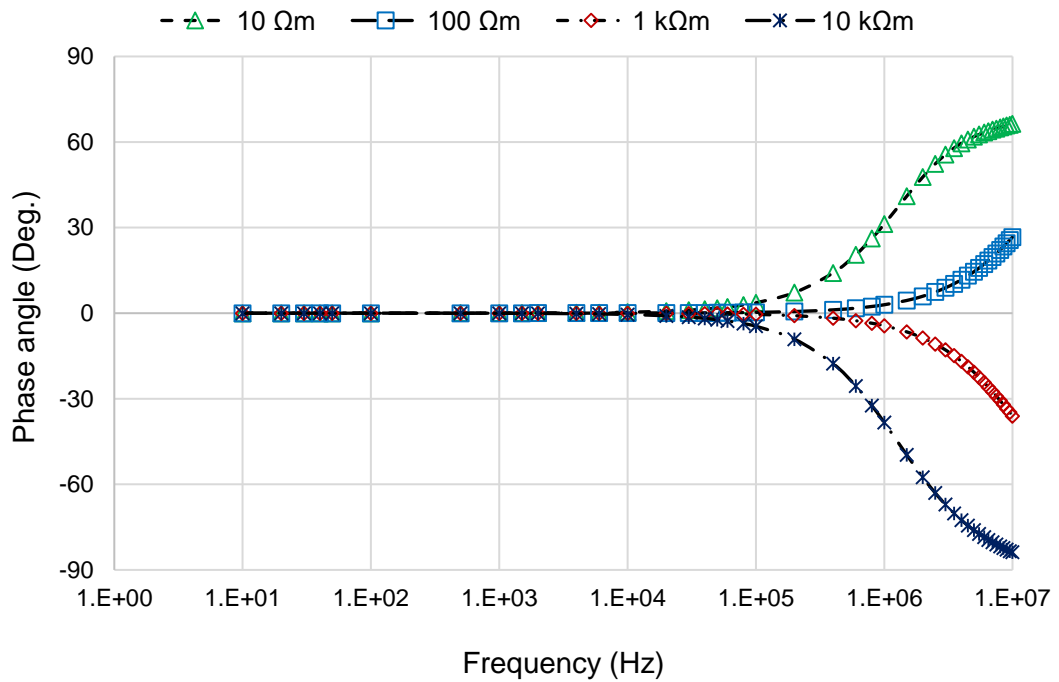
(b) Phase angle of simulated earth rod.

Figure 4.2: Frequency response of a 1.2 m (14 mm diameter) vertical rod for different soil resistivities (ε_r=1).

4.2.3 Effect of Soil Permittivity

The frequency response of vertical earth rods was examined under different values of soil relative permittivity to quantify the effect of permittivity on the performance of the earthing system. Simulations were conducted for 1.2 m and 6 m earth rods with soil resistivities of 10 and 10000 Ωm and a soil relative permittivity range 1-50, over frequencies DC to 10MHz.

The variation of permittivity at low frequency did not show the marked effect on the impedance magnitude of the earthing rod for both conditions of soil resistivity as shown in Figure 4.3. However, at high frequency, the impedance exhibited a reduction as the permittivity increased, that reduction becoming more evident at high soil resistivity.

In addition, the expected characteristic frequency occurred earlier as permittivity increased. At high soil resistivity (10kΩm) and a relative permittivity of 50, the earthing impedance decreased up to 8MHz, after which an oscillation occurred. At high soil resistivity, it was observed that the phase angle exhibited an oscillation over a relative permittivity range (15-50). The higher the relative permittivity is, the earlier oscillation occurs.

Figure 4.4 shows the simulation results of a 6 m earth rod. The effect of soil permittivity becomes more evident as the earth rod length increases. At low resistivity soil medium of 10 Ωm, the impedance decreased as the permittivity increased from 1 to 15; after that, the soil permittivity had no major effect on the performance of the earthing system. However, at high resistivity soil conditions of 10kΩm, the characteristic frequencies occurred at 30, 20 and 10) kHz when the permittivity changed as 15, 30 and 50 respectively. After those frequencies, a reduction in impedance magnitude was expected up to a specific frequency depending on the permittivity value; then, an oscillation occurred and continued over the rest-energised frequency. The phase angle was conducted as well over different values of

permittivity for a 6 m earth rod. At low frequency, current leads voltage by a small and almost constant angle. However, at high frequency, the high permittivity showed a greater increase in the phase angle up to a specific frequency, and then the oscillation occurred.
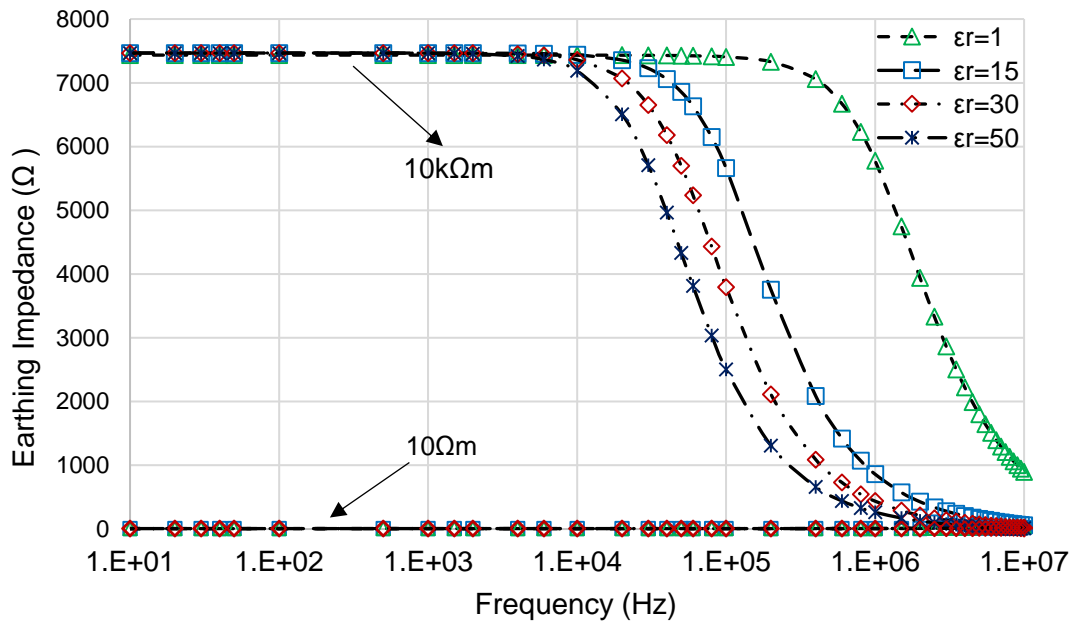
(a) Impedance of simulated earth rod.
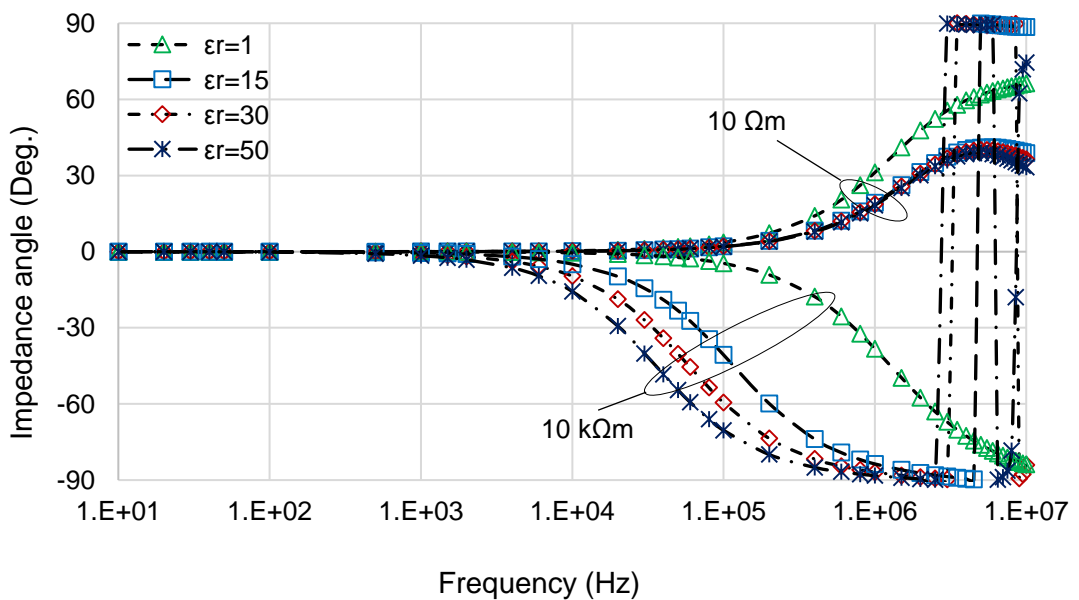
(b) Phase angle of simulated earth rod.

Figure 4.3: The effect of permittivity on the frequency response of a 1.2 m vertical rod.
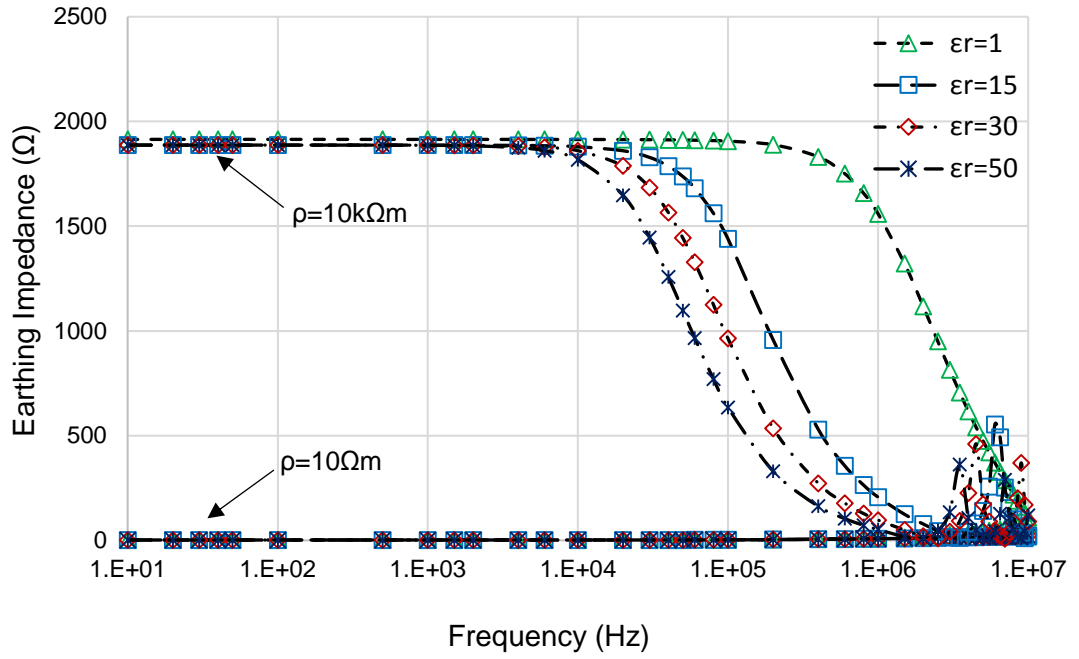
(a) Impedance of simulated earth rod.
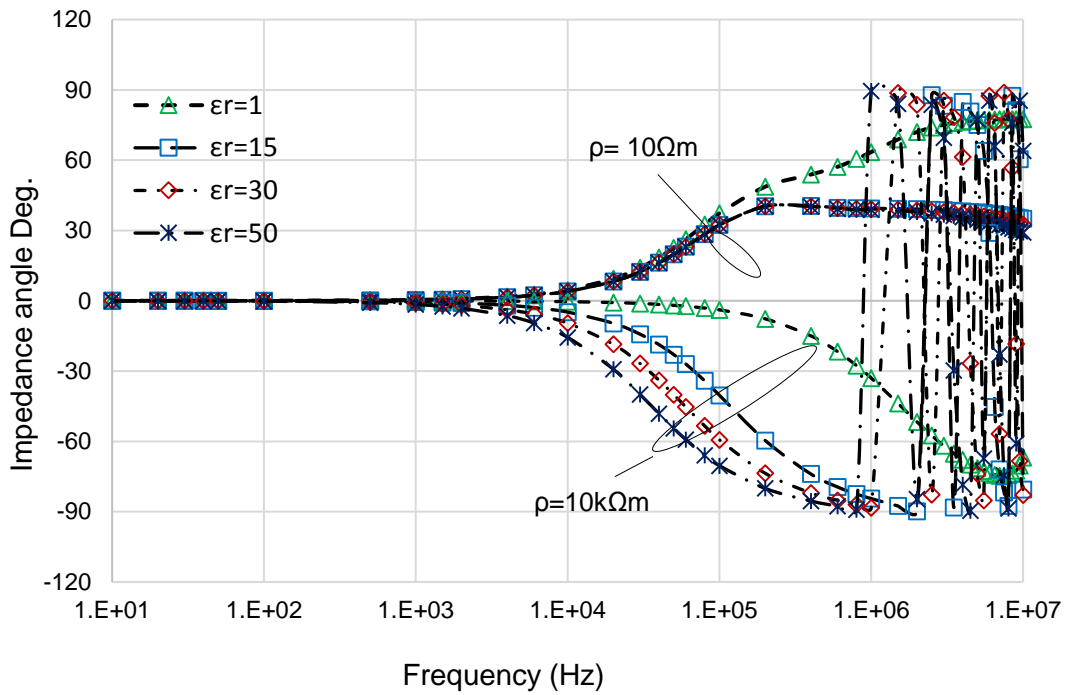
(b) Phase angle of simulated earth rod.

Figure 4.4: Effect of relative permittivity on the frequency response of a 6 m vertical rod.

4.2.4   The Effect of Earth Electrode Length

A key factor governing the performance of the earthing system is the length of the electrode. Figures 4.5 (a, b, c, and d) show the effect of simulated electrode length on EPR, which is defined as the maximum electrical potential that an earth electrode may attain relative to a distant earthing point assumed to be at the potential of remote earth, under different soil medium conditions. The EPR at the feed point of the simulated rod exhibited a reduction in its value with the increase in electrode length at low and high frequencies. Therefore, the longer earth rod gives a greator reduction in EPR at the injection point. Although the same frequency response can be seen for the rods buried at the same soil resistivity medium, however, the characteristic frequency, which is defined as the transition point in the electrode response from low frequency to high frequency behaviour, is smaller for the longer electrode at the same soil resistivity value [4.7]. Therefore, the electrode length is selected to achieve satisfactory earthing system performance.
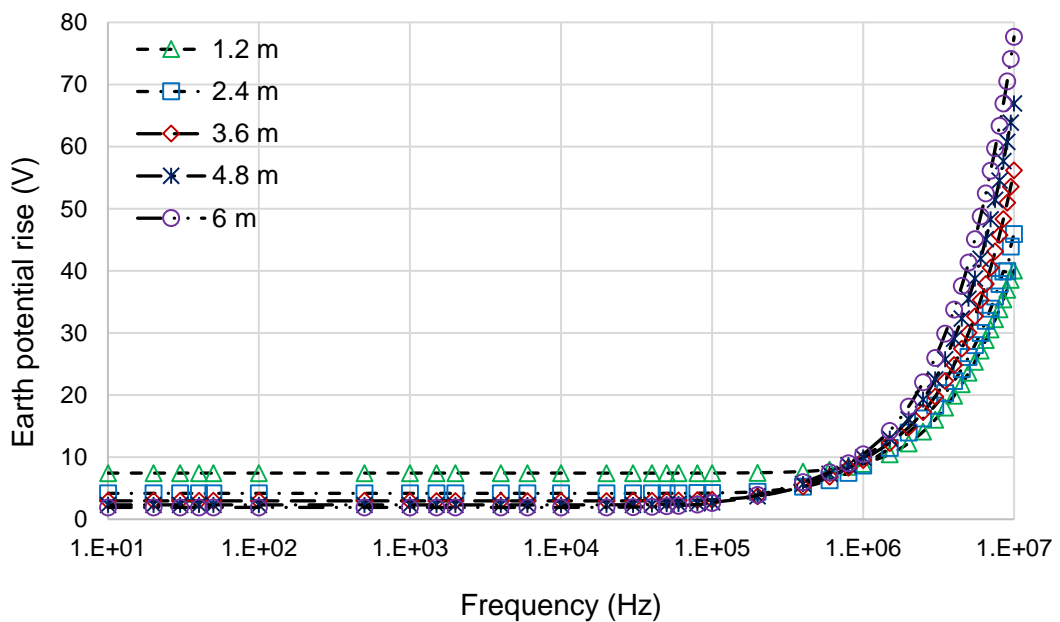
(a) 10Ωm Soil resistivity
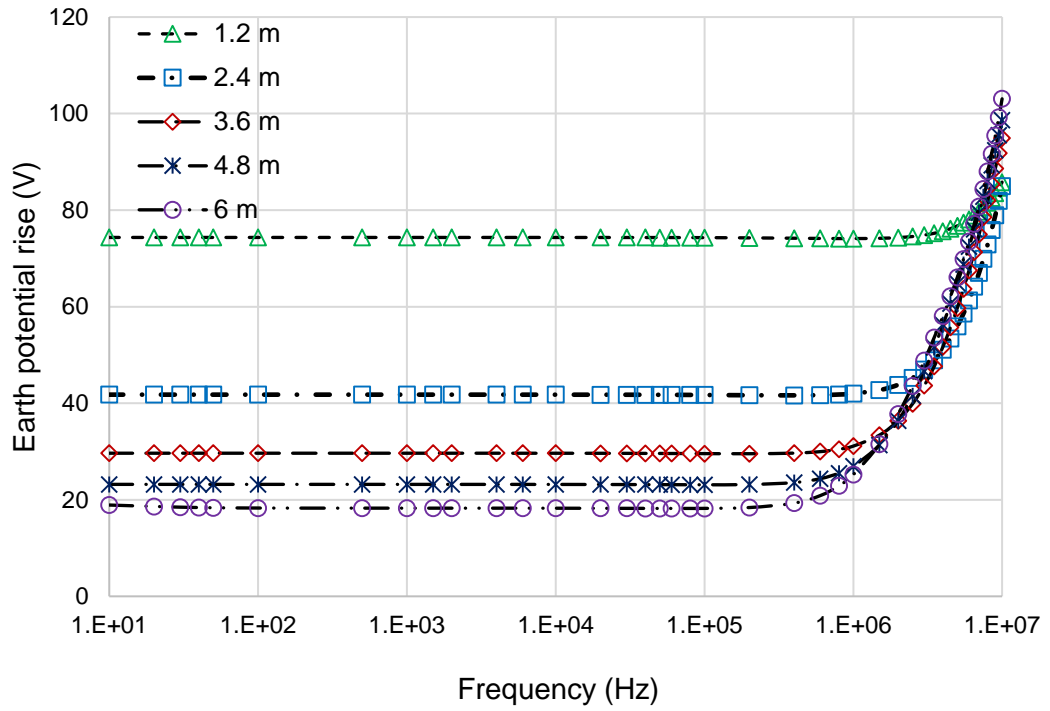
(b) 100Ωm Soil resistivity
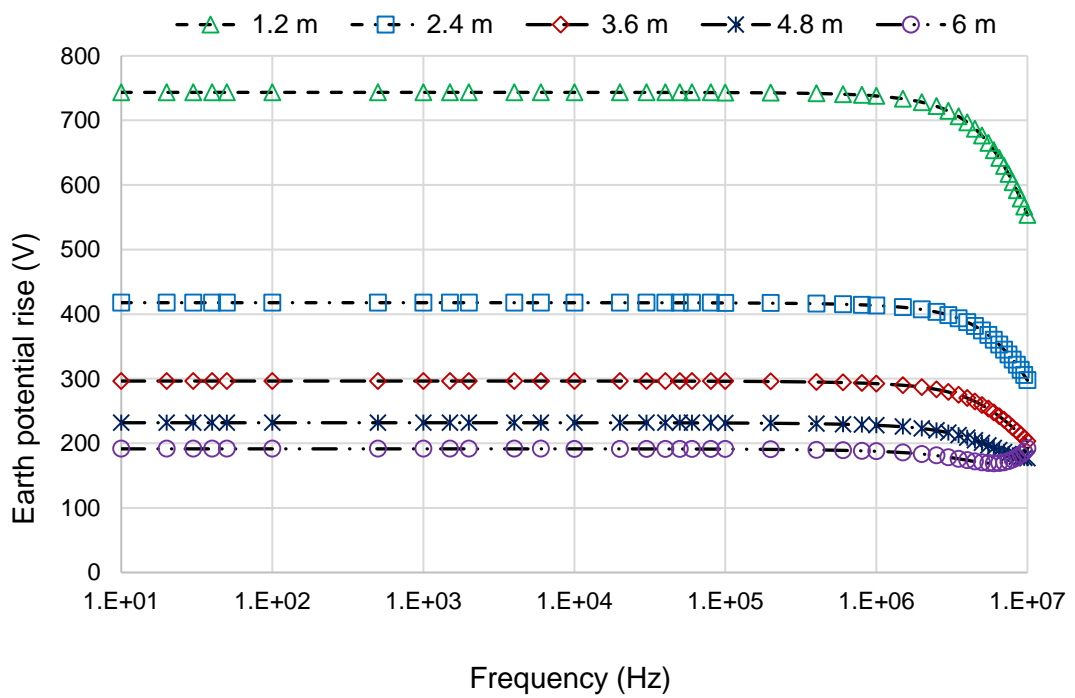
(c) 1kΩm Soil resistivity
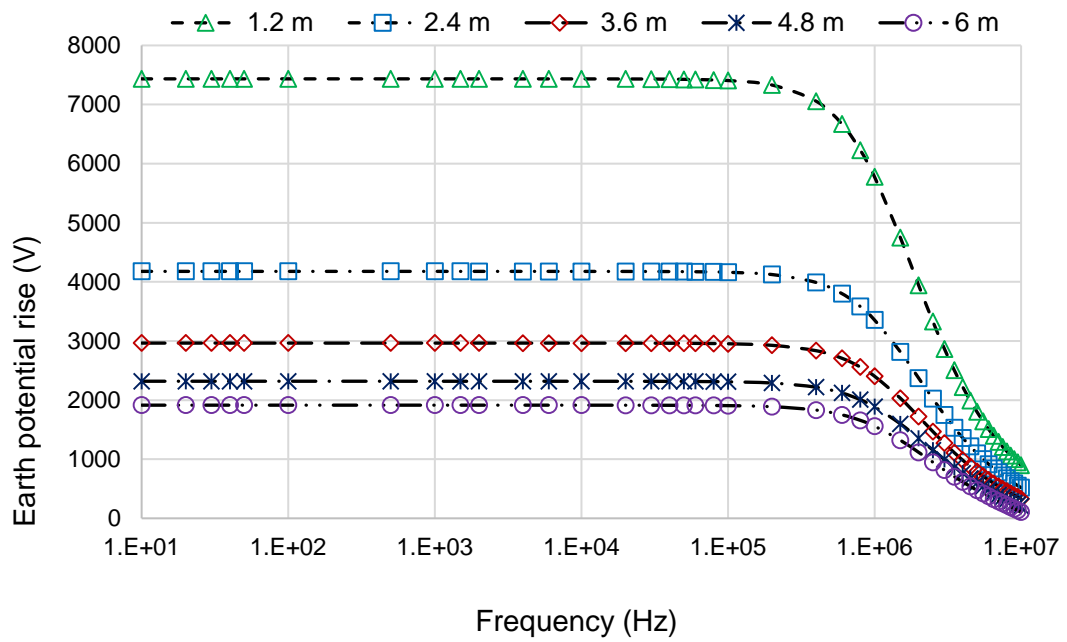
(d) 10kΩm Soil resistivity

Figure 4.5: Effect of earth rod length on the earth potential rise of vertical rod for different soil resistivities (ε_r=1).

4.3   Frequency Response of Horizontal Electrode

Figure 4.6 represents the setup used to obtain the frequency response of a horizontal earth electrode using CDEGS-HIFREQ. A 100m electrode buried under 0.5 m depth was simulated over a range of frequencies and soil resistivities. The dimensions and properties of the simulated rod are shown in Table 4.2.
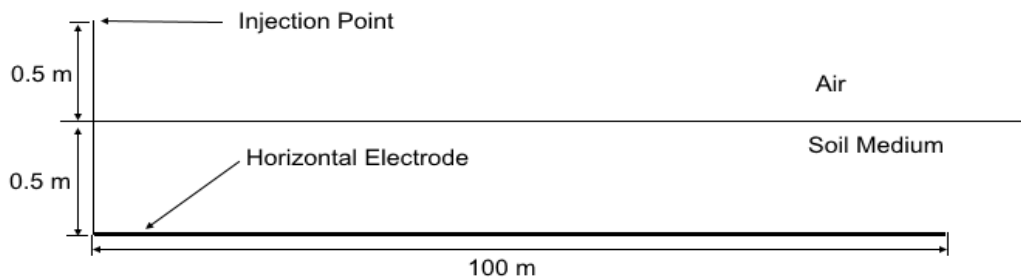
Figure 4.6: Simulation arrangements of the horizontal electrode.

Table 4.2: Dimensions and properties of simulated horizontal electrode and soil medium.

Earth rod properties		Down lead	Medium properties
Material:	Copper	Copper	Resistivity: 10^1, 10^2, 10^3, and 10^4 Ωm
Resistivity:	1.7×10^{-8} Ωm	1.7×10^{-8} Ωm	
Length (m):	100	0.5	
Diameter(mm):	14	35	Relative permittivity and permeability =1

4.3.1   Effect of Soil Resistivity

Figure 4.7 (a) shows the predicted earthing impedance magnitude for a 100 m horizontal rod over a range of frequencies from DC to 10 MHz in different soil media. As estimated, at low soil resistivity, the horizontal rod exhibits the same behaviour as the vertical rod over a range of frequencies. At low frequency, the impedance value is equal to the DC resistance up to the characteristic frequency, which is much lower compared with a vertical electrode for the same resistivity values. After that frequency, the impedance magnitude shows an increase due to inductive effects. However, for high soil resistivity media (1, and 10kΩm), the frequency response of the earth rod can be classified into three intervals:

1. Resistive behaviour up to a characteristic frequency: this depends on soil resistivity. In this range, $Z = R_{DC}$.

2. Inductive behaviour: this starts above the characteristic frequency. In this interval, the inductive effect occurred and dominated up to 100 kHz for 1kΩm and 1MHz for 10kΩm.

3. Capacitive effect: in this range, with 1kΩm soil medium, the capacitive effect occurred and dominated the remaining range of frequency.

However, with 10kΩm soil resistivity, an oscillation occurred over the rest of the frequency range. Figure 4.7 (b) shows the phase angle of the simulated rod. The phase angle for low soil resistivity medium demonstrates how the inductive effect occurred and showed a marked increase with an increase in frequency. In addition, with 1kΩm soil resistivity, the capacitive effect caused a reduction in phase angle. However, in the high soil medium, the electrode exhibited a capacitive effect trend accompanied by a resonant effect on the phase angle.
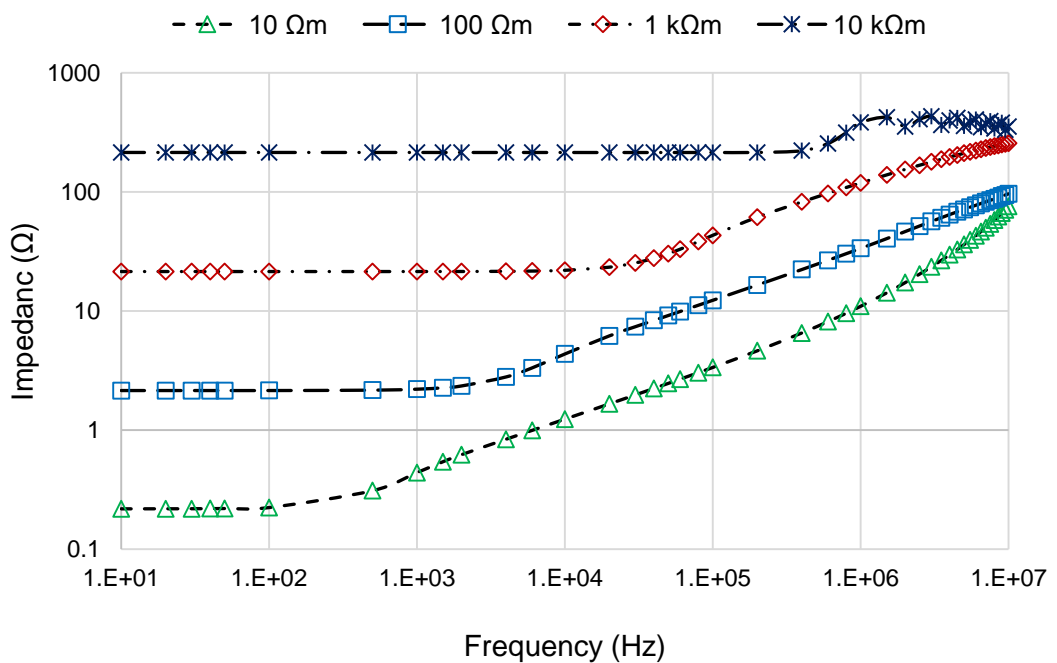
(a) Impedance of the simulated electrode
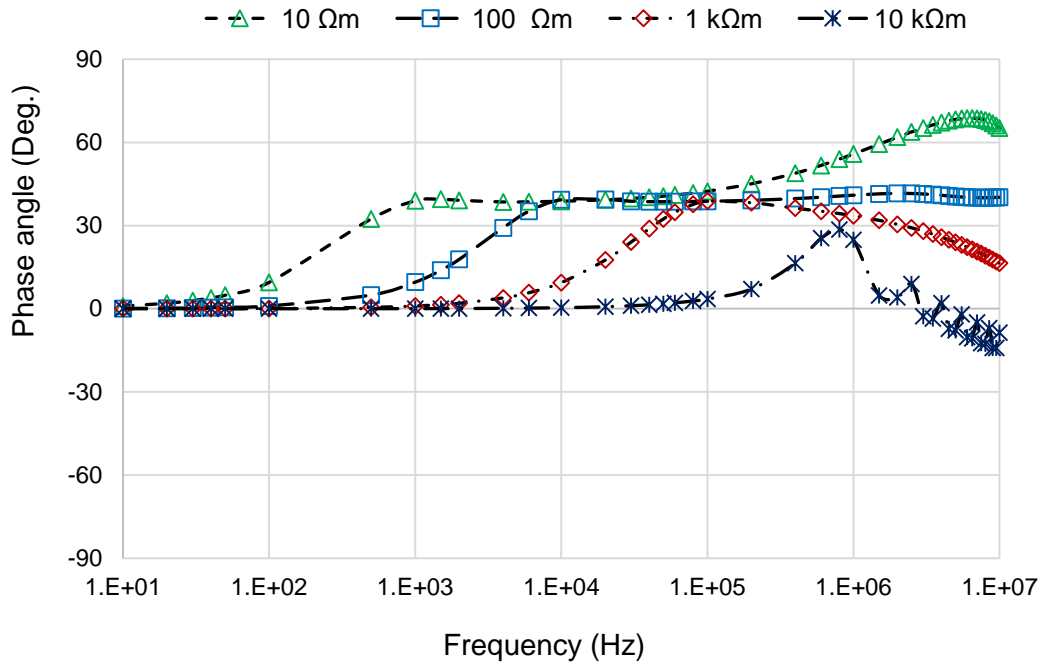
(b) phase angle of the simulated electrode

Figure 4.7: Frequency response of 100 m horizontal electrode for different soil resistivities

($\varepsilon\_r=1$).

4.3.2 Effect of Soil Permittivity

Figure 4.8 shows the effect of soil permittivity on 100 m horizontal earth rod impedance magnitude and phase angle over the frequency range DC to 10 MHz at low and high soil resistivity medium ($\rho= 10\Omega$m, $100k\Omega$m). The variation in relative permittivity has no marked effect on the impedance value and phase angle of the rod at low soil resistivity medium, as shown in Figure 4.8. At high soil resistivity condition ($\rho= 10k\Omega$m) and low frequency, the performance of the earthing rod did not exhibit any response changes to permittivity variation up to the threshold frequency. Above that frequency, increasing the relative permittivity from 1 to 50 resulted in a significant reduction in the impedance magnitude and phase angle due to the capacitive effect. This decrease continued for a short frequency interval, after which an oscillatory behaviour was observed.

4.3.3 Effect of Earth Electrode Length

The frequency response of horizontal earth rods of different lengths was predicted for low and high homogeneous soil resistivity media 10Ωm and 10kΩm respectively. A range of electrode lengths was considered (10 m, 50 m, 80 m and 100 m) to study the behaviour of horizontal rods. At low soil resistivity and low frequency, the impedance magnitude is equal to DC resistance, and this value depends on electrode length, as seen in Figure 4.9 (a). The impedance magnitude exhibits a reduction as the electrode length increases up to a specific length, termed the effective length. After that, there is no benefit in further increasing the rod length [4.8]–[4.11]. In addition, the length of the electrode affects the characteristic frequency, as mentioned previously. Therefore, the shorter electrode gives a much higher earthing impedance magnitude and characteristic frequency. However, at high frequency, the inductive effect dominates the behaviour, and the earth electrode shows the same frequency response for different lengths.

Figure 4.9 (b) illustrates the effect of length on the frequency response of the rod over a range of frequencies by examining the impedance angle of different rod lengths in low soil resistivity. The effect of length in high soil resistivity is much greater compared with the low soil resistivity medium, as shown in Figure 4.9 (c). The horizontal electrode exhibits a significant reduction in impedance magnitude when the length increased from 10m to 50m. However, that reduction gradually decreased as the rod length increased up to the effective length. Therefore, in high soil resistivity medium, the longer rod gives a low value of earthing impedance. Figure 4.9 (d) explains the impedance angle behaviour with different rod lengths. It is shown that the phase angle oscillated between positive and negative values due to the interaction between the capacitive and the inductive effect. The oscillation start point depends on the length of the electrode.
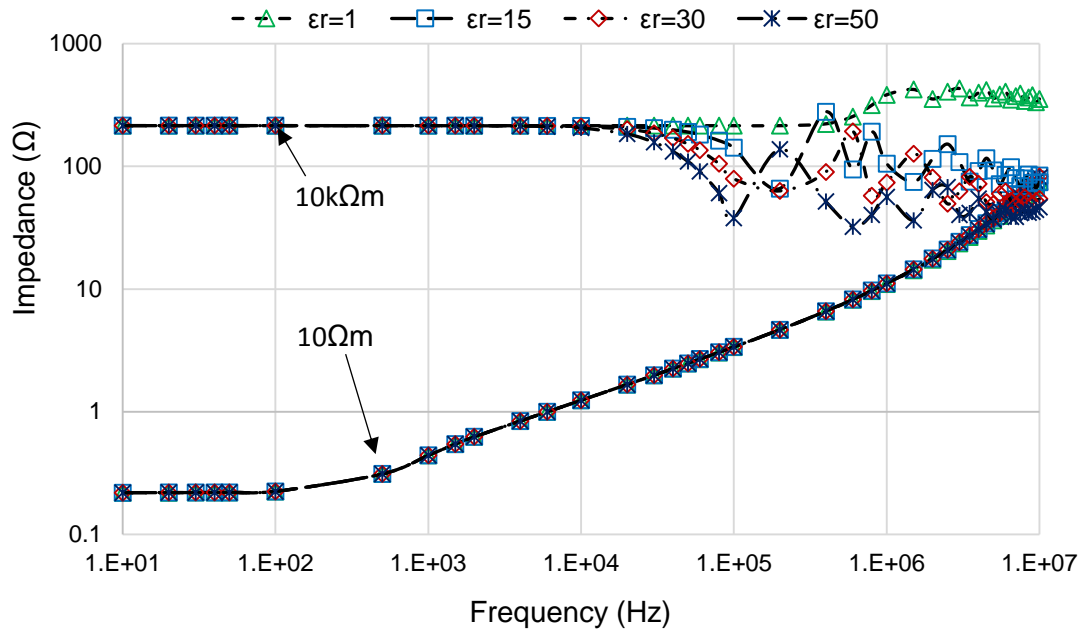
(a) Impedance of the simulated electrode
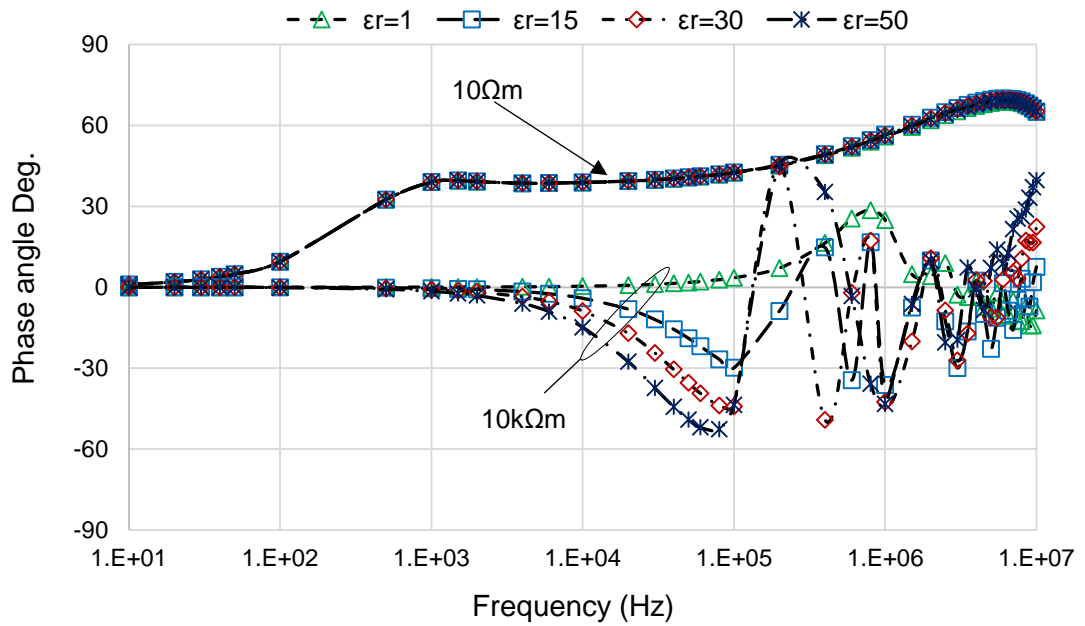
(b) Phase angle of the simulated electrode.

Figure 4.8: Effect of relative permittivity on the frequency response of 100m horizontal electrode
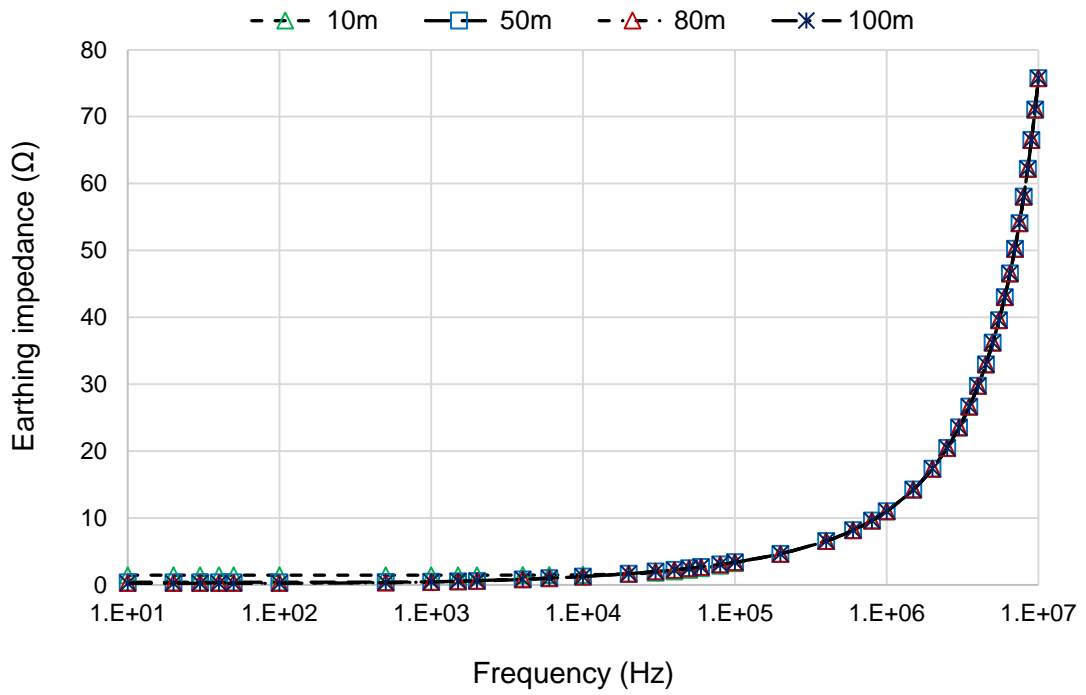
(a) Impedance of the simulated electrode at 10Ωm Soil resistivity
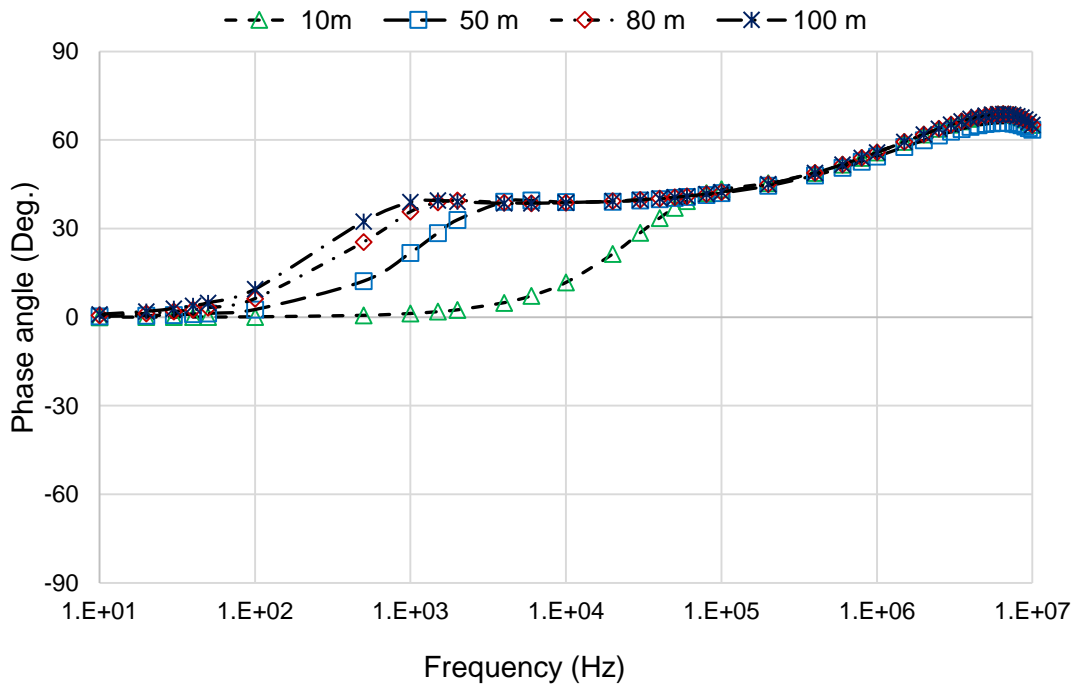
(b) Phase angle of the simulated electrode at 10Ωm Soil resistivity
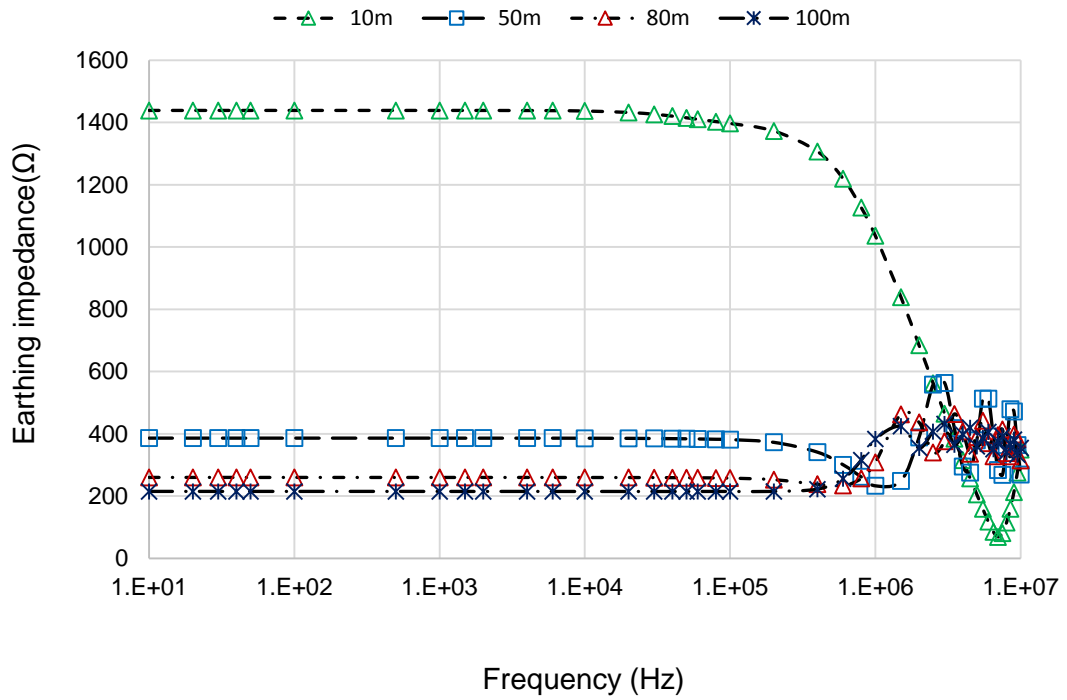
(c) Impedance of the simulated electrode at 10kΩm Soil resistivity
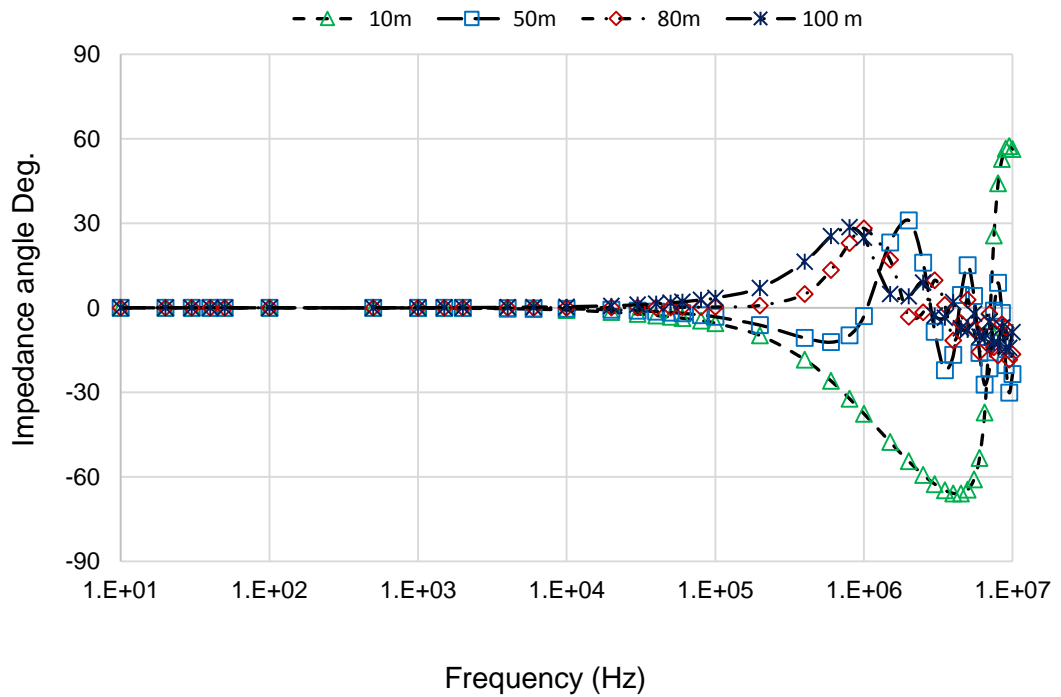
(d) Phase angle of the simulated electrode at 10kΩm Soil resistivity

Figure 4.9: Effect of earth rod length on the computed impedance of a 100 m horizontal electrode for different soil resistivities (ε_r=1).

4.4 Voltage distribution along profile

When electric power systems parts, such as substations and transmission lines, are subjected to lightning or are energised with a variable frequency source, the majority of the current is dissipated to the earth via the earthing system, causing an EPR in the earthing objects and the surrounding area. The EPR was investigated under different conditions for both vertical and horizontal earth rods to examine its change about the factors that affect the rate at which the energy is dissipated, such as soil resistivity, electrode length, and the amount of energized frequency. In addition, the potentials at the ground surface along a 100m profile were computed.

Figures 4.10 (a, and b) illustrate the potential fall with distance along the profile away from the injection point. The rate of change of potential is highest near the injection point and start to decrease along the profile away from the injection point. A higher soil resistivity medium exhibits a higher EPR and potential for the same current and frequency. These high EPR and potentials generated step and touch voltages magnitudes that are dangerous to humans in the vicinity. In the case of a lightning strike and variable frequency energization, soil resistivity value plays a major role in an electrical potential gradient along the earthing electrodes. This leads to a potential difference being generated, which will cause a current to flow in all the conductive bodies in the working zone. Therefore, many publications have focused on DC resistance reduction. Resistance reduction can be achieved by using a low resistivity material [4.12]-[4.14] or by applying various techniques [4.15]-[4.18].   As discussed before, the length of the earthing rods affects the behaviour of the earthing system by changing the earthing impedance magnitude and characteristic frequency. At the same frequency and soil resistivity, the longer electrode is exhibited higher rate of ESPR fall-off, because it can dissipate a significant amount of energy to the earth.
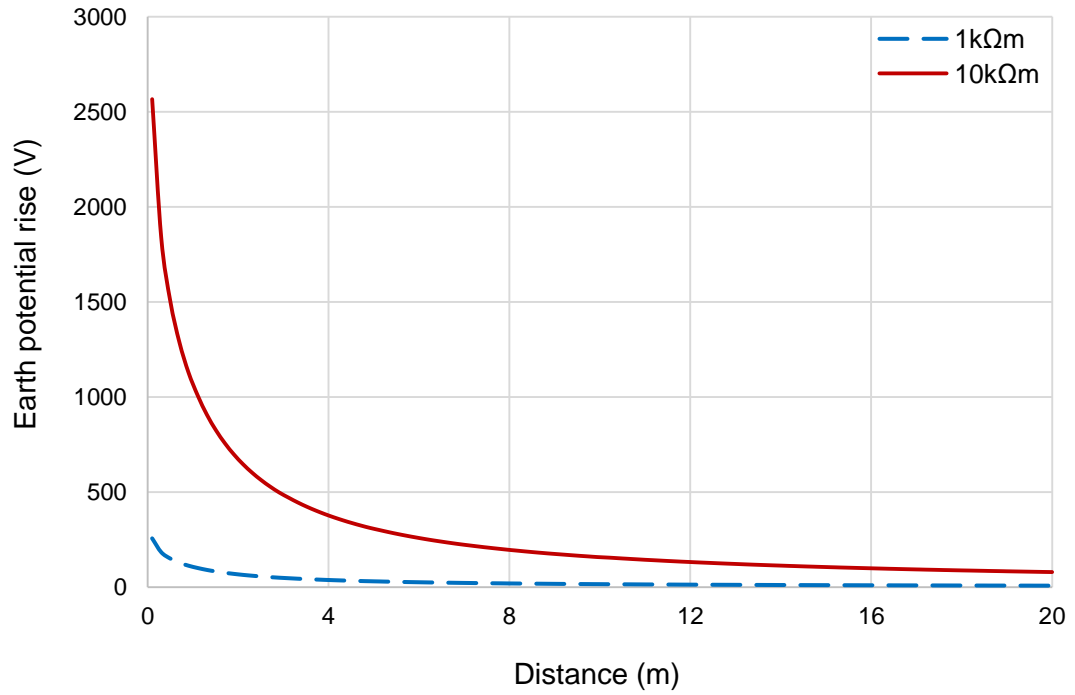
(a) 2.4m Vertical rod
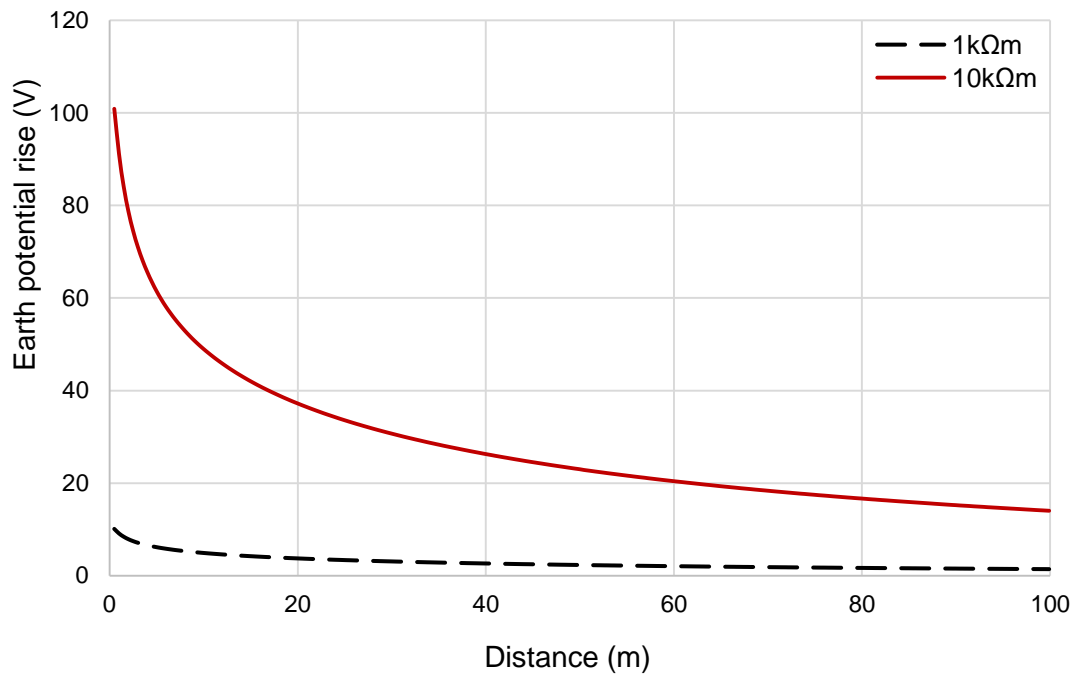
(b) 100m Horizontal electrode

Figure 4.10: Voltage distribution along surface profile.

4.5 Segmentation

A simulation study has been conducted using the commercially available computer software CDEGS HIFREQ to examine the effect of segmentation on homogenous soil resistivity (ρ=10 Ωm) for different lengths of the vertical earth rod and a 100 m horizontal rod. HIFREQ computer software assumes that the earth rod is a cylindrical conductor or it converts into the equivalent cylindrical conductor. Then the cylindrical conductor is divided into a number of segments, and a suitable number of segments should be chosen to obtain accurate earthing impedance calculation. The model segmentation must satisfy two conditions:

1. Thin wire approximation should be such that the segment length must be greater than five times the electrode radius, to ensure uniform current distribution over each segment.

2. The segment length should be less than 1/6 of the wavelength (λ), which is expressed according to [4.4] in the following equation.

$$\lambda \ (in \ soil) = 3160 \ \times \ \sqrt{(\rho/f)} \tag{4.3}$$

Where ρ is the soil resistivity and f is the frequency. Within these constraints, the number of segments used in the model has a significant effect on the predicted impedance. A set of simulations implemented on the rods over 50Hz, 1kHz, 100kHz, and 1MHz energisation frequency considered a different number of segments. Figure 4.11 illustrates the variation in the earthing impedance magnitude of the 1.2 m vertical rod in relation to the chosen number of segments. The maximum allowable number of segments for a 1.2 m earth rod with respect to thin wire approximation is 34 segments. Therefore, the frequency response is predicted over 2 to 30 segments. From Figure 4.11, it is clear that there is an increase in impedance magnitude as the number of segments increased over

high-frequency energization. However, at low frequency up to 100 kHz the impedance decreased as the number of segment increases. Therefore, a small number of segments is suggested for vertical electrodes to obtain good accuracy. That agrees with the published work in [4.19]-[4.20]. For the horizontal earth electrode, increasing the number of segments results in a more accurate earth impedance calculation, particularly in high-energised frequencies, as shown in Figure 4.12.
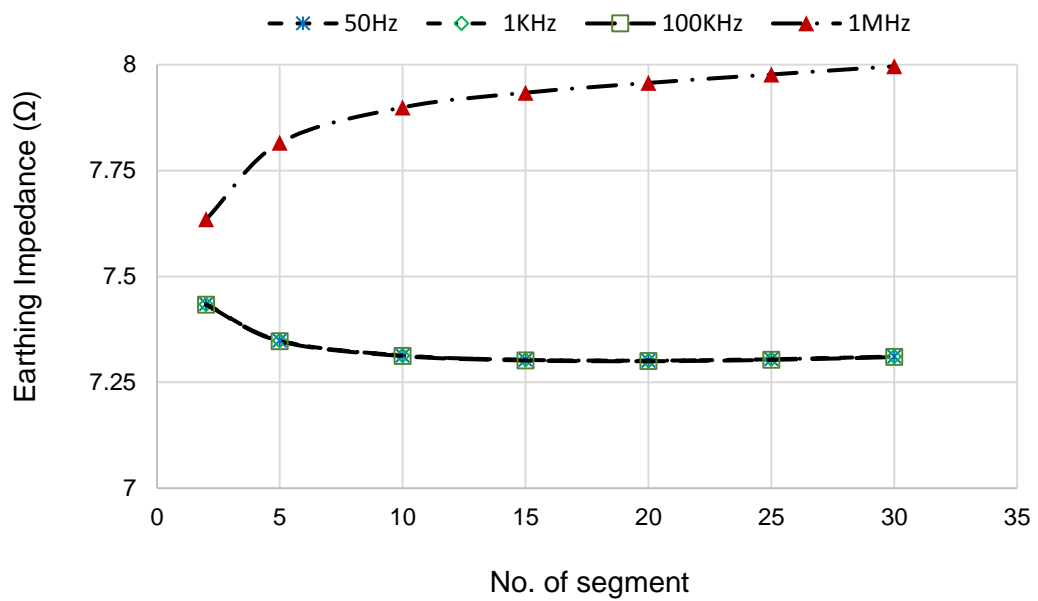
Figure 4.11: The Influence of Segmentation on Frequency Response of 1.2 m Vertical Rod.
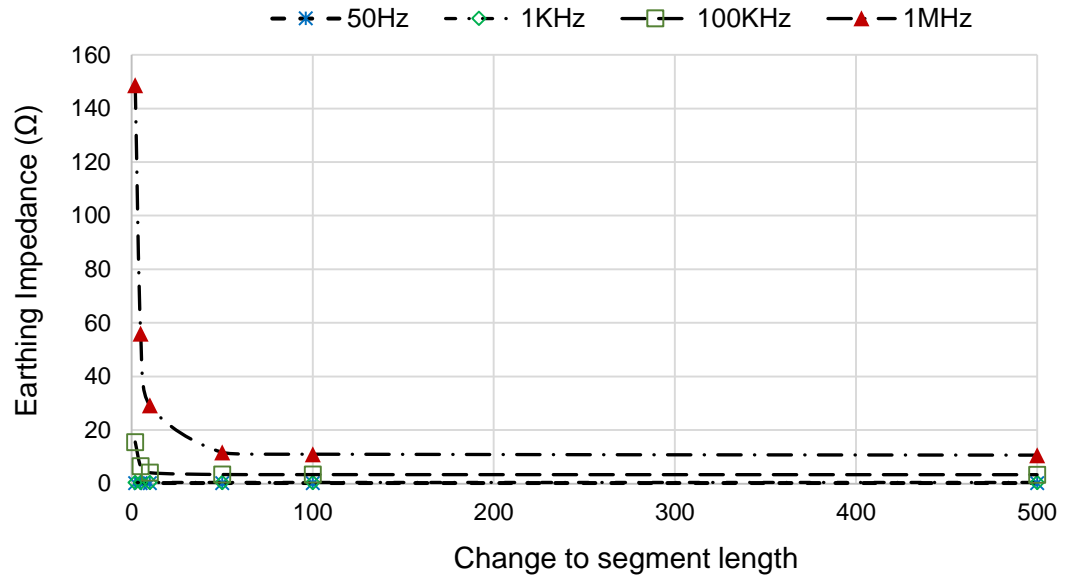
Figure 4.12: The influence of segmentation on frequency response of 100m horizontal electrode.

4.6   Conclusions

This study introduces detailed numerical simulations of rod electrodes, using a software programme (HIFREQ) to examine the main characteristics of frequency response taking into account the influence of soil medium resistivity, soil permittivity and electrode length. These studies implemented vertical and horizontal earth rods considering a range of frequencies from DC to 10 MHz and soil resistivity values of 10, 100, 1000, 10,000 Ωm, and with soil permittivity values between 1 and 50.

The investigations have confirmed the well-known low-frequency response of the earthing system for different rod configurations. The impedance magnitude at low frequency is equal to DC resistance over a range of spectra up to the characteristic frequency. Not only have soil resistivity and permittivity a significant influence on the characteristic frequency values, but they affect the length of the electrode as well. Above this frequency, the studies have shown the effects, including an upturn in impedance with frequency in low resistivity soil (inductive effects). Conversely, in high resistivity soil,

the capacitive effects become influential at high frequency, which causes a fall off (downturn) in impedance. In addition, the investigations have been implemented over a range of permittivity values. At low frequency, the variation in relative permittivity no longer affects the performance of the earthing system for different soil resistivity conditions. However, at higher frequencies and for a high soil resistivity, the impedance magnitude of an electrode tends to decrease with an increase in frequency, which could be attributed to the capacitive effects. The impedance also exhibits an oscillation under the same conditions.

In these studies, a range of electrode lengths has been simulated to predict the effect of electrode length on the impedance magnitude and EPR in the vicinity area. As expected, the rod impedance and EPR decrease with increases in the length of the rod up to the effective length. After that, there is no benefit in increasing the electrode length.

The effect of segmentation of the earth electrode has also been investigated by varying the number of segments of the simulated electrode. Then, the corresponding electrode earth impedance was compared. It was found that the variation in the number of segments affects the calculated response significantly. Therefore, the results suggest there should be a small number of segments for a short vertical electrode. However, for the horizontal electrode, more accurate earth impedance calculations were obtained particularly in high-energised frequencies by increasing the number of segments as much as possible, taking into consideration the thin wire approximation assumption.

CHAPTER FIVE: CHARACTERISATION OF EARTH ELECTRODES SUBJECTED TO IMPULSE AND VARIABLE FREQUENCY CURRENTS

5.1   Introduction

Earthing systems are an integral part of power systems. The main purpose of power system earthing is to maintain reliable operation and provide protection for personnel and apparatus during fault conditions. In order to obtain the best design of an electrical system that can protect power system installations against anomalous events, it is useful to analyse the behaviour of earthing systems when they are excited by impulse and variable frequency currents.   In earthing systems, different types of electrodes - vertical, horizontal, and grid - are usually used. The purpose of using vertical earth rods in earthing systems and lightning protection systems are either as main earth electrodes or as reinforcing electrodes to help in earth-impedance reduction and improve high frequency and transient performance [5.1].

Numerous studies on the performance of grounding systems have been published, and several models are proposed to analyse and predict the impulse and high frequency behaviour of earthing systems [5.2] and [5.3]. Experimental and theoretical studies explain how grounding systems show a variation in their characteristics according to the soil composition, the electrode geometry, the spectrum of frequency, current wave-shape and the magnitude of the injected current [5.4]-[5.8]. In addition, grounding system electrodes are designed to achieve a low ground impedance and should be capable of dissipating high currents. Under these conditions, the potential differences arising between exposed metallic earth parts and the ground should be limited to avoid danger to both human life and damage to or failure of equipment. Field-based and theoretical studies have been carried out to investigate the behaviour of horizontal earth electrodes under variable frequency and impulse energisation [5.9]-[5.14]. Recent publications have

considered the frequency dependence of soil parameters on the behaviour of grounding systems at high frequency and transient conditions [5.15]-[5.20].

In this chapter, an experimental set-up at the Advanced High Engineering Research Centre at Cardiff University is presented, including a vertical earth electrode of 1.2 m length and 14 mm diameter installed at the centre of 30 m diameter ring electrode to ensure a uniform radial current distribution [5.21]. Both DC and AC low voltage and variable frequency tests were conducted, and low voltage and high voltage impulse tests were performed. The results were compared with the frequency response of the same tested electrode computed by simulation software with a different value of soil resistivity and relative permittivity to understand how the soil parameters affect the behaviour of the system. The study describes tests carried out on a new field-based test configuration comprising an industry standard horizontal earth electrode energised with a low voltage AC variable frequency and a low voltage impulse. The tested electrode and the test circuit were modelled in the computational software program (HIFREQ/FFTSES-CDEGS).

In addition, controlled large-scale investigations of a practical earthing system were implemented at the Dinorwig power station in North Wales. The earthing grid was immersed in homogenous conducting medium energised by a DC, low voltage AC variable frequency and low and high voltage impulses. The measured DC resistance, AC impedance and impulses resistance are compared with the results obtained by numerical modelling

5.2   Vertical Earth Electrode

5.2.1   Description of Earth Electrode Test Setup

All the methods used to measure the earthing impedance of earth electrodes involve injecting current on the earth electrode and measure the voltage drop across it, and then

79

Ohm's law applied to obtain the impedance value. In practice, one of the terminals is available, which is the injection point, however the other taken over infinite area in the main body of the earth. To insure that the current passed through the electrode, an auxiliary electrode installed at sufficient distance to absorb the return current.

The test configuration shown in Figure 5.1 represents the test set up used for DC, low voltage AC and impulse tests. A concentric ring current return arrangement was installed to ensure uniform radial current distribution around the test electrode. The ring, which had a 15 m radius and which was buried at a depth of 0.3 m, consisted of eight parts connected to each other by an inspection pit. A current transformer (CT) and a differential probe were used to measure respectively current and voltage with a reference as a remote earth point with a direction perpendicular to the earth electrode to avoid the mutual effect on the measurement. For the DC test, the same configuration was used. The four channels of ABEM Terrameter and Megger DET 2/2, C1 and C2 were connected to the injection point of the tested electrode and the return electrode while P1 and P2 were connected to the injection point of the tested electrode and the remote earth point respectively.

The general test layout of the high voltage test is shown in Figure 5.2. In this test, the current is injected from the impulse generator, along a 15m-long elevated transmission line, into a test electrode installed at the centre point of the ring. The current dissipated by the test electrode is collected at the ring and returned to the common terminal on the chassis of the impulse generator. Power for the impulse generator charging unit and control gear is supplied by a 25 kVA diesel generator and regulator. A potential remote reference for the EPR measurements is taken from a point 60m away from the test electrode, in a direction perpendicular to that of the current injection lead. Voltage measurements were taken using a 150 kV gas-insulated capacitive divider. A differential

probe and a CT are connected to a LeCroy WaveRunner 64Xi oscilloscope energised from a small secondary petrol generator, each mounted on insulating platforms.
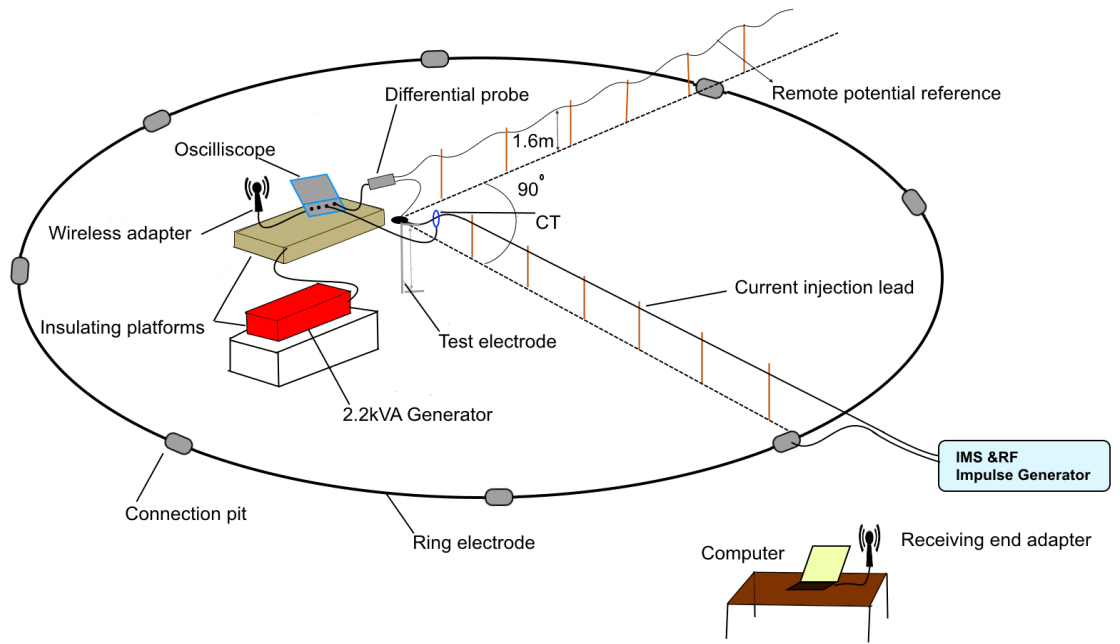
Figure 5.1: DC, AC low voltage variable frequency and low voltage impulse test configuration.
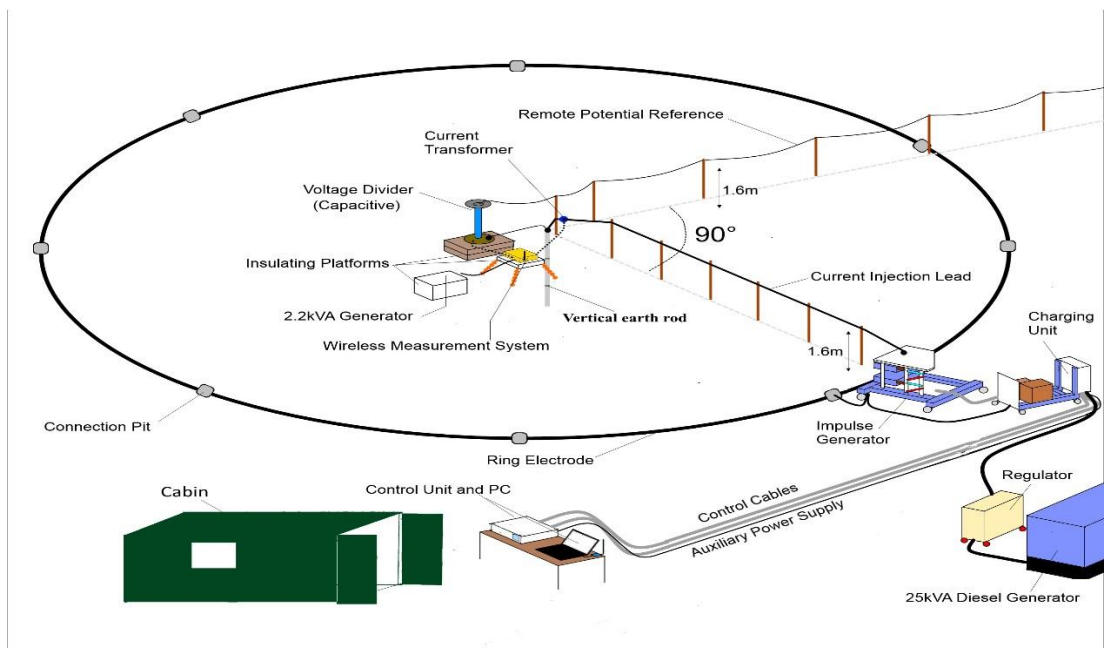
Figure 5.2: High voltage impulse test configuration [5.22].

5.2.2 Wireless Data-Acquisition system.

Two important conditions should be achieved during the test.

1. Measurement equipment and personnel are isolated from the test set up for adequate protection and safety conditions.

2. The mutual coupling between the 'current' and 'voltage' test leads is minimised by recording the current and voltage measurements at the point of current injection into the test object.

These requirements provide a satisfactory measurement and a safe environment for both staff and measurement devices. Therefore, the wireless system arrangement was used to send the recorded voltages and currents back to the test cabin by wireless adapters. The components of the wireless measurement system are shown in Figure 5.3. The signal lines of voltage and current transducers, located adjacent to the test object, are passed to the terminals of a PC-based oscilloscope, which is powered from a small petrol generator. A long-range wireless adapter connected to the scope is configured to form a point-to-point network with an identical device connected to the remote control PC. A robust remote desktop application (TightVNC) is employed to manipulate the scope controls directly from the cabin.
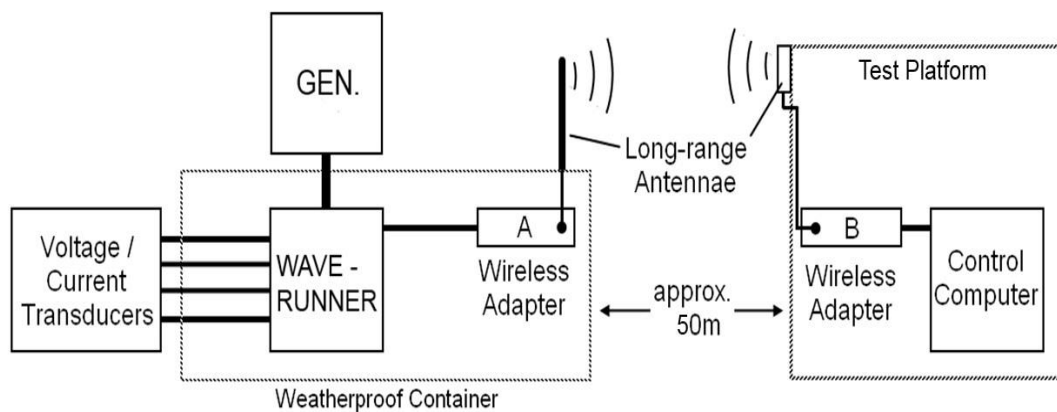
Figure 5.3: Block diagram of the developed wireless measurement system [5.23].

5.2.3 Results and Discussion

A DC test was carried out with an ABEM Terrameter SAS1000 and Megger DET2/2 in the same season (winter), taking into account the effect of rainfall on the measured DC resistance. The first test was done one day after rainfall and the second was carried out one week after rainfall. The DC resistance was measured with the ABEM was seen to decrease as the injected current was increased from 1 mA up to 0.5A. The difference in water level was reflected in the soil resistivity value, as shown in Figure 5.4. The results showed that the soil resistivity and DC resistance decreased when the water content increased. Such an effect should be considered in the design of the grounding system especially in places, which show a significant weather change over the seasons. Tests were also performed with the Megger DET2/2 at (8 and 40mA) current settings. The results of the measured ground resistance are constant over the values of the currents.
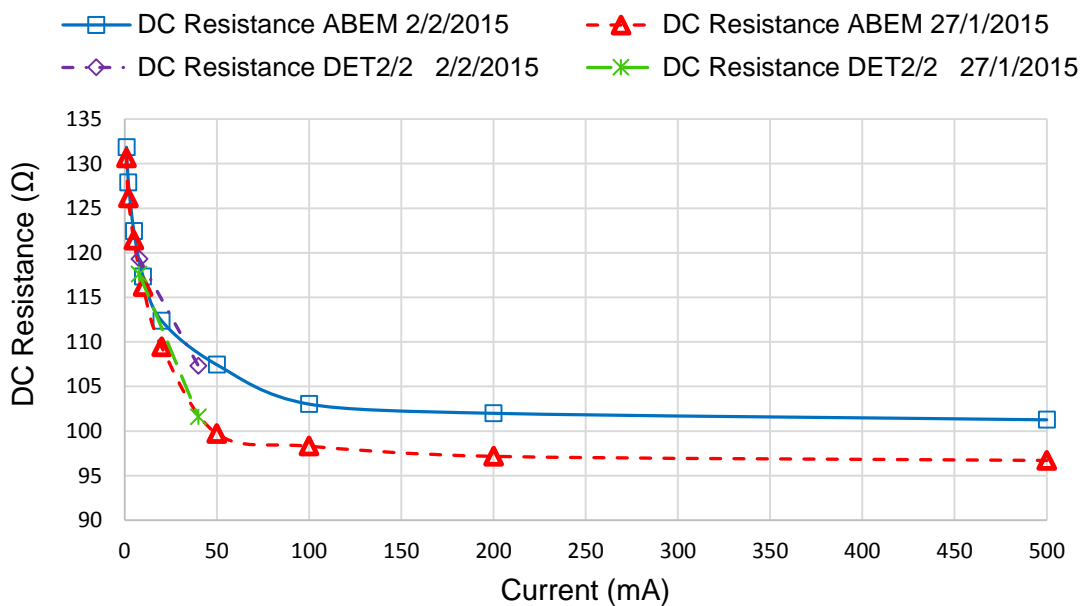
Figure 5.4: Effect of rainfall of 1.2 m earth electrode on the DC resistance value.

For the AC low voltage variable frequency test, a sinusoidal current waveform with a frequency range (50 Hz up to 1 MHz) is injected at the earth rod in the central point of the ring electrode using both the impedance measurement system (IMS) [5.24] developed

at Cardiff University and the radio-frequency generator. A remote potential reference for the EPR measurements is taken from a point 60m away from the test electrode, in a direction perpendicular to the current injection lead. The test set up at the field was installed to determine the frequency response of the vertical earth rod shown in Figure 5.1. Deferential probes and CTs were used to obtain the EPR and injected current by connection directly to the wave runner oscilloscope.

The ratio of voltage to current represents the measured impedance. At low frequency, the impedance is the same value as the resistance, which means the electrode behaviour is purely resistive. Above the characteristic frequency, the impedance showed an increase with frequency, due to inductive effects. A simulation study with HIFREQ [5.25] was carried out taking into account the effect of soil resistivity value and variation in relative permittivity. When compared with the field results, it showed good agreement.

As shown in Figure 5.5, simulations of the experimental arrangement were carried using the simplified 150Ωm uniform soil model, and this model produces an excellent agreement with the measured results. Additional simulations were carried out at 125 Ωm and 100 Ωm to examine the sensitivity of the result to changes in soil resistivity. However, the results showed that the simulated earth impedance was not sensitive to changes in ε_r over the range 1 to 30, as shown in Figure 5.6.
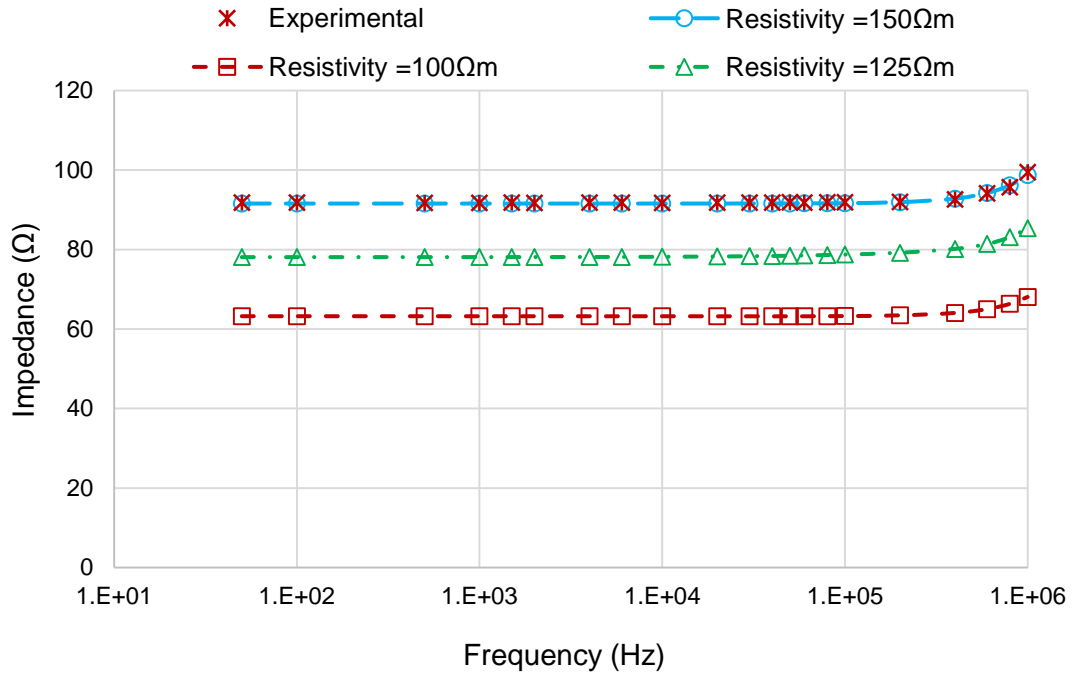
Figure 5.5: Measured and simulated frequency response of 1.2 m earth electrode with different soil resistivities.
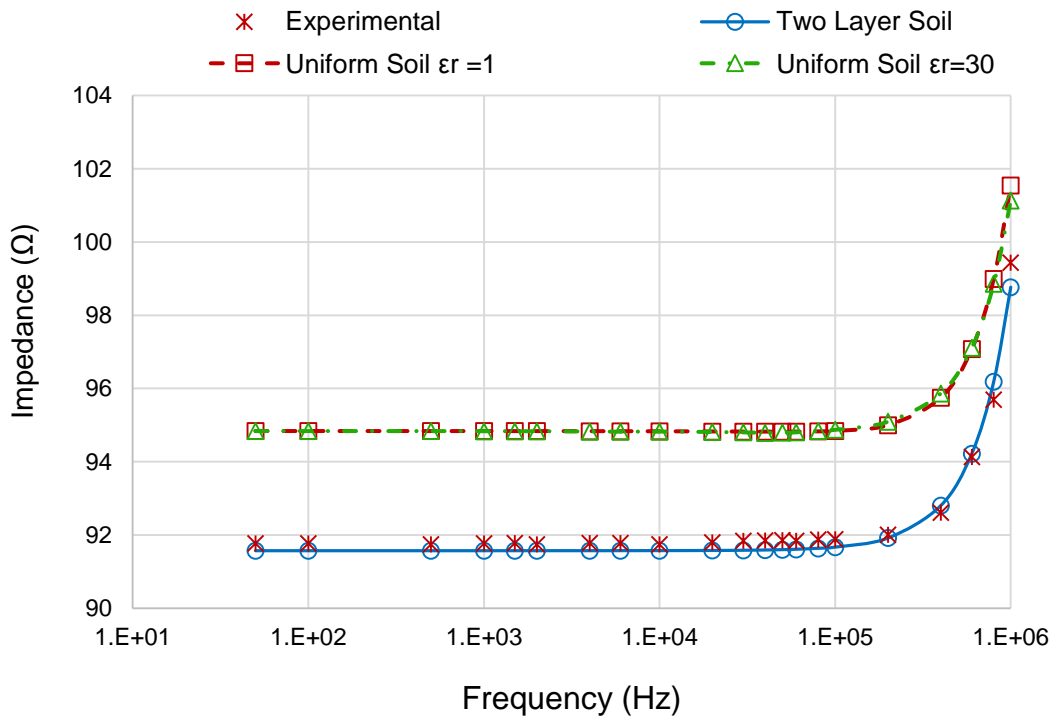
Figure 5.6: The effect of soil permittivity and soil structure on the behaviour of 1.2 m earth electrode.

A low amplitude current wave with front time 1.2 µs and time-to-half peak value 50 µs was injected into the vertical earth electrode driven in soil of resistivity 150Ωm. The peak value of current and voltage were 2.1A and 195.8V respectively. As shown in Figure 5.7, it can be seen that for this particular impulse, EPR and current peaks occur more or less at the same instant. In addition, good agreement between measurements and the calculated transient responses using CDEGS (HIFREQ-FFTSES) using the uniform soil model. Using the impulse test data, the impulse resistance is calculated to be 91.7Ω using the voltage/current ratio at the instant of peak current, which is similar to the DC and low frequency AC values.
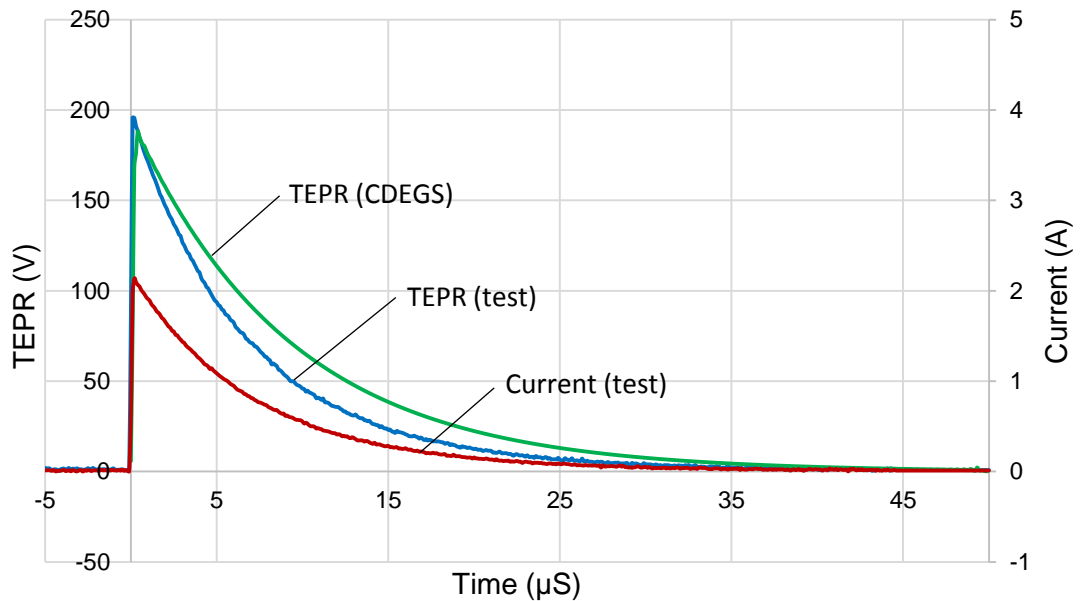
Figure 5.7: Transient response of the ground electrode to 1.2/50 µs current impulse: Computed and measured values.

The transient behaviour of the 1.2 vertical earth electrode subjected to a high voltage impulse was measured and compared with the CDEGS computations, as shown in Figure 5.8. The impulse current has a peak value of 313A, a rise time of 3µs and a time-to-half value of 45µs. The corresponding peak voltage is 27.8kV and the results indicate that the current peak occurs before the voltage peak. The impulse impedance is calculated to be

86

86Ω, which is slightly lower than the low voltage impulse resistance and the low voltage, low frequency impedance and DC resistance. The calculated transient response of the test rod using CDEGS (HIFREQ-FFTSES) and based on the uniform soil model shows reasonably good agreement with the measured voltage response.
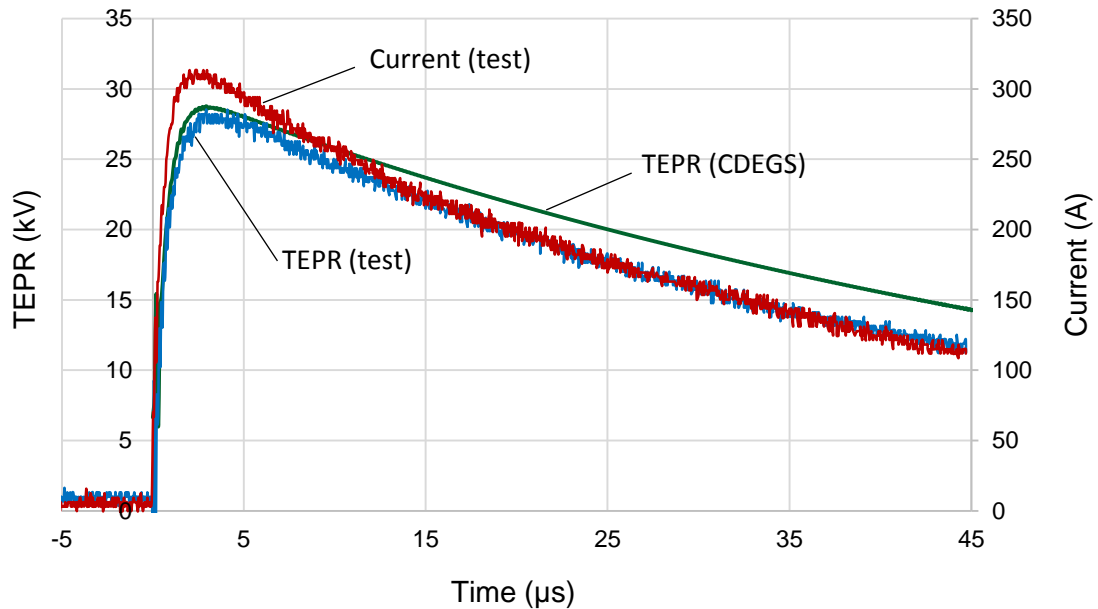
Figure 5.8: Transient response of the grounding electrode to high voltage 2.98/44.7 µs current impulse.

5.3   Horizontal Earth Electrode

5.3.1   Description of Test Electrode and Test Setup

The horizontal electrode used in the tests is an industry standard arrangement for the 'LV earthing system' of an 11 kV/415 V pole-mounted transformer. The electrode system comprises a 24 m length 3-stranded copper conductor with an overall cross-section area of 35 mm^2 buried horizontally at a depth of 1.5 m. A set of vertical rods are connected along the length of the buried horizontal conductor. The first three rods are positioned 1.5 m apart and starting 6 m from the pole base. The remaining six rods are separated by a distance of 3 m as shown in Figure 5.9.
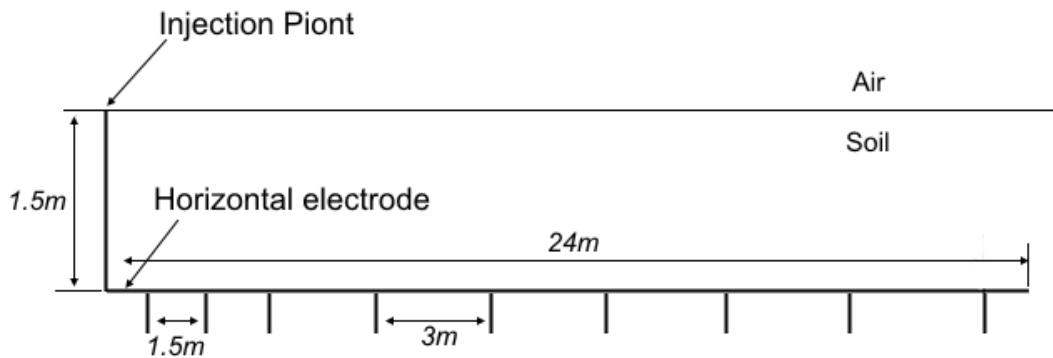
Figure 5.9: The arrangement of horizontal electrode.

5.3.2 Fall of Potential Earth Resistance Measurements Method

Investigation of the grounding resistance of the horizontal grounding electrode was performed using the fall-of-potential (FOP) method. This method is based on passing a current between the ground electrode under test and an auxiliary current probe and then measuring the voltage between the ground electrode and a potential probe. In order to reduce the inter-electrode influence due to mutual resistance, the auxiliary current probe should be installed at a substantial distance from the ground electrode under test. The principle of the FOP method is shown in Figure 5.10.

A minimum distance of at least five times the largest dimension of the ground electrode under test is recommended in IEEE standard 81 [5.26]. In practice, the distance between the potential probe and the grounding electrode under test is chosen to be 62% of the distance between the grounding electrode and auxiliary current return electrode, X=0.62×D. Therefore, this method is also known as the 62% rule. This distance is obtained based on two assumptions: (i) uniform soil resistivity and (ii) a relatively large distance between the auxiliary current electrode and the ground electrode under test. This technique is a suitable method for measuring the earth resistance of high voltage substation earthing systems [5.26]-[5.28].

88
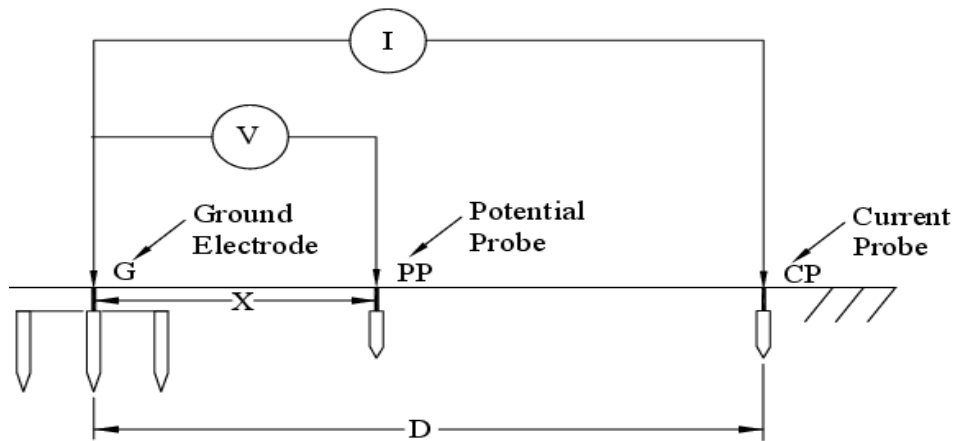
Figure 5.10: Test electrodes arrangement in Fall of Potential method [5.27].

Based on the schematic diagram of the FOP method, an auxiliary current probe (CP) with a diameter of 10 mm and a length of 500 mm was installed at a distance of 100 m from the grounding electrode under test. Another electrode with a diameter of 10 mm and a length of 300 mm was implemented as the potential probe (PP). In the DC test, the potential probe was installed at a distance of 62 m (X=0.62 D) from the grounding electrode under test, in line with the current return lead. To eliminate the influence of inductive coupling between the current and voltage leads in the AC variable frequency test, the potential probe was installed perpendicular to the current return lead [5.26].

5.3.3   Results and Discussion

The DC resistance measurement was performed based on the schematic diagram shown in Figure 5.10. The first DC test was performed using a Megger DET 2/2 to measure the earth resistance of the grounding electrode at two selectable current amplitudes: 8 mA and 40 mA, then the equipment inject this current followed by a resting period with no injection, using a switching frequency of 128 Hz. A second DC resistance test was carried out with the same test configuration and using the ABEM Terrameter SAS1000 with a current range from 1 mA up to 200 mA and a switching frequency of 1 Hz. The results from both DC tests are shown in Figure 5.11.

It can be seen from the figure that the ABEM instrument gives a significantly higher value of electrode earth resistance. In addition, for the ABEM readings, the measured resistance falls with increasing current injection. The DET2/2 instrument gave the same resistance value for both the 'low' and 'high' current settings. These tests show similar trends to those obtained with tests carried out on different rods in low resistivity water [5.29] and a vertical rod electrode in soil [5.21]. This non-linear trend in resistance with current magnitude, and influence of the energisation frequency, may be attributed to the electrical nonlinearity of the soil itself and at the metal/electrolyte interfaces.
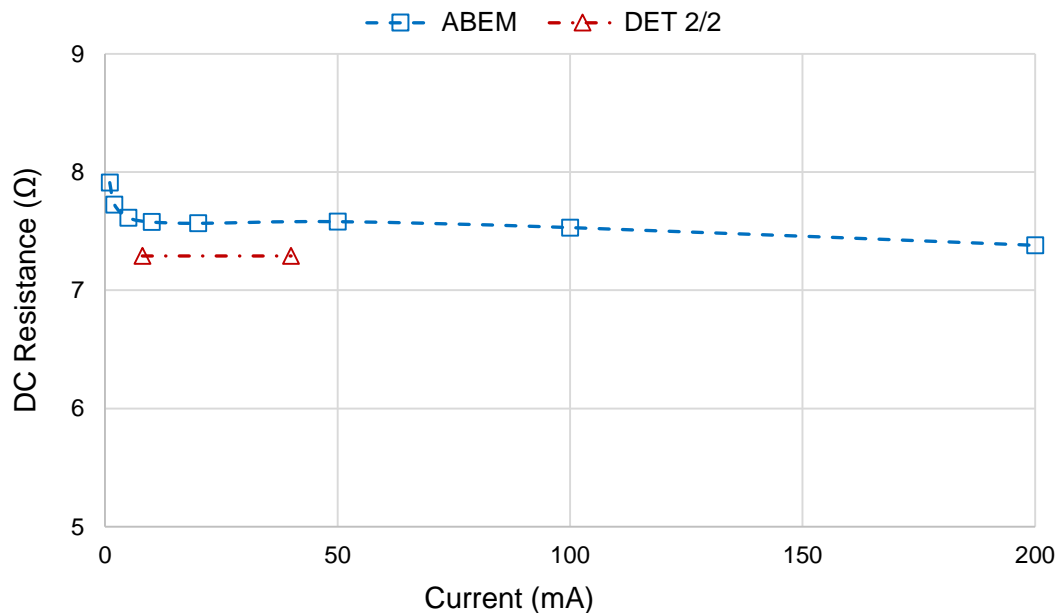
Figure 5.11: Current dependence of the horizontal grounding electrode resistance.

For the AC tests, two different instruments were used: 1) the impedance measurement (IMS) [5.24] developed at Cardiff University and 2) a radio frequency (RF) measurement system. The IMS incorporates two lock-in amplifiers, which can measure magnitude and phase values of two signals (voltage and current) with respect to a common reference signal and is capable of excellent noise rejection. The system incorporates a power amplifier, which generates output voltages up to 120 V RMS and operates over the frequency range 20 Hz–100 kHz. The RF system consists of a Marconi 2019A signal

generator and an Amplifier Research-type 25A250 RF amplifier. The RF system can operate at frequencies between 10 kHz and tens of megahertz. Due to very low background noise above 10 kHz at the test site, voltage and current signals in this frequency range can be measured directly using a digital storage oscilloscope. Wideband differential attenuation probes and wideband current transformers were implemented in the voltage and current measurements. The RMS and phase angle of the injected current and EPR were acquired using a PC-based 4-channel oscilloscope (LeCroy Wave runner 64Xi). The acquired data were recorded to determine the earth impedance of the rod seen at the point of injection. The measurement set-up of the AC low voltage variable frequency tests is shown in Figure 5.12.
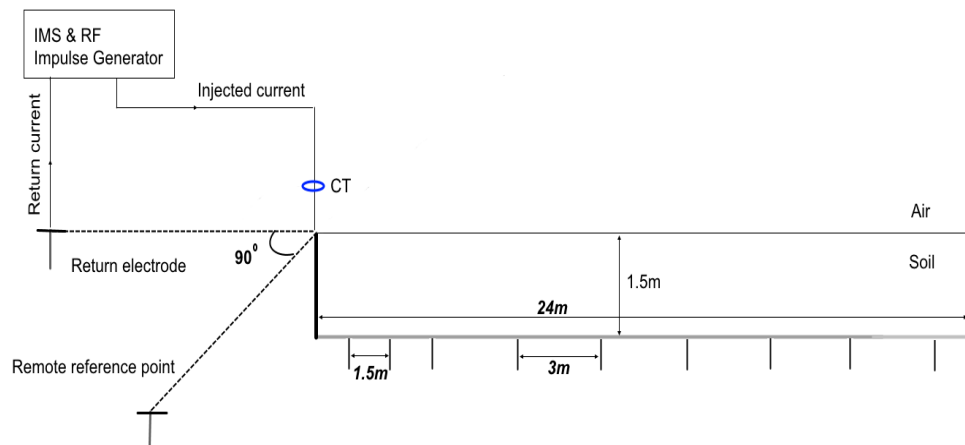
Figure 5.12: Measurement set-up of AC variable frequency.

In order to support the experimental results, numerical simulations were performed using HIFREQ-CDEGS, taking into account the detailed geometry of the electrode and soil medium parameters. A comparison between the experimental and numerical results of the electrode impedance versus test frequency is shown in Figure 5.13.

91
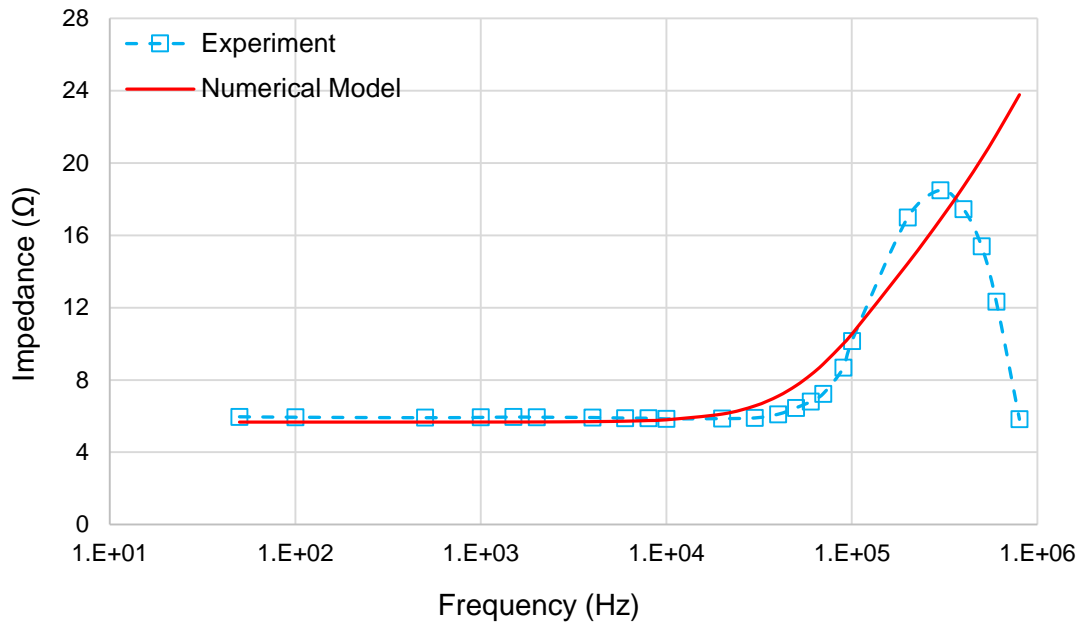
Figure 5.13: Frequency variation of 24 m horizontal earth impedance.

The figure shows that over a frequency range of 50 Hz to 30 kHz, the AC impedance is about 6Ω, which is of the same order as the measured DC resistances obtained with the DET2/2 and the ABEM at its higher current setting. Above an upturn frequency (~40 kHz), the impedance increases due to the inductive effect of this relatively long electrode. Furthermore, in the frequency range of 50 Hz up to 100 kHz, a close agreement was found between the experimental results and numerical modelling. At higher frequencies (>100 kHz), however, the trend in the measured values of impedance differs from the simulation results. The measured impedance rises to a maximum of 18Ω at about 300 kHz and then decrease sharply to a value close to the DC resistance. Such a trend is predicted by the distributed parameter circuit model of a horizontal earth electrode [5.30] and can be explained by resonance due to the interaction of the capacitive and inductive components of the model. In addition, the simulation model does not account for the frequency dependence of resistivity or permittivity.

Additional numerical simulations were performed to consider the sensitivity of the calculated electrode impedance to soil parameters (resistivity ρ and relative permittivity ε_r). For these additional simulations, soil resistivity varied from 50 Ωm to 80 Ωm, and relative permittivity was varied from 1 to 80. The results are shown in Figure 5.14 and Figure 5.15 respectively.

Figure 5.14 shows that changes in soil resistivity have a significant impact on the calculated electrode impedance while the effect of soil permittivity variation is negligible as shown in Figure 5.14. However, none of the simulations over the ranges of resistivity and permittivity produces high-frequency impedance characteristic similar to that obtained from the field tests.
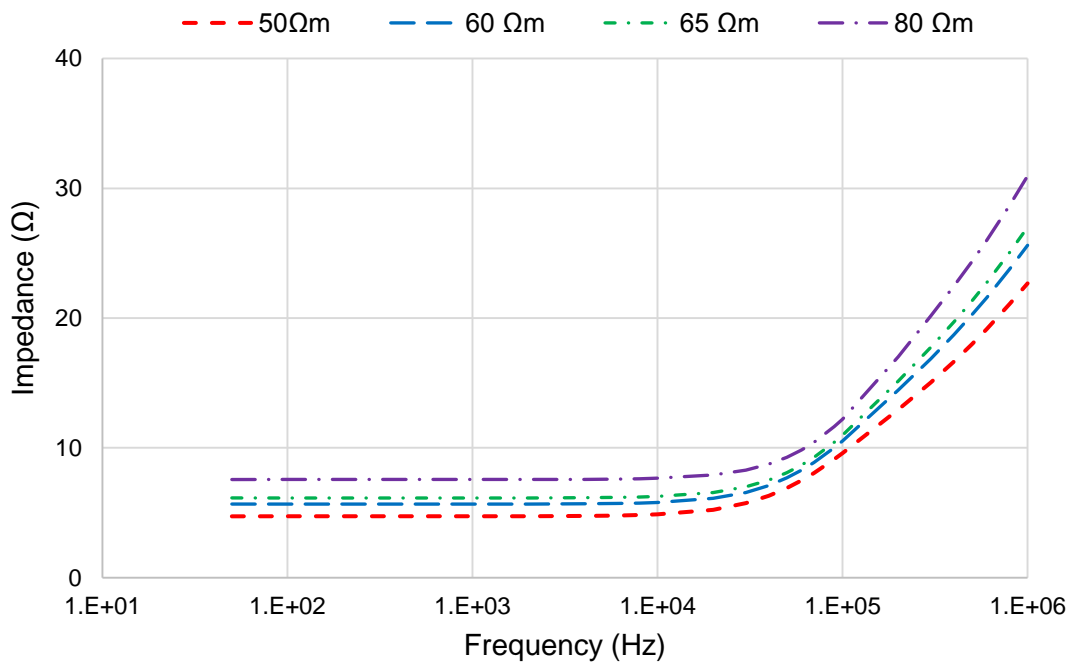
Figure 5.14: Effect of soil resistivity on the impedance value of horizontal earth electrode ($\varepsilon_r = 9$).
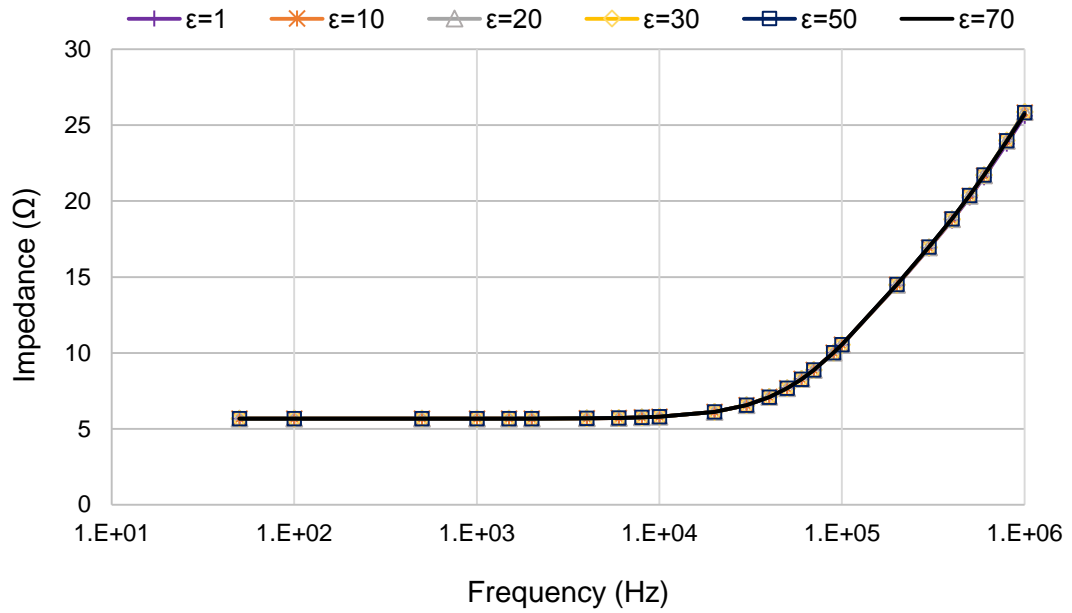
Figure 5.15: Effect of relative permittivity on the impedance value of horizontal earth electrode (ρ = 6Ωm).

Low-voltage impulse tests were performed using a Haefely RSG481 recurrent surge generator, having a maximum output voltage of 500 V. The instrument is capable of generating different impulse shapes by changing the circuit components over wide ranges. In this work, a current impulse of amplitude 24.5 A with a front time of 2 µs and a time-to-half peak value of 50 µs was injected into the grounding electrode under test. The transient voltage response of the grounding electrode was calculated using CDEGS (HIFREQ-FFTSES), and the simulation results together with the measured injected current and TEPR (transient earth potential rise) are shown in Figure 5.16.
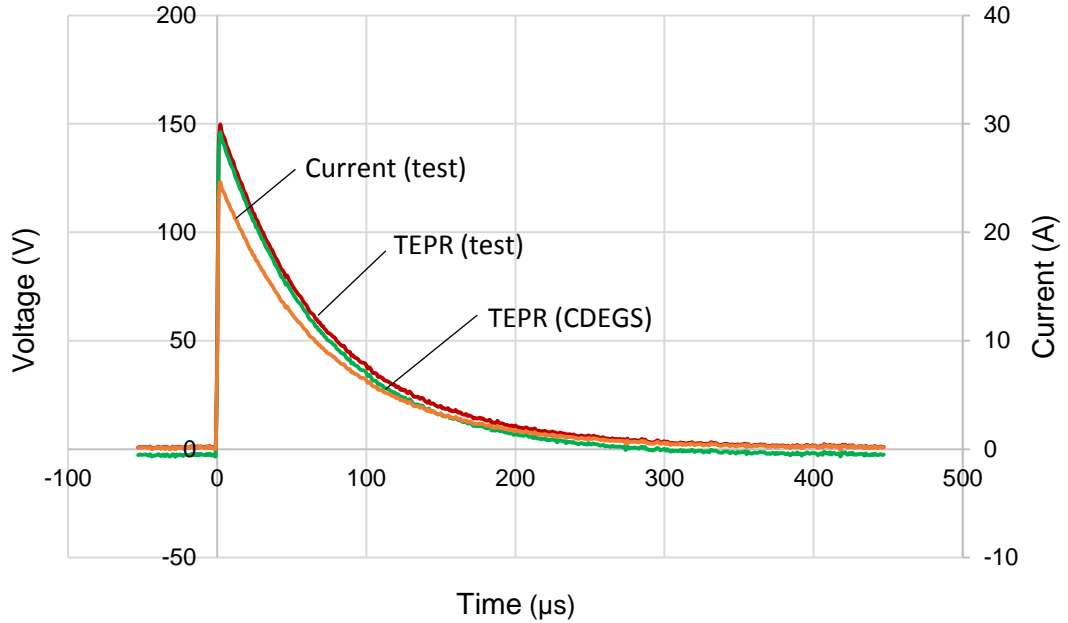
Figure 5.16: Transient response of the horizontal ground electrode to 2/50 µs current impulse.

Close agreement was obtained between the measurement and simulation results. From the tests, the measured peak values of current and voltage are 24.5 A and 149.4 V, respectively. The "impulse impedance", Z_1, given in Equation (5.1) and defined as the ratio of maximum voltage V_p to maximum current I_p [5.31],

$$Z_1 = V_P/I_P \tag{5.1}$$

is calculated to be 6.1 Ω. The impulse impedance, Z_2, given in Equation (5.2) and defined by the ratio of voltage and current values occurring at the instant of current maximum,

$$Z_2 = V_{@IP}/I_P \tag{5.2}$$

gives a value of 6.1 Ω. Both values are reasonably close to the DC and low-frequency AC values.

5.4   Characterisation of the earth grid in a homogeneous conducting medium

Usually, a low current magnitude is injected to measure the earth resistance/impedance of operational power system installations [5.32]. For the DC test, there are many commercial testers available. With these testers, a variable switched frequency is used for DC energisation to measure the electrode earth resistance [5.33]. However, sinusoidal signals with variable frequency away from power frequency are injected to the earth electrodes to measure the earth impedance [5.24] [5.33]-[5.35]. The earth potential rise is measured at the injection point and then the earth impedance is calculated by taking the ratio of the measured voltage to the injected current. The earthing resistance/ impedance shows variation in the magnitude depending on the test conditions or the nature of the conducting medium. Therefore, several studies have focused on the behaviour of the earthing system, taking into consideration all the factors, to clarify the performance of the earthing system.   Extensive investigations involving an analytical approach and numerical simulation models have been developed to analyse the earthing electrodes and to design earthing systems [5.36]–[5.39]. Several laboratory studies have been performed in controlled environments to clarify some aspects of earthing-system behaviour, such as soil ionization [5.40]–[5.45]. However, the validity of these tests is highly dependent on the test parameters of the laboratory such as the temperature, the composition of the conducting material and the test arrangements. Therefore, the current and the potential distribution have significant influence when these parameters are scaled up to the full-scale system [5.46]. Full-scale tests, including field tests [5.3], [5.15], [5.47], [5.48] and at operating electrical substations and tower lines [5.49]–[5.52] have been performed. In these tests, the earthing system installations were buried in the soil, which is a non-uniform medium due to the variation in soil structure both horizontally and vertically. Therefore, the test results are highly affected by the nonlinear conduction of the medium,

in particular at impulse resistance [5.24], [5.43]-[5.45], [5.47]. For the above reasons, further work is required to validate the results obtained from computational modelling techniques. An outdoor facility was established and low-voltage DC, AC, and impulse tests on different earthing electrodes were conducted [5.29], [5.46]. However, the behaviour of earthing systems under high voltage impulse energisation still needs more clarification.

5.4.1   Dinorwig Measurements Set Up Description

Full-scale tests were performed at a large area outdoor earthing facility at Dinorwig pumped storage power station in North Wales, as described in Chapter 4, to investigate the behaviour of a practical earthing system subjected to high voltage impulse different energisation. Measurement configurations were investigated for energising a 5 m x 5 m earthing grid comprising a 25 (1 m x 1 m) mesh earth grid. The test grid was suspended at the end of the floating pontoon at a depth of 0.8 m. A preliminary numerical model was used to simulate the earthing test grid using a single-layer medium to determine the most appropriate test layout.

Figure 5.17 shows the test configuration used to energise the test object with DC current. The ABEM Terrameter and DET2/2 located near the injection point were used to inject currents of different magnitudes at the corner of the test grid. Current was injected at the test electrode in the water and returned via a 60 m horizontal electrode positioned near the shore and immersed just below the reservoir water surface. For this setup, a remote voltage reference was obtained from a single-rod electrode immersed in the reservoir water over 50 m away, and arranged in an orthogonal direction to the current injection lead. Both channels C1 and P1 were connected directly to the test grid with a 1 m down lead. C2 was connected to the current return electrode and P2 to the remote reference point.

For AC measurements, the previous test configuration is not valid for two reasons: first, if the test equipment is positioned near the injection point, this requires someone present to record the measurements, and that might affect the safety requirements for the personnel. The second reason is that, if the AC current is energised from the cabin, then the current is measured at the output of the test source, and the voltage lead connected to the test object is brought back along the pontoon and parallel to the current lead, which will lead to measurements being influenced by mutual coupling between the two leads, particularly at higher test frequencies [5.46].

Therefore, it is replaced by the configuration shown in Figure 5.18. With this configuration, voltage and current measurements were taken close to the injection point, while the test source was located and controlled from the test cabin. To achieve this desirable test arrangement, a non-wired data transmission system between the test electrode end and the test cabin was required. Therefore, the wireless system in Figure 5.3 was used successfully to control and record the signals.

The same configuration was used with low/high voltage impulse energisation. However, the differential probe was replaced with a resistive voltage divider, and an invertor was used supply the oscilloscope from a battery supply.
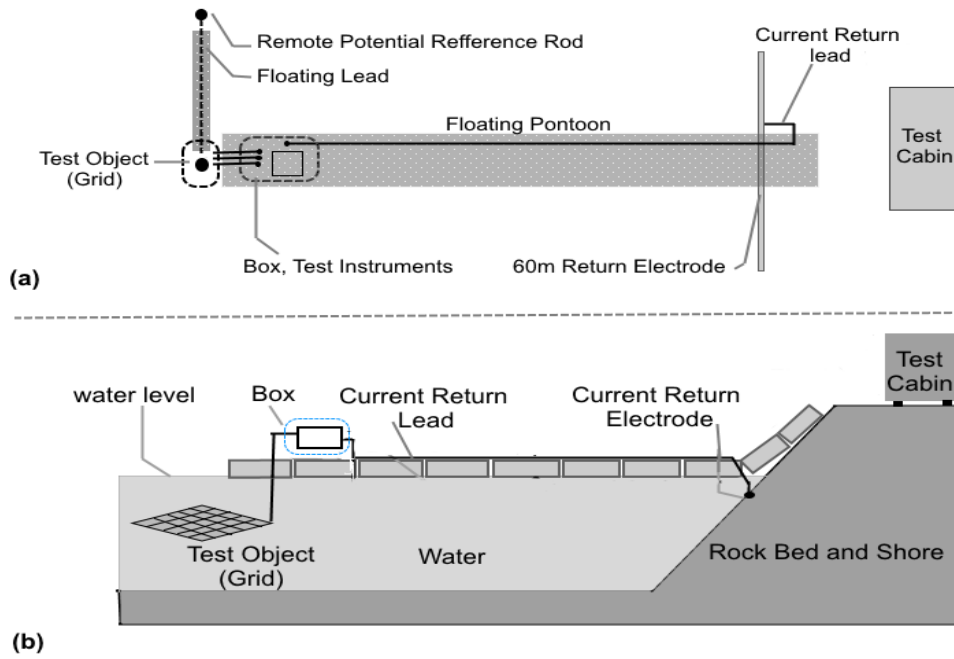
Figure 5.17: Schematic diagram of the DC test set up showing the plan and elevation view of the test configuration: (a) plan view and (b) elevation view
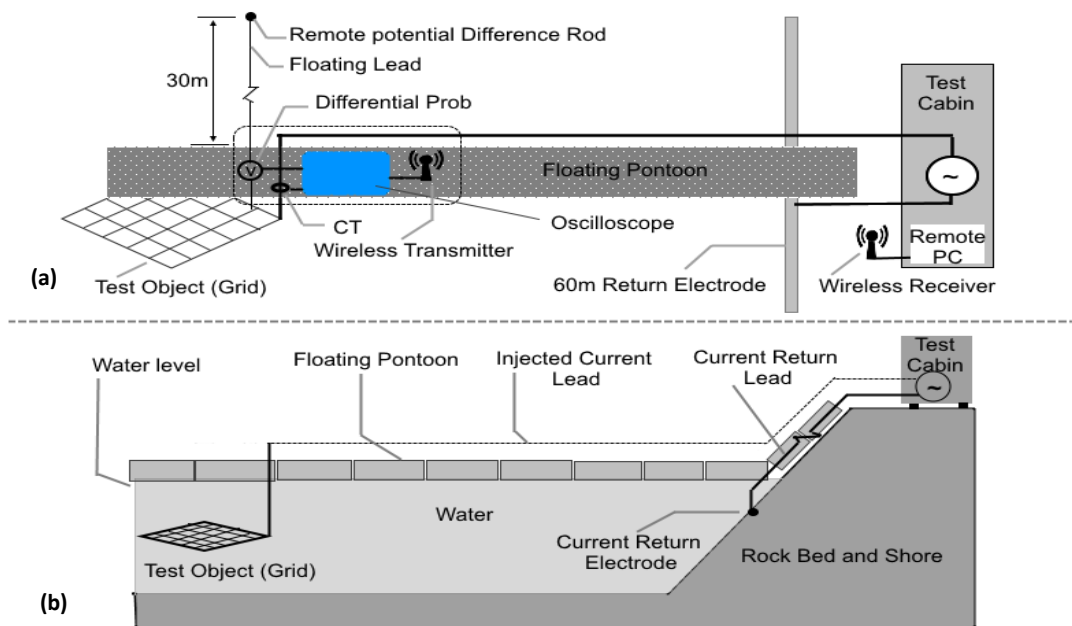
Figure 5.18: Schematic diagram of the AC test set up showing the plan and elevation view of the test configuration: (a) plan view and (b) elevation view.

5.4.3 Experiments Results Discussions

DC measurements were conducted using a DET2/2 instrument with two current settings, specifically, a low current of 8 mA and a high current of 40 mA, giving values of 10.65 Ω and 10.03 Ω respectively. The same test was performed with the ABEM Terrameter at different current values from 1 mA up to 1 A. Figure 5.19 shows the DC test results. It is clear from the figure that there is a decrease in the resistance magnitude with injected current up to 10 mA. This nonlinear behaviour is due to the interface between the electrode metal/electrolyte [5.53]. The resistance value was then observed to be constant for the currents up to 1 A. The repeatability of the test results was checked, and the results are shown in Table 5.1.
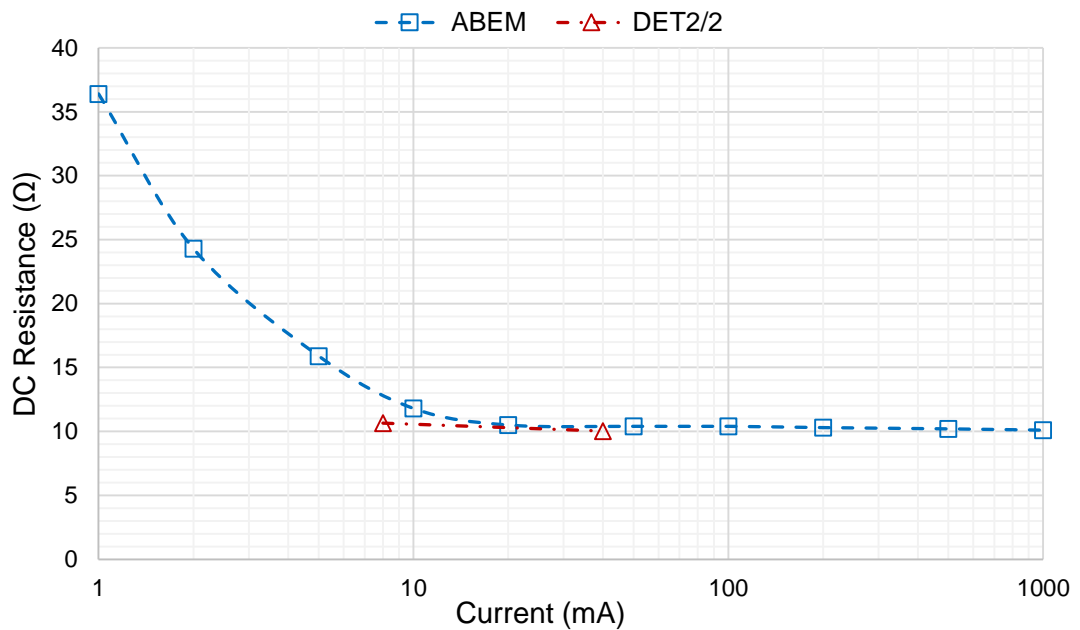
Figure 5.19: Measured DC resistance of earth grid under different low current energisations

Table 5.1: DC resistance measurement at Dinorwig earthing test site.

Current (mA)	Resistance (Ω)				Repeatability
	Repeat 1	Repeat 2	Repeat 3	Average	
1	36.4	37.3	38.9	37.5	0.73
2	24.3	25.4	26.0	25.2	0.50
5	15.9	16.0	16.1	16.0	0.06
10	11.8	11.8	11.9	11.8	0.04
20	10.5	10.5	10.5	10.5	0.00
50	10.4	10.4	10.4	10.4	0.01
100	10.4	10.4	10.4	10.4	0.02
200	10.3	10.4	10.2	10.3	0.04
500	10.2	10.3	10.3	10.3	0.01
1000	10.1	10.1	10.1	10.1	0.00

For low voltage AC variable frequency measurements, low-magnitude AC currents were injected into the test grid over the frequency range of 20 Hz to 1 MHz using the IMS and RF test systems. A low constant current of magnitude 50 mA was injected over the frequency range of each instrument. The measured frequency response of the grid electrode is shown in Figure 5.20. The measured impedance is constant up to about 50 kHz at a value of 11.4Ω. Then, a small reduction in impedance value was noted up to 500 kHz, which is the same as the reduction in the impedance value of the vertical electrode [5.46]. After this frequency, there is a sharp upturn in the measured impedance with an increase in frequency. The measured impedance was compared with the simulation results using CDEGS, based on the simplified two-layer soil model. The CDEGS calculated values of earthing impedance for the same frequency range exhibited a flat

region up to 10 kHz, and then the simulation showed the same trend as the measured impedance. The computed impedance decreased up to 500 kHz. After this frequency, it exhibited a sharp upturn in impedance, but it was still smaller than the measured values. The difference in impedance values at high frequency might be due to the limitations of the computational model.
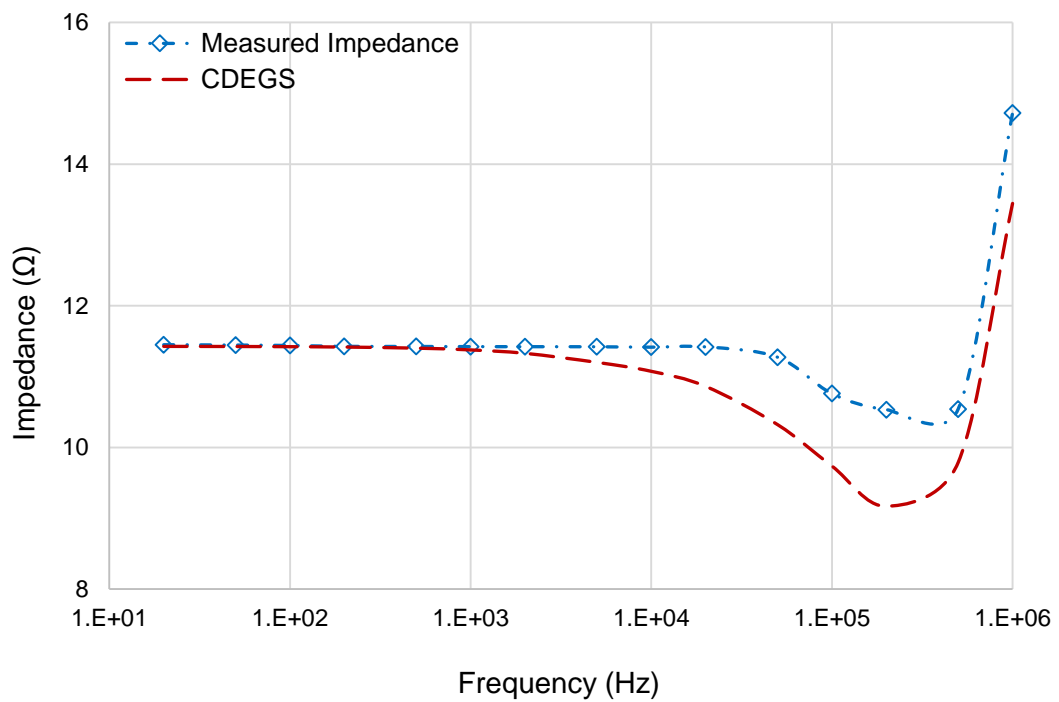
Figure 5.20: Frequency response of the test grid.

Further measurements were performed to highlight the effect of current variation on the measured impedance. An AC test with current varying from 100 mA to 3 A was performed on the same day, and the test results can be seen in Figure 5.21, the measured earth impedance showed a reduction in its value over an increased current by about 9% at different tested frequencies.
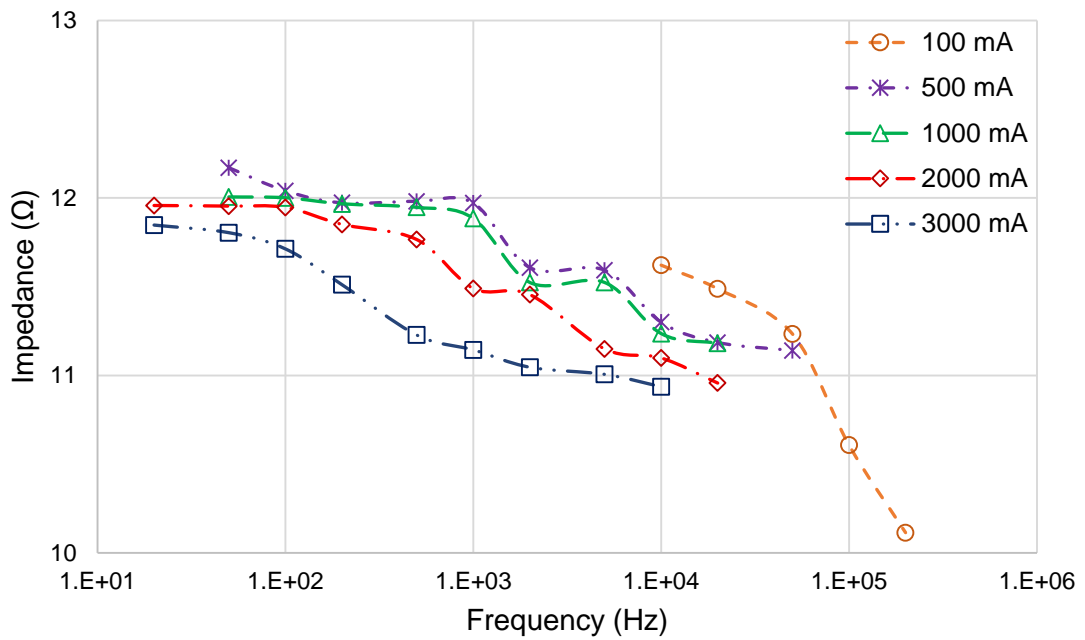
Figure 5.21: Effect of test current magnitude on the measured earthing resistance over different frequencies.

Further tests were carried out to investigate the transient response of the test grid. An impulse generator was used to energise a fast impulse at the corner of the test object. The impulse generator has a maximum output voltage of 6 kV and is capable of generating impulse waves with different rise-time and time-to-half values. In these tests, a standard lightning voltage impulse with a rise-time of 1.2 μs and a time-to-half peak value of 50 μs was applied to the test circuit at the sending end, inside the test cabin. A resistive divider with a voltage ratio of 500/1 located close to the injection point was used to measure the transient earth potential rise (TEPR) of the test grid. The measured signals were sent back to the test cabin using the wireless system. The peak voltage of the impulse waves varied from 250 V up to 6 kV.

The results of the low-voltage impulse tests performed on the grid electrode are shown in Figure 5.22. The figure shows that the EPR and current traces for the impulse test indicate a mainly resistive behaviour. The computed transient response using the computational

model CDEGS (HIFREQ-FFTSES) is also shown in the figure and a reasonably good agreement was obtained with the measurements.
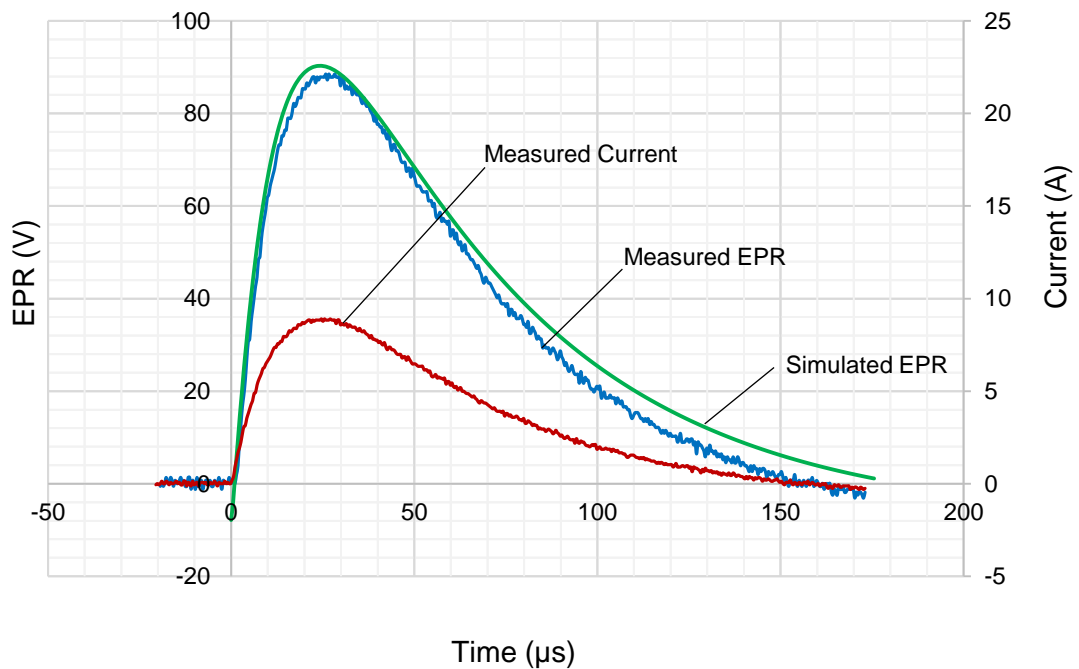
Figure 5.22: Transient response of the grid electrode to low voltage impulse.

In addition, Figure 5.23 shows the results of the high voltage impulse test. The test grid electrode was energised with an impulse voltage of 6 kV, and the TEPR and current peaks occurred at the same instant. This indicates a resistive behaviour for the test grid. The results were compared to the computed high voltage transient response using the CDEGS (HIFREQ-FFTSES) model and showed a reasonably good agreement. The impulse resistance was measured for different voltage magnitudes, and the measured peak values of current and voltage are shown in Table 5.2.
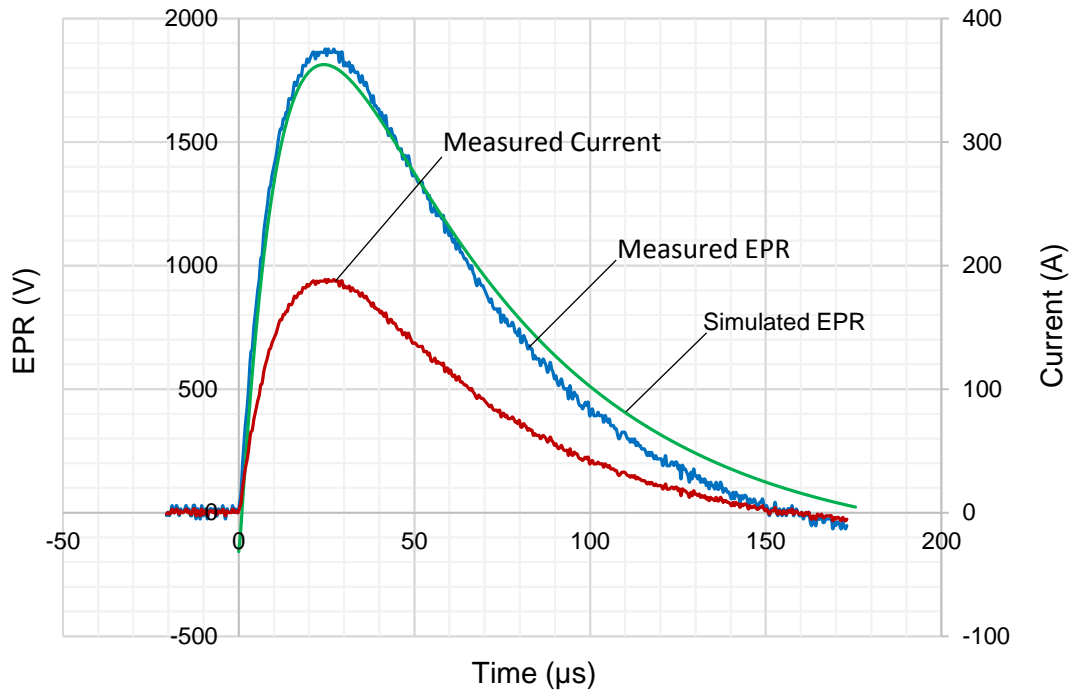
Figure 5.23: Transient response of the grounding electrode to high voltage 25/75.6 current impulse.

Table 5.2: Impulse resistance of the test electrode at different peak values of voltage and current.

Peak Voltage V_{pk} (V)	Peak Current I_{pk} (A)	Impulse resistance R_{Imp} (Ω)
82.7	8.3	9.96
155.34	15.63	9.94
321.89	32.52	9.90
682.5	64.04	10.6
981.5	94.24	10.4
1333.5	127.5	10.4
1563	154.5	10.1
1899	188.6	10.1

The impulse resistance at different peak values of voltage and current, V_{pk} and I_{pk}, is calculated based on the definition of impulse resistance R_{imp} (Equation (5.1)). For this particular test electrode and energisation conditions, the test grid has a resistive behaviour, and the results are shown in Figure 5.24.
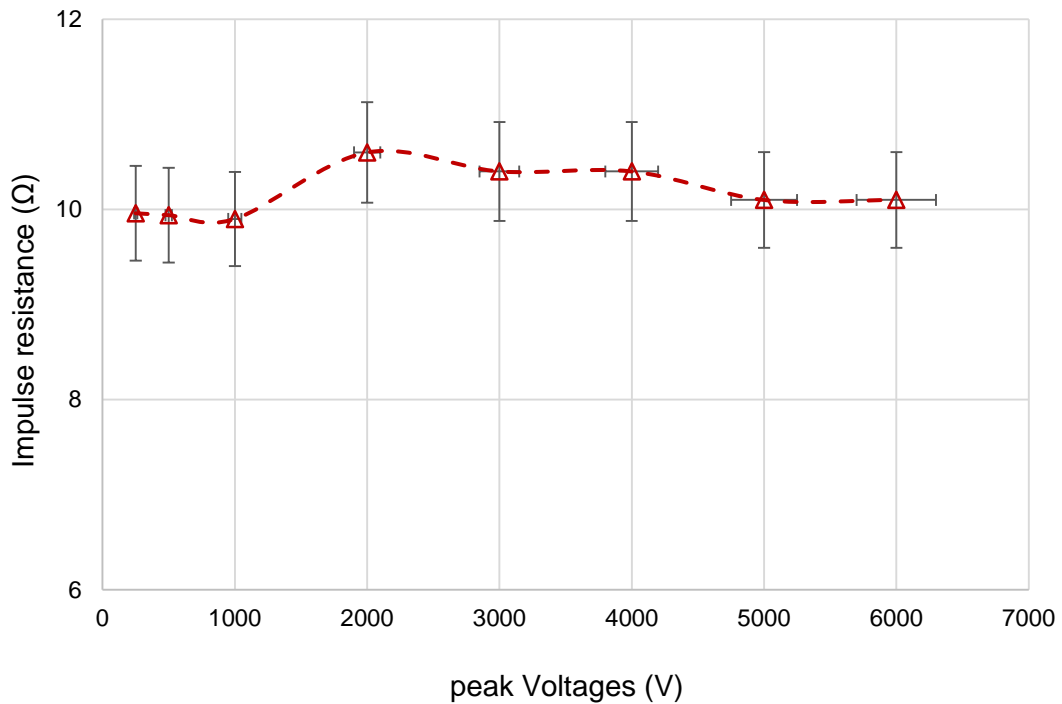
Figure 5.24: Measured impulse resistance of the test grid at different peak voltages.

5.5   Conclusions

Extensive variable frequency AC/DC and impulse tests were performed on several full-scale earth electrodes at the university test site at Llanrumney and the Dinorwig power station earthing test facilities. Tests were carried out on a 1.2 m earthing rod at a new test location at the Cardiff University earthing test facility at Llanrumney fields and showed good agreement between measured low voltage AC, DC, and impulse resistance values. The current dependence of measured resistance is significant in the low voltage tests and particularly so over a low current range at low switched DC frequencies. For these tests,

an approximate average uniform soil model obtained from a detailed local resistivity survey was implemented in detailed numerical models of the test setups and was able to produce very good agreement with the preliminary test results. The simulations allowed investigations into the variations of soil resistivity and permittivity parameters. For this setup, it was shown that changes in relative permittivity had little effect on the results over the tested range of frequencies and rise times. High voltage tests indicated a slightly lower impulse resistance compared with the low voltage impulse tests.

Further field tests were carried out on a 24 m horizontal electrode installed in a low resistivity soil medium. A reasonably close agreement was found between DC, AC variable frequency, low voltage impulse impedance and impulse resistances. The earth electrode DC resistance exhibited significant current dependence with the low switching frequency test meter. With regard to AC, satisfactory agreement was obtained between the measured and simulated values of electrode earth impedance up to 100 kHz. However, above this frequency, there was a significant difference in the frequency responses. The computer model did not provide a close match to the experimental results at high frequency; this might be due to the frequency dependence of soil resistivity and relative permittivity. Further, the variation in relative permittivity did not produce any appreciable effect.

Investigations were performed at Dinorwig pumped storage substation at North Wales to clarify the behaviour of the practical earthing system at a controlled full-scale test environment. The 25-mesh grid earth electrode made of aluminium was subjected to DC/AC energisation, and the earthing resistance and impedance were measured. The measured DC resistance showed a decrease with increasing current up to 10mA. This current dependence under DC may be due to nonlinearity at the electrode-electrolyte interface. AC constant current was injected into the earth electrode grid over frequencies

ranging from 20 Hz up to 1 MHz, and the measured impedance showed good agreement with the DC resistance at low frequency. The measured impedance was compared with the computed impedance based on the simplified two-layer model. The computed impedance magnitude exhibited a reduction over high frequencies. In terms of current dependence, the measured earth impedance shows a reduction in its value over increased current.

Further tests were carried out on the earth electrode grid to clarify the earthing system response under low and high voltage energisation. A surge generator was used to apply different voltage magnitudes from 250 V to 6 kV. Resistive behaviour dominated the earthing system response for all the implemented tests, and the impulse resistance was calculated over different impulse magnitudes. The obtained results were compared with the computed results by using CDEGS (HIFREQ-FFTSES) and showed good agreement with both low and high voltage tests.

CHAPTER SIX: LABORATORY CHARACTERISATION OF SOIL PARAMETERS UNDER HIGH FREQUENCY AND TRANSIENT CONDITIONS

6.1 Introduction

Earthing systems are installed in the soil to mitigate against the effects of system faults and lightning surges. Their main function is to dissipate lightning and fault currents into the earth without generating hazardous potential differences between contact points of grounded structures and the earth that may be bridged by people or sensitive electrical equipment. When the currents are dissipated into the earth, the soil exhibits a significant variability in its behaviour. Many factors are responsible for this variation, some of them related to the frequency contents of the energized currents and current magnitude and wave shape; others to the grounding electrode itself, such as the materials and dimensions; and yet other factors related to the nature of the soil, such as moisture, salt content, and size and soil components [6.1]–[6.4]. The behaviour of earthing systems energised by low-frequency current is well known. However, when earthing systems are subjected to a lightning surge, they exhibit a different behaviour to that at low-frequency energization, and such behaviour requires more investigation, in particular, the frequency dependence of soil parameters remains not clearly understood and warrants further work.

Investigations of frequency dependence of soil parameters began almost a century ago [6.5]. Further studies in both the laboratory and the field have shown how soil conductivity and permittivity is related to the frequency, and the studies modelled the frequency dependence of these soil parameters by a number of analytical models [6.6]–[6.12]. According to these models, the frequency dependence of soil parameters has a significant impact on earthing system performance, in particular when subjected to a lightning surge. Also, applying the conservative approach, in which the resistivity value

is chosen to be the measured DC or low-frequency resistivity and the permittivity value varies from 4 to 81 with respect to water content, leads to a significant error [6.12].

In this study, a set of laboratory experiments was established to determine the behaviour of the soil under DC and AC energization over a range of frequencies (50 Hz to 1 MHz) and variety of current magnitude. The objective of these investigations was to observe the frequency dependence of soil parameters with different percentages of water content. Finally, the results were compared with the previous published models of the soil conductivity and permittivity frequency dependence expressions.

6.2   Soil Sample Preparation

The soil medium used in this investigation was extracted from Cardiff University's earthing system facility at Llanrumeny near the injection point of the buried electrode. In the first step, the soil was dried by using an oven at a maximum temperature of 100º C. The soil samples then allowed cooling to reach the laboratory temperature. Finally, the soil was weighed and wetted with different levels of water content (10%, 15% and 20% by weight) using tap water (volume conductivity 300 µs/cm).

6.3   Frequency Dependent Soil Parameters Models

Models have been developed to describe the properties of soil parameters with respect to energised frequency. In this section, three models are highlighted and compared with the results obtained in the experiments.

6.3.1   Scott Model

Scott et al. [6.6] proposes a model to determine the electric properties of soil conductivity (ϭ) and permittivity (ε) relying on laboratory and field measurements for different soil samples with a range of moisture level over frequency range 100 Hz to 1 MHz. These

investigations resulted in curve-fit expressions for the electrical soil parameters as a function of frequency and water content .

$$\varepsilon_r\,(f) = 10^D \qquad (6.1)$$

$$6\,(f) = 10^K\,[mS/m] \qquad (6.2)$$

Where

$$D = 5.491\ +\ 0.946\log_{10}(\sigma_{100Hz})\ -\ 1.097\log_{10}(f)\ +\ 0.069\log_{10}{}^2(\sigma_{100Hz})$$

$$-\ 0.114\log_{10}(f)\ \log_{10}(\sigma_{100Hz})\ +\ 0.067\log_{10}{}^2(f)$$

$$K = 0.028\ +\ 1.098\log_{10}(\sigma_{100Hz})\ -\ 0.068\log_{10}(f)\ +\ 0.036\log_{10}{}^2(\sigma_{100Hz})$$

$$-\ 0.064\log_{10}(f)\log_{10}(\sigma_{100Hz})\ +\ 0.018\log_{10}{}^2(f)$$

f is the energised frequency in [Hz] and σ_{100Hz} is the conductivity at 100 Hz in [mS/m].

6.3.2 Smith and Longmire Model

The model proposed by Smith and Longmire [6.7] is called the universal soil model, which is depended on the measured conductivity and permittivity of samples of concrete and grout. Their model was able to present the frequency of soil parameters over frequencies ranging from 1Hz up to 200MHz. The conductivity and permittivity frequency dependence are expressed as follows:

$$\varepsilon_r\,(f) =\ \varepsilon_\infty + \sum_{i=1}^{13}\frac{a_i}{1 + (\frac{f}{F_i})^2} \qquad (6.3)$$

$$\sigma(f) = 2\pi\varepsilon_\circ \sum_{i=1}^{13} a_i\,F_i\,\frac{(\frac{f}{F_i})^2}{1 + (\frac{f}{F_i})^2}\ [mS/m \qquad (6.4)$$

Where σ_{DC} represents the DC soil conductivity, ε_∞ is the high frequency limit of the dielectric constant, which was set to 5, and F_i was calculated as follows:

$$F_i = \left(F_{6_{DC}} \right) . 10^{i-1} \ [Hz] \tag{6.5}$$

$$F_{(6_{DC})} = (125 \ 6_{DC})^{0.8312} \tag{6.6}$$

Finally, the coefficients values a_i are listed in Table 6.1

Table 6.1: Coefficients a_i for the Smith-Longmire soil model.

i	a_i	i	a_i
1	$3.4 * 10^6$	8	$1.25*10^1$
2	$2.74 * 10^5$	9	$4.8*10^0$
3	$2.58 * 10^4$	10	$2.17*10^0$
4	$3.38 * 10^3$	11	$9.8*10^{-1}$
5	$5.26 * 10^2$	12	$3.92*10^{-1}$
6	$1.33 * 10^2$	13	$1.73*10^{-1}$
7	$2.72 * 10^1$		

6.3.2 Visacro and Alipio Model

Visacro and Alipio proposed a model to determine the frequency dependence of soil parameters according to the results obtained by a series of field experiments for 30 locations [6.12]. They applied their methodology to 31 soil samples with a wide range of resistivity, from 60 to 9,100 Ωm. It was found that both soil resistivity and permittivity exhibited strong variations in their values for the frequency interval in the range 100 Hz to 4 MHz. Based on their obtained data, they proposed a new curve-fit expression for the frequency dependence of the soil's relative permittivity and conductivity. The permittivity expression is valid from 10 kHz up to 4MHz. However, for the conductivity, it is valid from 100 Hz to 4MHz.

$$\varepsilon_r \ (f) = 7.6 \times 10^3 f^{-0.4} + 1.3 \quad \geq 10kHz \tag{6.7}$$

$$6 \ (f) = 6_{100Hz} \times \left\{ 1 + \left[1.2 \times 10^{-6} \times \left(\frac{1}{6_{100Hz}} \right)^{0.73} \right] (f - 100)^{0.65} \right\}^{-1} \tag{6.8}$$

6.4   Test Configuration

A series of experiments were performed in the laboratory under controlled conditions in order to characterise the frequency dependence of soil parameters. Figure 6.1 shows the test setup that was used to observe the behaviour of soil energised by DC and variable frequency AC currents. The conducting medium was brought from Cardiff University's earthing system facility, prepared in the laboratory, and mixed with different moisture levels (10%, 15% and 20%) according to weight rates. The test cell used in the investigations was first developed in [6.13] with different material electrodes. Two rectangular copper plate was bonded to the cell and separated by an insulated mounting panel. The copper plate consisted of two parts: a central circular electrode forming 1/3 of the whole plate area and the remaining frame of the plate. Thin insulation was used to separate the circular electrode from the rectangular electrode frame.
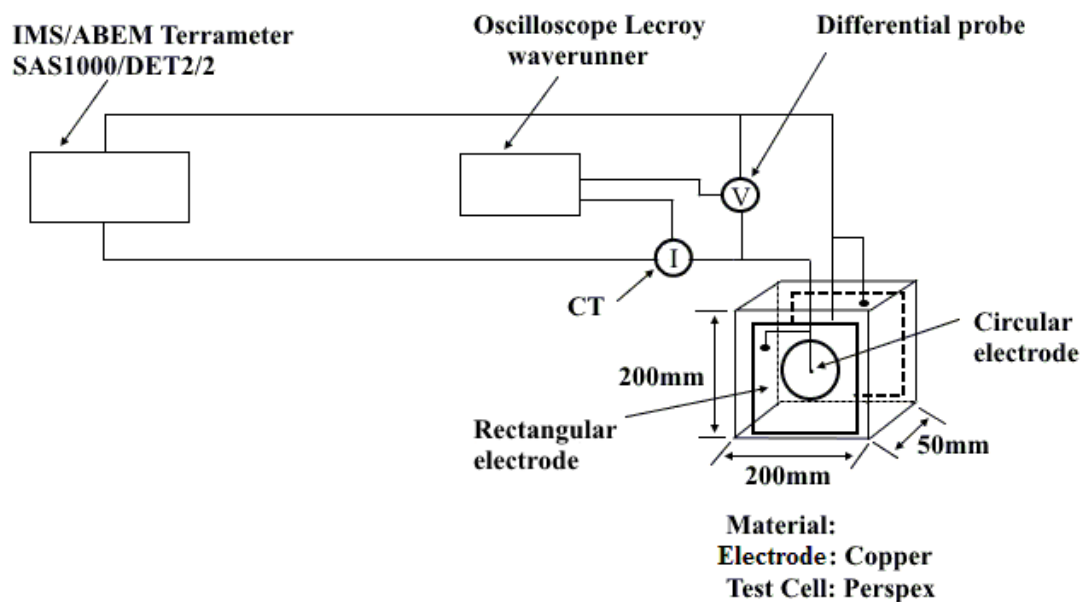
Figure 6.1: Experimental setup of DC and AC tests at Cardiff University high voltage Laboratory.

DC tests were implemented with two instruments. The first DC tests were performed using DET2/2 to measure the sample resistance. This instrument can inject at two current levels (8 mA, 40 mA) at a 128 Hz frequency. The four channels of the instrument were connected directly to the test cell by a short connector to minimise the series impedance. The second set of tests was performed with the ABEM Terrameter SAS1000. The ABEM test configuration is identical to that of the DET2/2 instrument. However, the ABEM is capable of injecting a much higher current. The injected DC currents ranged from 1mA up to 1A over a 1 Hz frequency. Due to the very low switching frequency of the ABEM, ohmic heating of the sample was more likely; therefore; the tests had to be implemented as quickly as possible.

The AC energisation was achieved by IMS and RF instruments. The Impedance Measurement System (IMS) developed at Cardiff University [6.14] was employed for the AC tests. The output of the power amplifier was connected across the test cell, as shown in Fig 6.1. A differential voltage probe and current transducer model 58MH100 were used to measure voltage and current respectively, and were connected directly to a digital storage oscilloscope (LeCroy Wave runner 64Xi). The same scenario was repeated with the RF instrument, which is capable of delivering test currents with a frequency from 10 kHz up to 10 MHz.

Figure 6.2 shows the test circuit for impulse energization. A resistive divider with a ratio of 500:1 and a current transducer with a ratio of 10:1 were used to measure the voltage and current respectively. These are then terminated with a measurements oscilloscope, Lecroy wave jet 314.
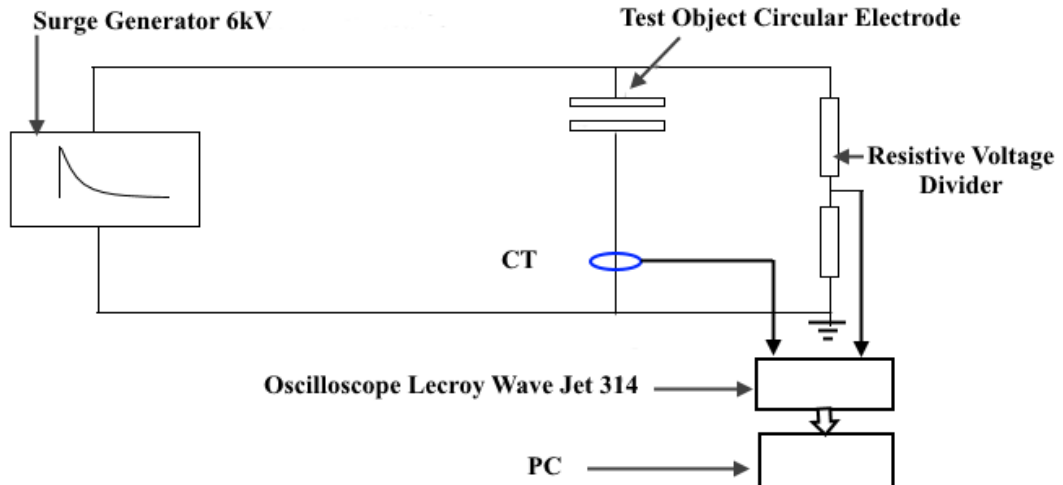
Figure 6.2: Laboratory Experiment of test setup for impulse tests.

6.4.1 DC Resistance and Resistivity measurements

The two DC instruments, DET and ABEM, described above were used to cover a wide range of injected currents up to 200mA. Three soil water content ratios (by weight) were used during these tests; 10%, 15% and 20%. From the measurements of resistance, the resistivity of the test soil was obtained using the geometry of the test cell.

As shown in Figure 6.3, the tests show similar trends to those obtained with tests carried out on electrodes in low resistivity water and the soil [6.15]–[6.17]. The non-linear behaviour with current magnitude was found to be more significant at very low frequencies, which might be attributed to the electrical nonlinearity of the soil itself and at the metal/medium interface. Moreover, as expected a clear and significant dependence of the resistivity on water content is obtained. Up to 75% drop can be seen when water content was changed from 10% to 20%. The implication of this for real earthing systems is that, under heavy rain the earth resistance drops significantly but, as the soil dries, it is important to consider its impact on the rise of earth potential and safety implications.
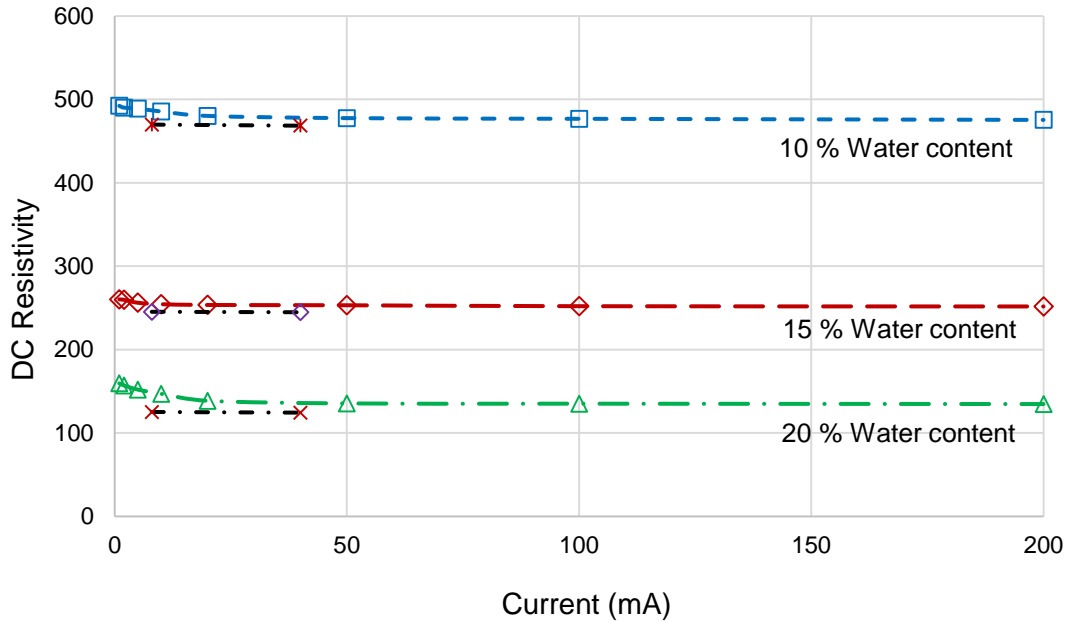
Figure 6.3: Effect of DC magnitude and moisture level on soil resistivity.

The test configuration described in Figure 6.1 was used to measure the impedance of the soil sample with a constant current (10mA) over a spectrum of frequencies from 50 Hz up to 1MHz. Figure 6.4 shows the behaviour of the soil sample with different percentages of water content. Due to the high impedance of dry soil, which limited the injected current, all the measurements were implemented with various moisture levels, starting with 10% according to weight ratios. For frequencies from 50Hz up to 6 kHz, an almost constant value of impedance was observed, which shows close agreement with the DC resistance. As the frequency increased further to 100 kHz, a reduction in impedance was observed. After this frequency, the capacitive effect of the soil was clearly observed, and the impedance magnitude was reduced to about 50% of the low-frequency impedance. Also, the impedance value showed a high percentage of reduction in its value with an increase in water content. This means that the higher the rate of moisture is, the lower impedance value will be. Moreover, the phase shift between the two measured signals of voltage and current are obtained. Due to the capacitive behaviour, the current led the

voltage by a small angle (almost zero) at low frequency, and an increase clearly occurs at high frequency, as shown in Figure 6.5.

In addition, for a number of frequencies, the ac variable frequency tests were conducted using different levels of injected current ranging from 3 to 25mA. As can be seen in Figure 6.6, for the test frequencies used in this experiment, a slight decay of impedance with increasing current magnitude is easily observable. Such observation in the impedance trend with current magnitude was previously highlighted in earlier work when testing ground electrodes in the field [6.15]-[6.17].
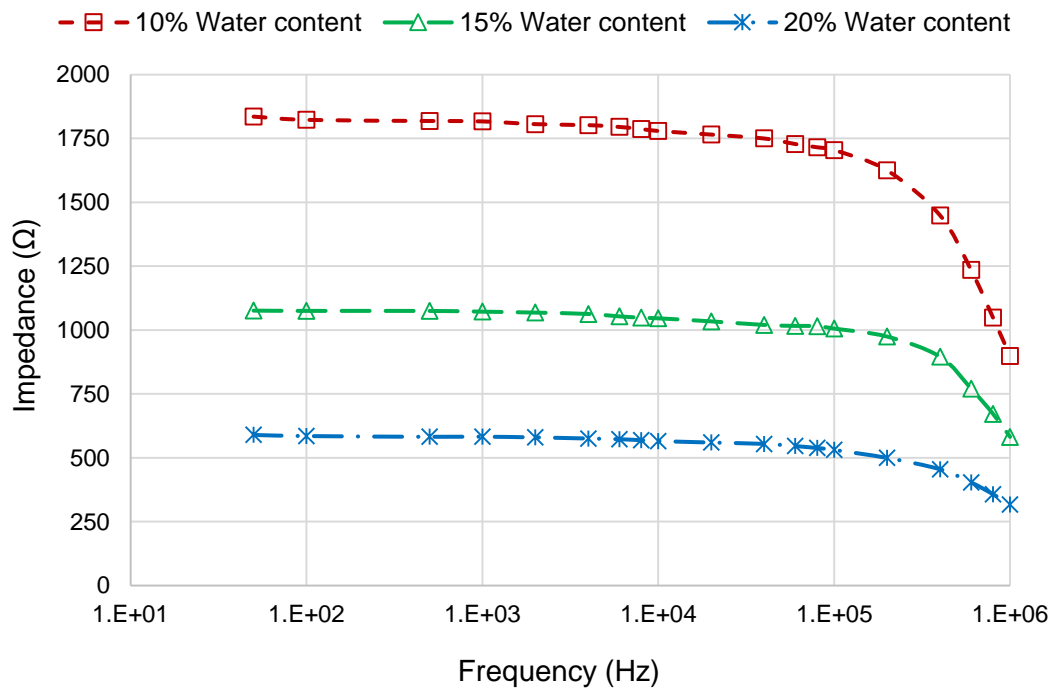
Figure 6.4: Measured impedance of soil sample as a function of energisation frequency and water content
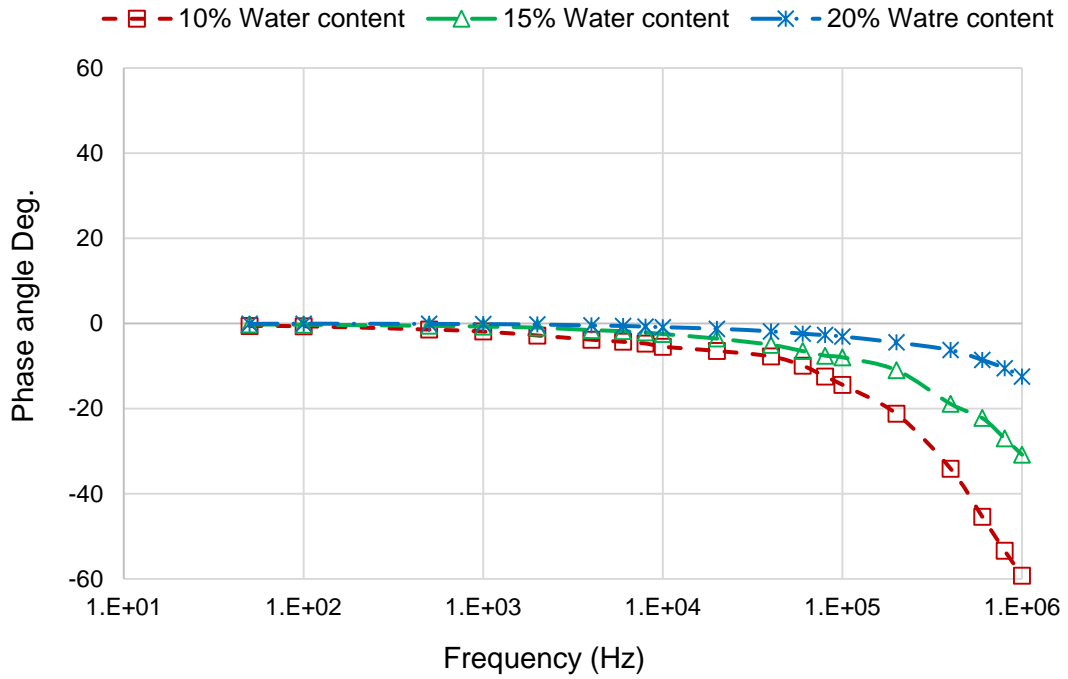
Figure 6.5: Phase shift of soil sample as a function of energisation frequency and water content.
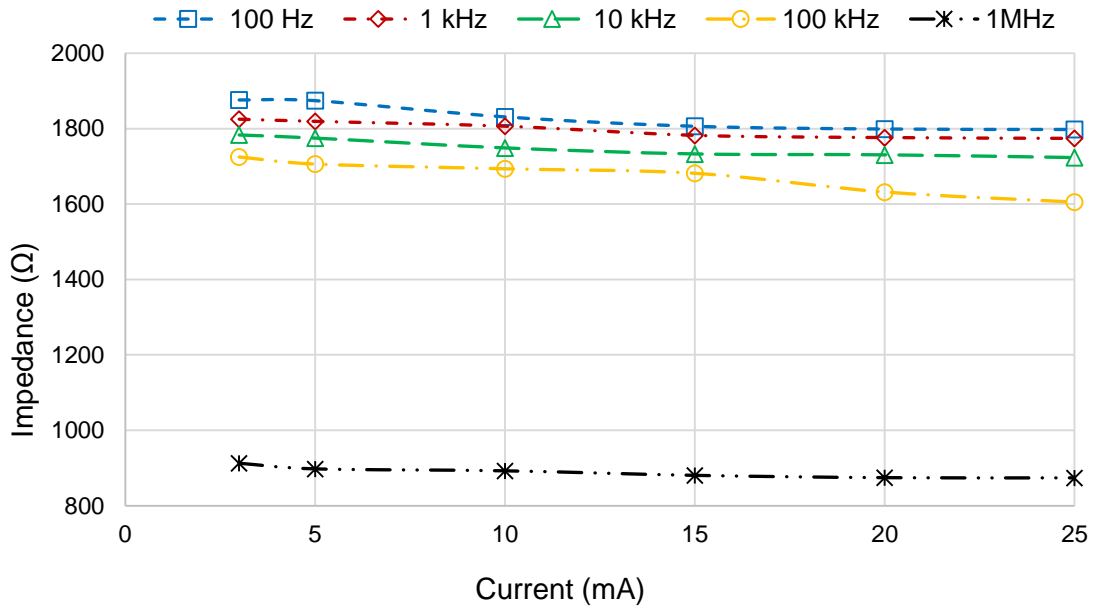
Figure 6.6: Effect of current magnitude on the measured impedance value with 10% water content.

6.4.2 Impulse tests

The test configuration described in Figure 6.2 was used to perform low and high voltage impulse injection, in soil with different percentages of water content. The waveforms of the current and the voltage at the injection point were recorded, and these are shown in Figure 6.7. It is clear from the figure that the current led the voltage by a small angle due to the capacitive effect. Moreover, under the same condition (water contents), the impedance value was seen to be decreasing as the injected current and frequency content increased, as shown in Figure 6.8. The figure indicates that the 10% water content soil had the highest rate of change in impedance value over the frequency and the injected current, and the impedance exhibited a reduction in the rate of change in both frequency content and injection current as the water content increased.

(a) Applied voltage peak 2kV

(b) Applied voltage peak 3kV

(c) Applied voltage peak 5kV

(d) Applied voltage peak 6kV
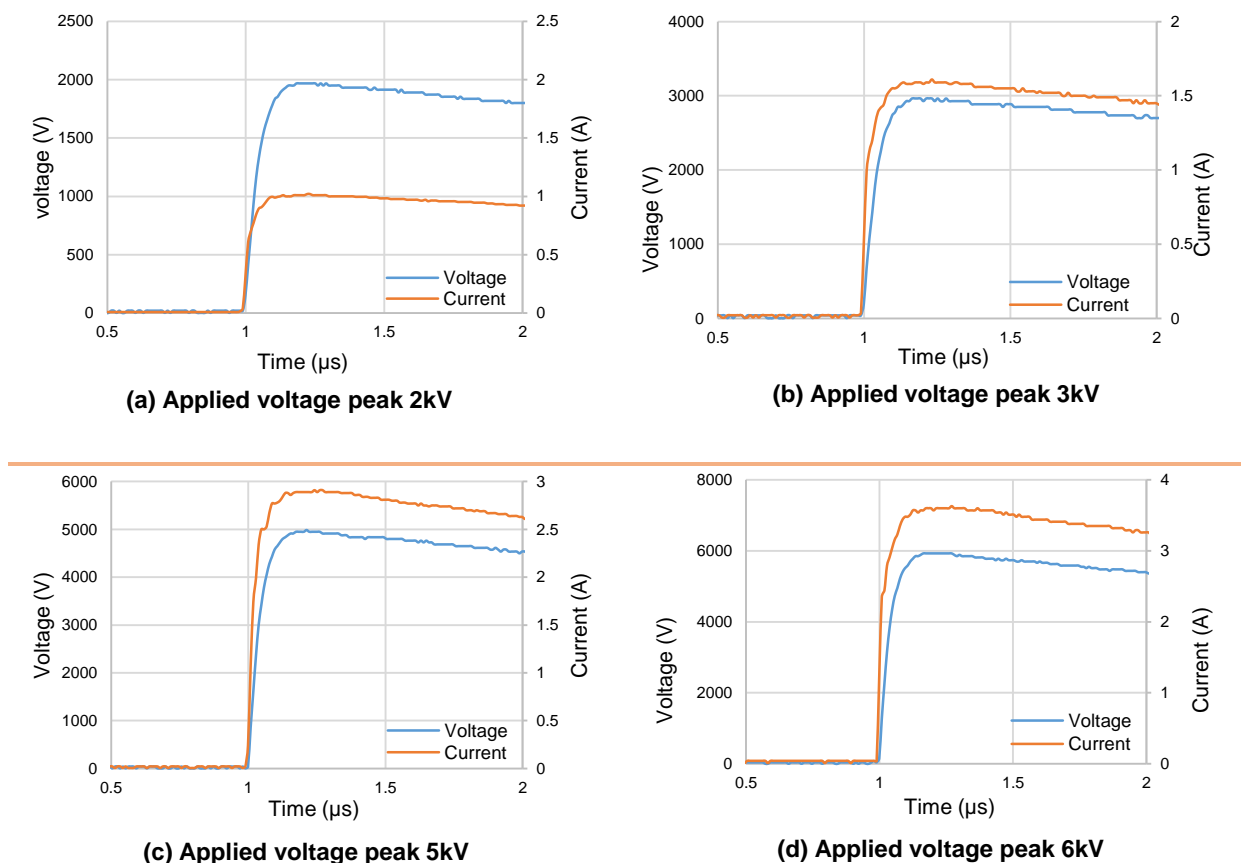
Figure 6.7: High voltage impulse test with soil having 10% water content.
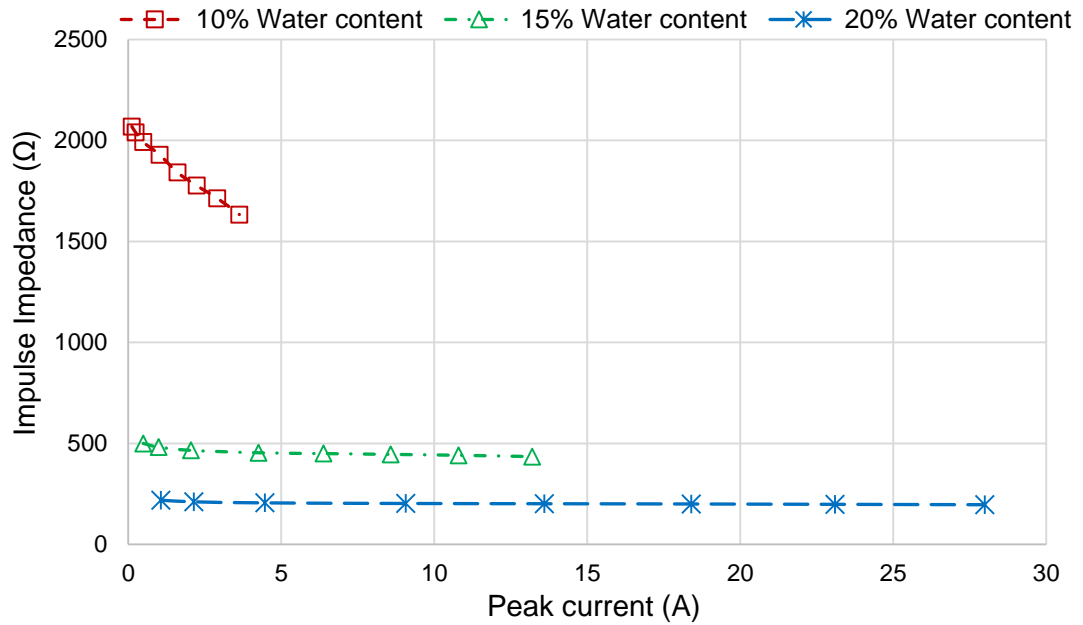
Figure 6.8: Impedance value of the soil with different percentages of water content versus peak injected current.

6.4.3 Frequency dependence of soil electrical parameters

The current was injected at the circular electrode, and both the input current and output current were measured to make sure that the current density was uniform (see Figure 6.9). The percentage error between the input and output current should be 1%; if the percentage error exceeds this ratio, this means the current density is non-uniform.
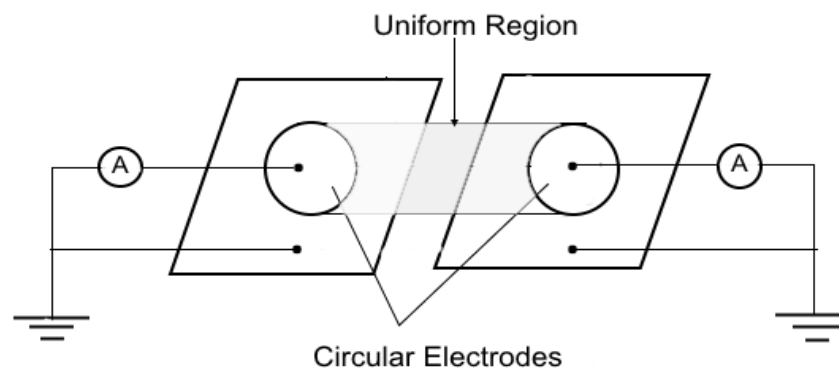
Figure 6.9: Test circuit.

Both voltage and current waveforms were recorded. Figure 6.10 and Figure 6.11 show examples of the waveforms for 10% water content.
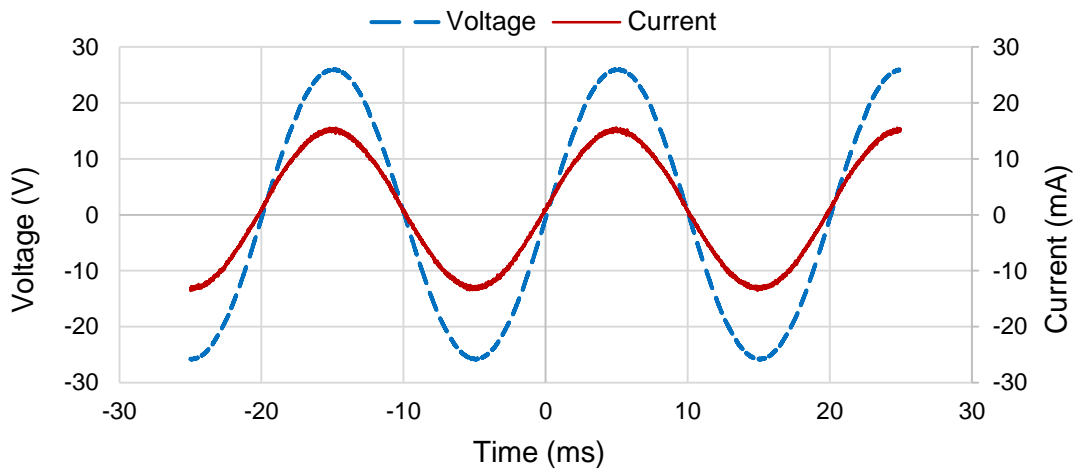
Figure 6.10: Measured voltage and current waveforms in a soil medium (AC test at 50Hz).
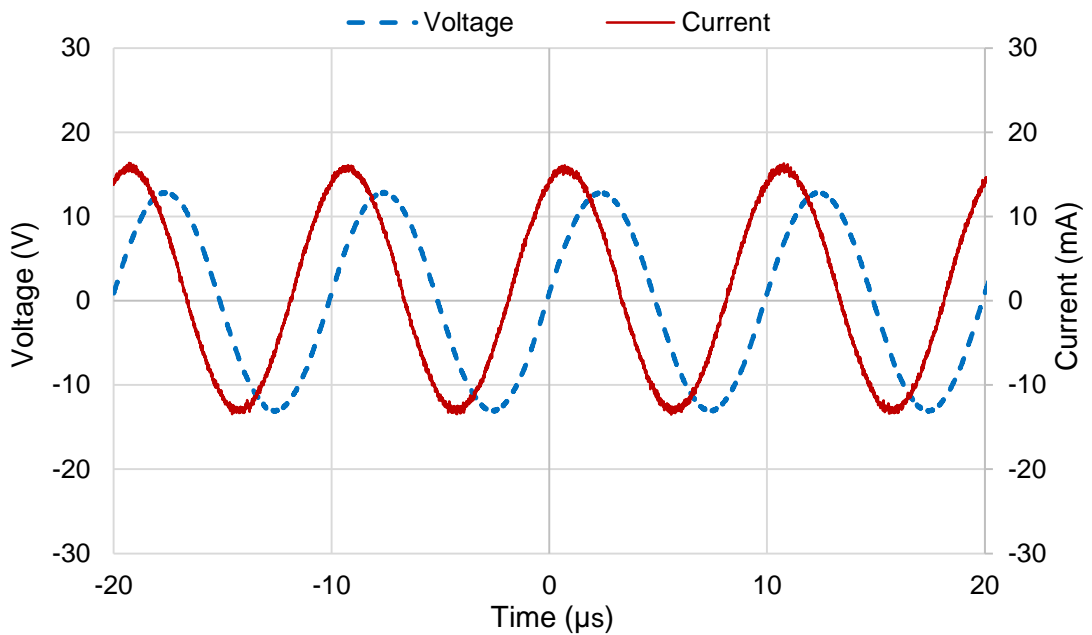
Figure 6.11: Measured voltage and current waveforms in a soil medium (AC test at 100 kHz).

The accuracy of the results obtained with the oscilloscope is essential. Therefore, a simple calculation was implemented on the waveforms of both voltage and current to calculate the phase shift between them. The measurement shows that the current led the voltage in

the small angle at low frequency and started to increase to become noticeable at high frequency.

The phase angle between the signals was calculated by determining the average power using Equation (6.9). Then Equation (6.10) was applied to calculate the cosine angle.

$$P_{av} = \frac{1}{T} \int_0^t v_{(t)} \times i_{(t)} \, dt \tag{6.9}$$

$$\cos \theta = \frac{P_{av}}{I_{rms} \times V_{rms}} \tag{6.10}$$

The admittance of the test sample is presented as

$$Y = \left| \frac{1}{Z} \right| \llcorner \theta \tag{6.11}$$

Moreover, it can be written as

$$\frac{1}{Z} = \frac{1}{R} + j\omega c \tag{6.12}$$

Therefore, the resistance component and capacitance component are expressed as

$$\frac{1}{R} = \left| \frac{1}{z} \right| \cos \theta \tag{6.13}$$

$$C_\omega = \left| \frac{1}{Z} \right| \sin \theta \tag{6.14}$$

According to these measured signals, the impedance components (resistance and capacitance) were calculated. The applied current was injected at the circular electrode of the cell. Therefore, the area of the cylinder is considered to calculate the resistivity and the permittivity by using Equations (6.15) and (6.16):

$$\rho = \frac{R\,A}{l} \tag{6.4}$$

$$\varepsilon_r = \frac{C\,d}{\varepsilon_\circ\,A} \tag{6.16}$$

R is the resistance, A is the area of the cylinder, d is the space between the circular electrodes ε_r is the relative permittivity, and $\varepsilon_\circ$ is the permittivity of the free space, which is $8.85 \times 10^{-12}\ F/m$.

Figure 6.12 presents the soil resistivity determined from the measurements of different percentages of water content. It shows a significant variation in frequency and exhibits the same trend as predicted in [18]–[20]. At low frequency, the resistivity is almost constant and shows good agreement with the calculated DC resistivity up to 6 kHz with all moisture levels. After this threshold frequency, the resistivity decreased dramatically up to 1MHz. Also, the increase in water content in the soil affects the performance of the earthing system. As shown in the figure, the resistivity exhibited a reduction in resistivity with increased moisture content.
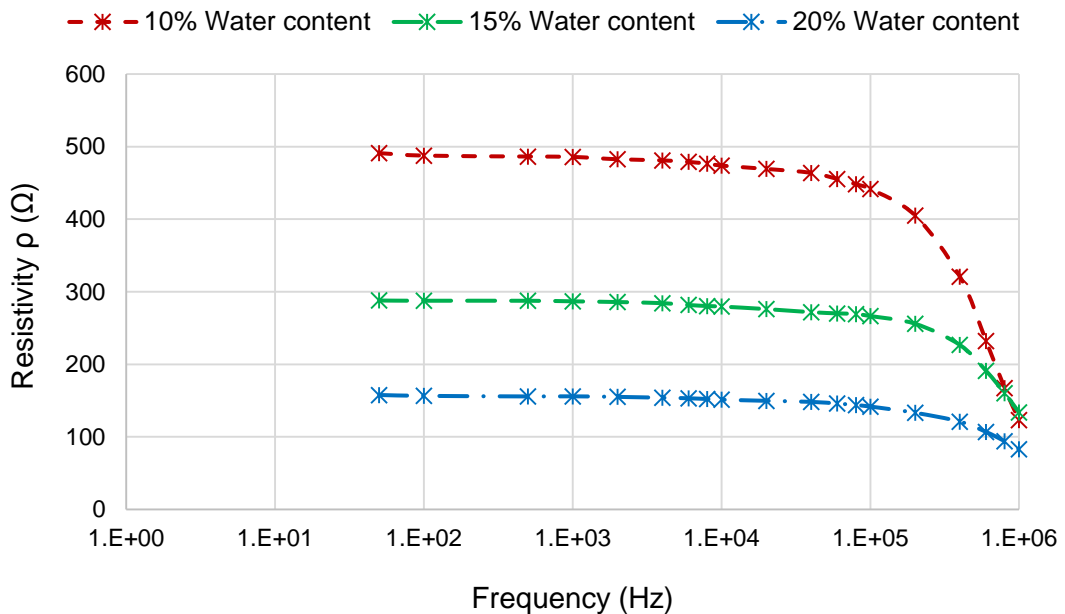
Figure 6.12: Resistivity variation with frequency at different water content levels.

The permittivity investigation was implemented over different moisture levels and a range of frequencies from 100 Hz up to 1 MHz. The relative permittivity magnitude decreased as frequency increased to about (65, 60, and 45) with 10%, 15%, and 20% water content respectively, as shown in Figure 6.17. Moreover, the moisture level of the conducting medium has a significant influence on the permittivity value. The figure shows a reduction in the permittivity as the water content increases in the soil medium.
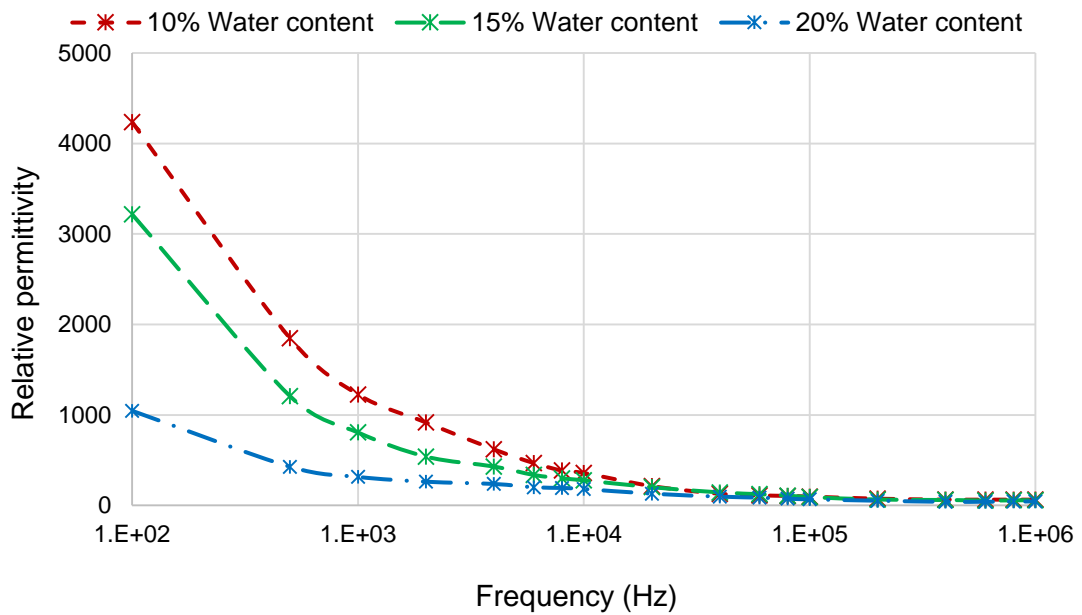
Figure 6.13: Relative permittivity variation with frequency at different water content levels.

6.5 Comparison of the Soil Models

The results obtained by the experiments were compared with the frequency dependence properties of the soil medium conducted by Scott, Smith, and Visacro [6.7], [6.8], [6.13]. The comparison holds with different moisture levels. With a 10% water content, the conductivity of the soil shows good agreement with the Scott and Smith models at low and high frequency up to 400 kHz, and with Visacro model upto 100kHz, as shown in Figure 6.14. Above this frequency, the conductivity shows a divergence and exhibits an increase in its value.

Figure 6.15 shows a close agreement between the Smith model and the obtained permittivity value of experiment at low frequency. However, the results does not show convergence to Scott model. At high frequency, the experimental results show good agreements with all models.

Figure 6.16 presents the conductivity of the soil determined by the frequency dependence models and the results of the experiment with 15% water content. The influence of moisture on the soil is reflected in the conductivity by increasing its magnitude. Close agreements was obtained between Visacro and Scott models and the results of the experiment. However, the Smith model diverged. Also, the permittivity of the soil was demonstrated by experiments, and compared with other models. Visacro and the Smith models show close agreements with the experimental results, see Figure 6.17.

As the water content increased, the resistivity of the soil medium decreased, which led to an increase in the conductivity of the soil. Figure 6.18 presents the conductivity comparison of other models with the results of the experiment at 20% water content. Good agreement was obtained between Smith model and the results of the experiment up to 100kHz, and then the experimental results show an increase in the conductivity values with frequency increase. Moreover, the relative permittivity of the soil was determined and compared with the models. There is a disagreement with all of models up to 10 kHz. After this frequency, good agreement was obtained with the results and other models, as shown in Figure 6.19.
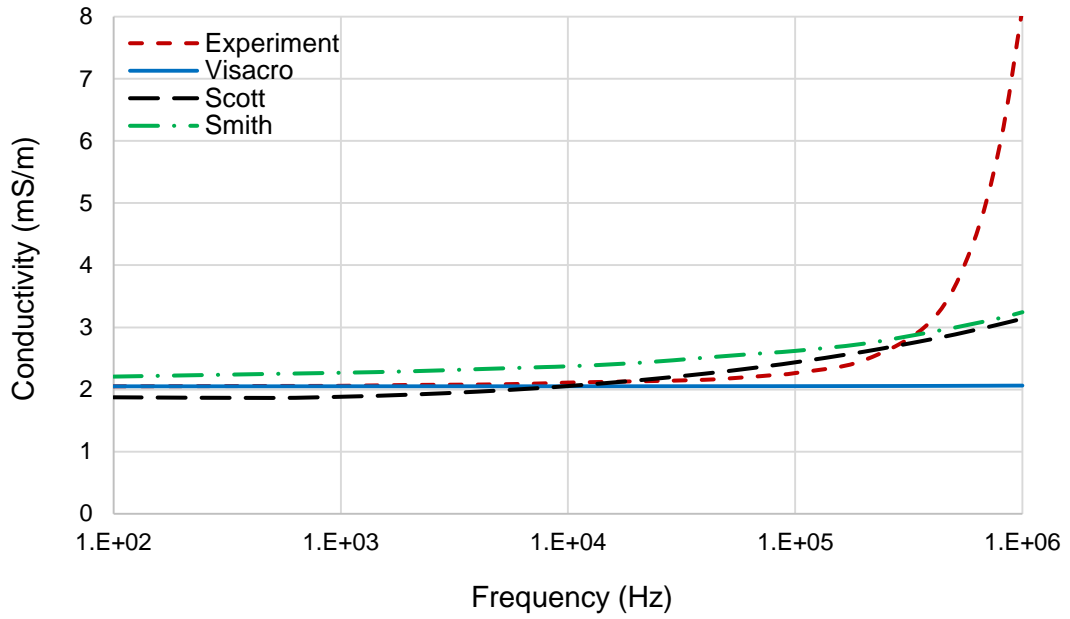
Figure 6.14: Frequency dependent soil conductivity obtained by different soil models ($\rho_\circ$=491Ωm according to water content).
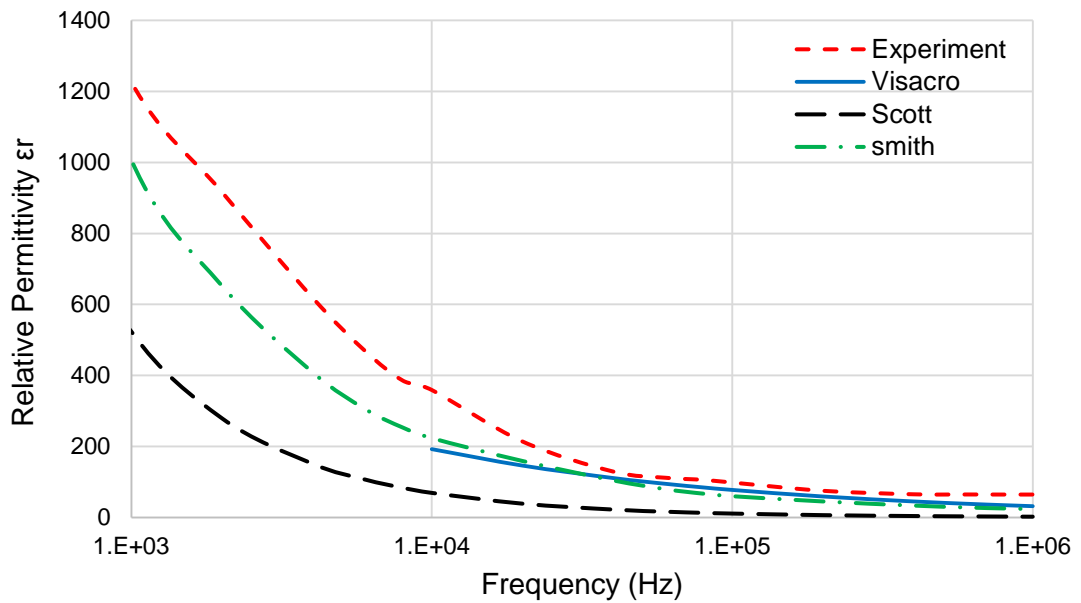
Figure 6.15: Frequency dependent soil relative permittivity obtained by different soil models ($\rho_\circ$ =491Ωm according to water content).
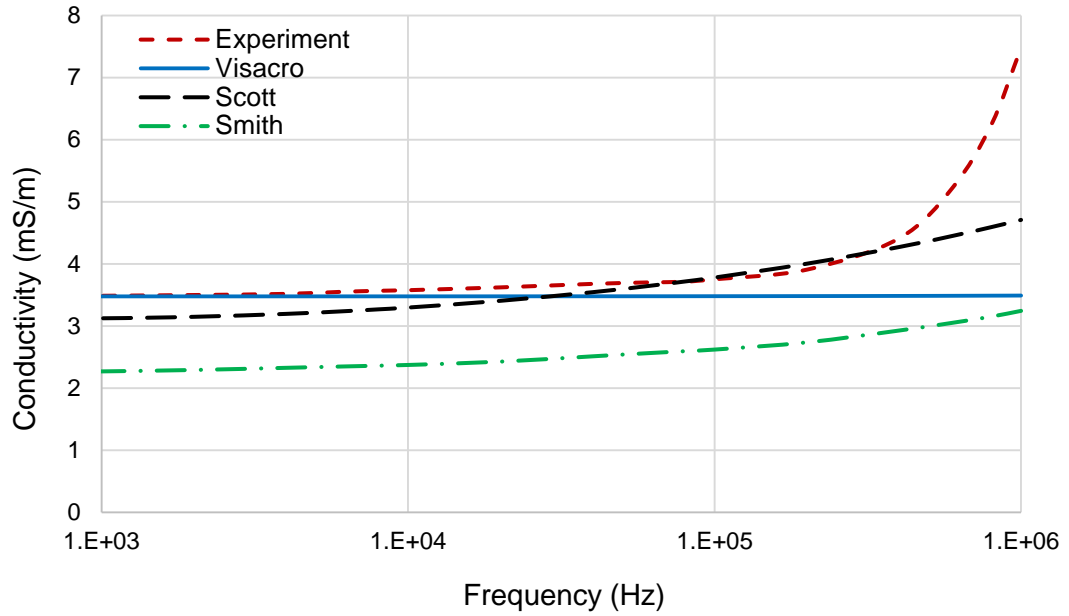
Figure 6.16: Frequency dependent soil conductivity obtained by different soil models ($\rho_\circ$=287Ωm according to water content).
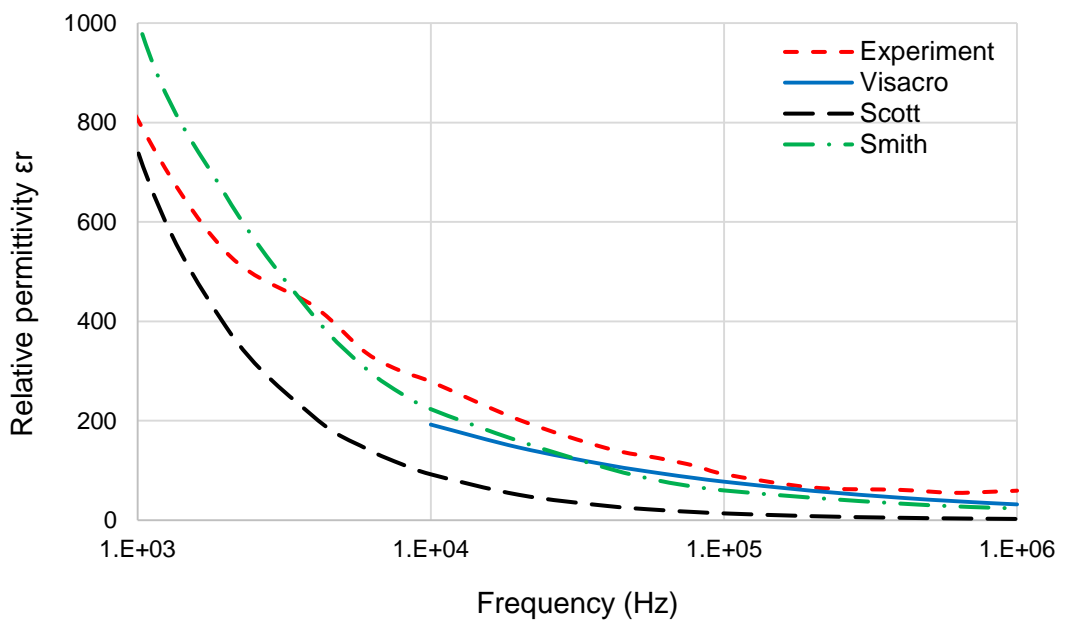
Figure 6.17: Frequency dependent soil relative permittivity obtained by different soil models ($\rho_\circ$ =287Ωm according to water content)
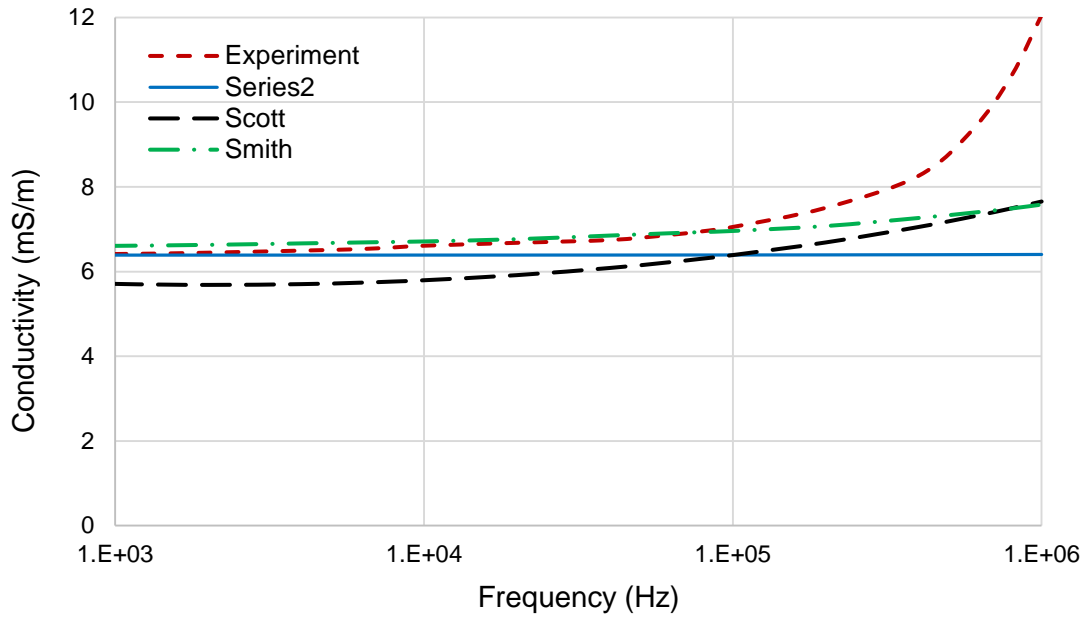
Figure 6.18: Frequency dependent soil conductivity obtained by different soil models

($\rho_\circ$=157Ωm according to water content)
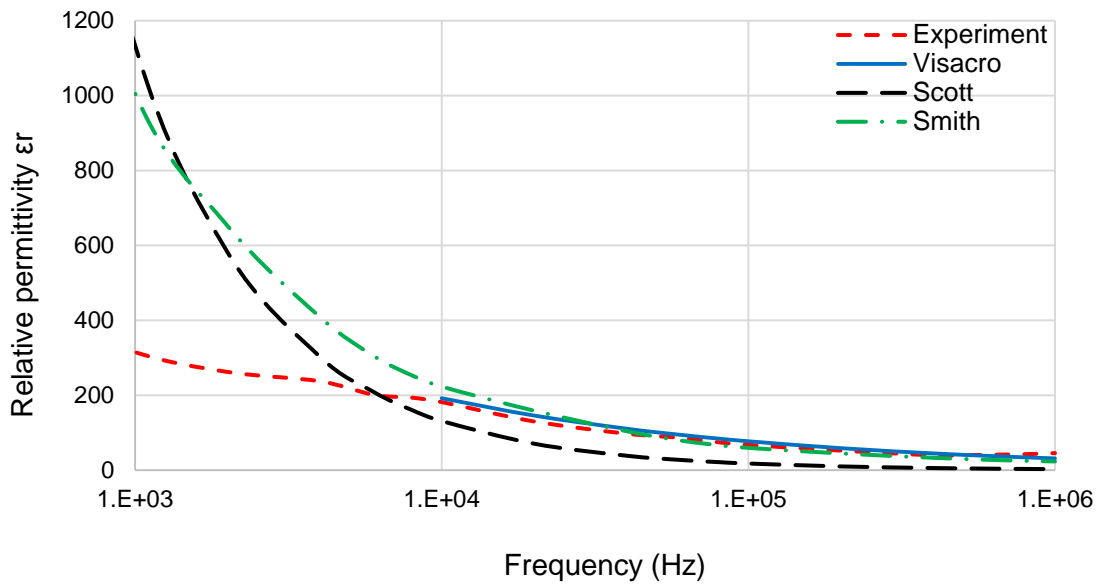
Figure 6.19: Frequency dependent soil relative permittivity obtained by different soil

models ($\rho_\circ$=157Ωm according to water content)

6.6   Conclusion

Clarification of earthing systems performance under normal and abnormal conditions is necessary to ensure the continuity of the power supply to consumers. Extensive studies have focused on the behaviour of an earthing system when subjected to low-frequency currents, and it is well understood. However, the earthing system exhibited a variation in its behaviour over surge and lightning conditions, and further investigation is required to clarify this variation. In this study, a series of laboratory experiments were performed to highlight the behaviour of the earthing system under DC, AC low voltage, and low/high voltage impulse energisation, and in particular, those factors related to soil parameters (conductivity and permittivity). In addition, the investigation discusses the application of the conservative approach in which the resistivity is assumed to be the same as DC resistance. However, the permittivity varied from 1 to 80, thus leading to significant errors. The soil medium used to implement the experiments was brought from Cardiff University's earthing system facility at Llanrumeny.

The DC resistance was measured using two instruments: DET2/2 and ABEM Terrameters SAS1000. Both instruments showed good agreement; however, due to the non-linearity of the soil and the interface between the metal and the conduction medium, at low currents, the resistance measured by ABEM Terrameter SAS1000 showed a reduction in its value. The same trend was noticed with resistivity.

For AC energisation, a sinusoidal waveform was injected with frequencies ranging from 50 Hz up to 1 MHz. Voltage and current signals were recorded using a DP (differential probe) and a CT (current transducer) respectively. At the first, the impedance and phase angle were calculated by energising the constant current of 10mA. At low frequency, as expected, the resistive characteristics dominated, and the impedance exhibited a constant value up to 6 kHz, which shows good agreement with the DC measurements. After this

frequency, the impedance decreased as the frequency increased due to the capacitive effect. Further calculation was carried out to calculate the phase angle. At low-frequency, the current led the voltage by small angle (almost 'zero') and started to increase as the frequency increased. Secondly, the impedance was measured at specific frequency points (100 Hz, 1 kHz, 10 kHz, 100 kHz, 1 MHz) by energising a range of currents (3, 5, 10, 15, 20, 25) mA. As explained before, due to the capacitive effect, the impedance shows a reduction in its value with the increase in frequency. Moreover, it is noticed that there is a decrease in the measured impedance magnitude with an increase in the injected currents over the same frequency.

In addition, impulse measurements were taken over a range of voltages starting with low voltages up to 6 kV. Fast impulse tests were performed on the central circular electrode to investigate the behaviour of the soil. The peak values of voltage and current recorded during the tests. At low voltage, the impulse test of the impedance value shows close agreement with those of both DC/AC measurements. As the frequency content and voltage level increase, the impedance value decreases, and the phase shift between signals (voltage and current) increases. Therefore, at high voltage energisation, the impedance value show a significant reduction in its value.

Further calculations based on the data collected from the experiments were implemented to explain the variation of the soil conductivity and permittivity as function of frequency. At 10% water content, the resistivity value was high and remained constant up to 6 kHz. Then, the resistivity decreased dramatically over frequency, and the capacitive effect occurred. This means that the conductivity of the medium increases over frequency. However, the permittivity exhibited a reduction in its magnitude as the frequency increased.

Moreover, the percentage of the water content of the soil has a significant influence on the behaviour of the earthing system. A high proportion of the reduction was noticed on the magnitude of DC resistance, AC impedance, and impulse resistance over the percentage of water on the medium. This reduction was about 50%, as the water percentage changed from 10% to 15% and increased to be about 70% at 20% water content. The low percent of water in the medium leads to the high permittivity and low conductivity. Therefore, the water content is a significant substantial factor affecting the behaviour of the earthing system, and this should be taken into consideration in earthing system design, in particular, in countries that have a high precipitation.

CHAPTER SEVEN: CHARACTERISATION OF HIGH RESISTIVITY SUBSTATION MATERIAL: LABORATORY INVESTIGATIONS

7.1 Introduction

The buried earthing systems of electrical substations are designed to ensure the continuity of power demands and provide a path for electrical currents under fault conditions. A core function is to limit the effect of any generated earth potential rise that might endanger life or significantly affect substation equipment. High resistivity materials, such as concrete, stone chippings and gravel, are typically used to cover ground surfaces at substations to provide an electrical safety barrier by increasing the contact resistance between the earth and any workers on the surface. The surfacing material usually chosen depending on the resistivity value, has a significant impact on the permissible body current for touch and step voltages involving the person's feet according to IEEE Std. 80-2000 [7.1]. During the fault conditions, the earthing system dissipates fault currents to the earth. This current flow will produce potential gradients within and around a substation. Adequate precautions should be taken when the earthing system is designed to limit the generated potential gradients along the earth's surface, which might be of sufficient magnitude during fault conditions to endanger a person's life in the area. One of the critical circumstances that makes electric shock accidents possible is the absence of sufficient contact resistance or other series resistances to limit current through the body to a safe value under fault conditions. According to IEEE Std. 80-2000 [7.1], the resistance of a human body from hand-to-feet and also from hand-to-hand, or from one foot to the other foot can be taken at around 1000 Ω. However, any resistances in series with the body resistance are neglected and assumed to be zero. For example, hand and foot contact resistances and glove and shoe resistances. It is important to mention that the chosen body resistance depends on the current path through the human body. In addition, the effect of

the passing currents on the human body depends on the current magnitude, shock duration, frequency and physical condition of the person.

Humans seem to be vulnerable to the effects of electric current of between 50 Hz and 60 Hz frequency range, [7.2]. In addition, under DC, the body can tolerate up to five times higher current than under AC [7.3]. In the case of higher frequencies, from 3 kHz to 10 kHz, even larger currents can be tolerated. Dalziel et al. [7.4] suggested that the maximum tolerable body current $I_{B(Max)}$ for a 50 kg person can be determined from Equation (7.1), and for a 70 kg person, Equation (7.2) can be used.

$$I_{B(Max)} = \frac{0.116}{\sqrt{t_s}} \tag{7.1}$$

$$I_{B(Max)} = \frac{0.157}{\sqrt{t_s}} \tag{7.2}$$

Where $I_{B(Max)}$ is the maximum tolerable current (A) and t_s is the electric shock duration (s).

Therefore, increasing the surface resistance is one of the important techniques to ensure the safety for the workers. The earth resistance is affected by several factors, such as the type of stone, the size and condition of the chippings and the moisture content, only a limit number of previous studies have investigated these materials [7.5]-[7.10]. Detailed information about high resistivity materials and the factors, which can affect resistivity, is given in [7.1].

In this work, four different types of commercially available gravel and concrete were subjected to DC and AC energization under both dry and wet conditions to investigate the effect of wetting on their resistivity.

7.2 Gravel Description and Preparation

The four types of gravel used in this work are shown in Figure 7.1 and described as follows:

(a) 20 mm Cotswold buff decorative stone chippings

(b) 20 mm limestone chippings

(c) 20 mm bulk gravel

(d) 10 mm bulk gravel

In each case, a small batch of gravel was dried in an oven at a temperature of $100^{\circ}C$ for 6 hours, and then cooled to room temperature over 2 hours. Further batches were dried and cooled over a period of 2 days until a sufficient quantity was acquired for experimentation. Experiments were carried out with the dry gravel, and then different amounts of water were added and the experiments repeated for each case.

Figure 7.1: Photographs of the four types of gravel: (a) 20 mm Cotswold buff decorative stone chippings. (b) 20 mm limestone chippings. (c) 20 mm bulk gravel. (d) 10 mm bulk gravel.

7.3 Experimental Setup

The experimental setup as shown in Figure 7.2. A 60x35x30 cm wooden box with two 60x30 cm aluminium plates fitted to opposite sides was used to contain the gravel. Electrical connections were made to the outside centre of each plate and connected to DC and AC measurement electronics. A CT and differential probe was used to measure the voltage and current of an AC low voltage circuit of frequency 50 Hz to 1 MHz, with both the CT and voltage probe connected to storage oscilloscopes.

The amount of water added to the samples depended on their saturation level. Sample (a) had 5% and 10% water by volume added, whereas samples (b) and (c) had 3% and 5%, and sample (d) had 3%, 5% and 10%.

The same configuration was repeated as shown in Figures 7.3 and Figure7.4 for concrete and work boots. A 60x30x20 cm concrete column with two 60x30 cm aluminium plates fitted to opposite sides was used to investigate the characteristics of the concrete. The concrete column was immersed in a water pool for three intervals (15, 30, and 60 minutes) to absorb water. Then, the measurement procedure was implemented.
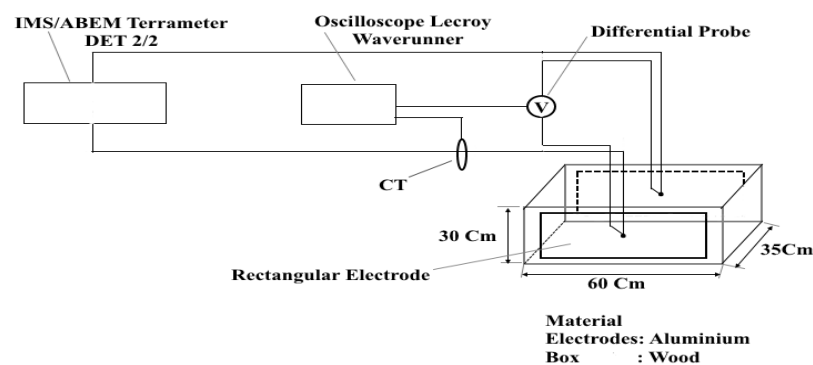
Figure 7.2: Experimental setup for DC and AC tests.
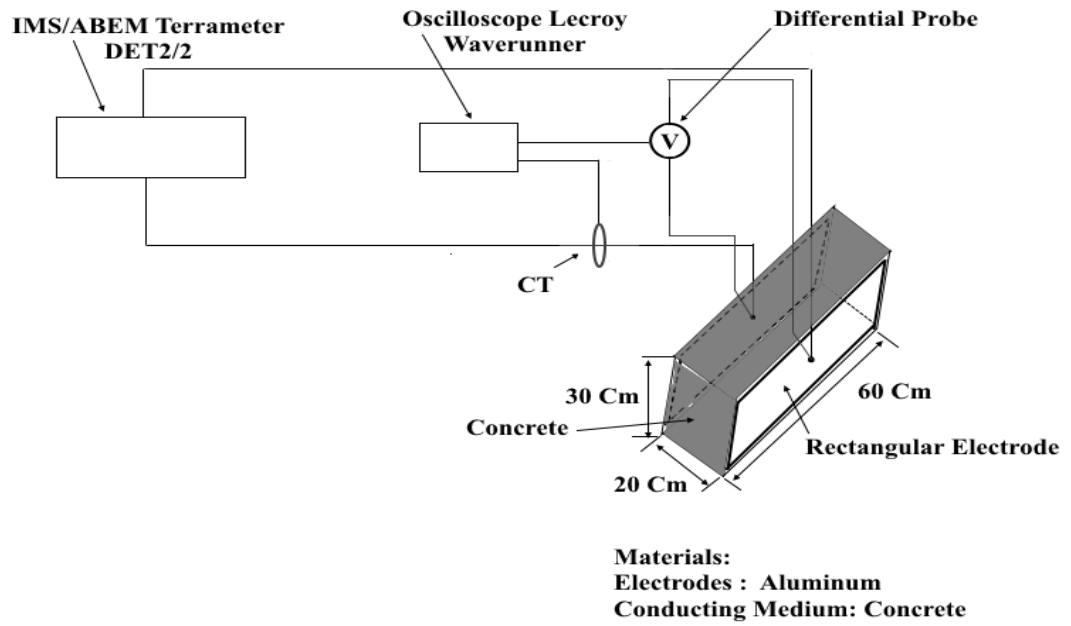
Figure 7.3: Experimental setup for DC and AC tests of concrete.
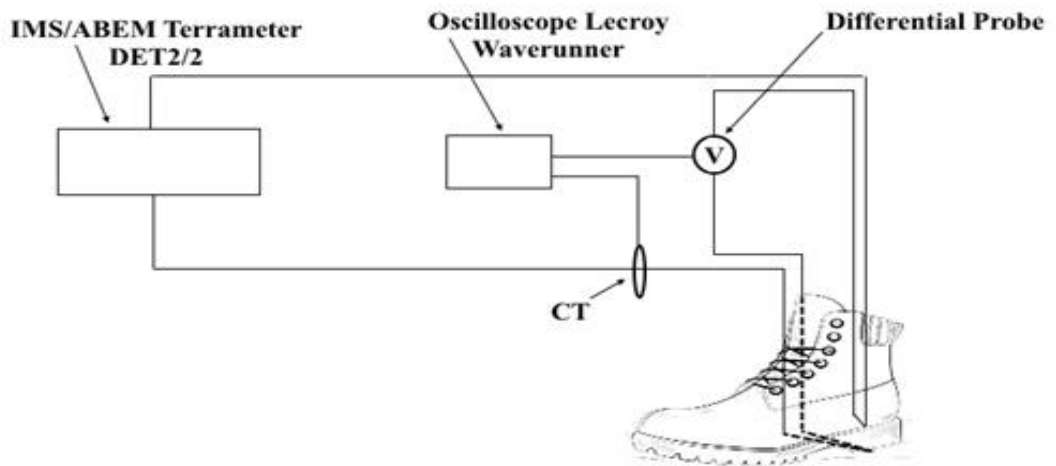
Figure 7.4: Experimental setup for DC and AC tests of work boots.

7.4   Results and Discussion

7.4.1   Gravel properties

DC resistance measurements were conducted using the ABEM Terrameter and DET2/2 instruments, and low currents were used to energise the test samples with switched DC frequencies of 1 Hz and 128 Hz. The measurements exhibited a reduction in DC resistivity for currents up to 5mA, after which it remained constant. This may be due to the non-linearity of the conducting medium or the interface between different materials [7.11] and[7.12].

The DC resistivity of the samples is shown in Figures 7.5 to Figure 7.8. In all cases, the resistance of the dry gravel was high, so it was measured as an open circuit. However, when water was added, the resistance decreased. Proportionally water was measured and added to the materials according to the volume in different percentages depending on the nature of the gravel. For instance, in Sample (a), the DC resistance was measured as an open circuit from 1% to 4% water content. Hence, measurments were taken at 5% water content. In addition, the test sample was found to saturate and could not obsorb effectively more than 10% of water content.

For AC, the RMS values for the voltage and current from the CT and differential probe were saved and the impedance calculated. As the frequency increased, the impedance decreased due to the capacitive effect. These results are given in Figures 7.9 to 7.12. The DC resistance compared to the AC tests at 50 Hz show close agreement, as shown in Table 7.1.
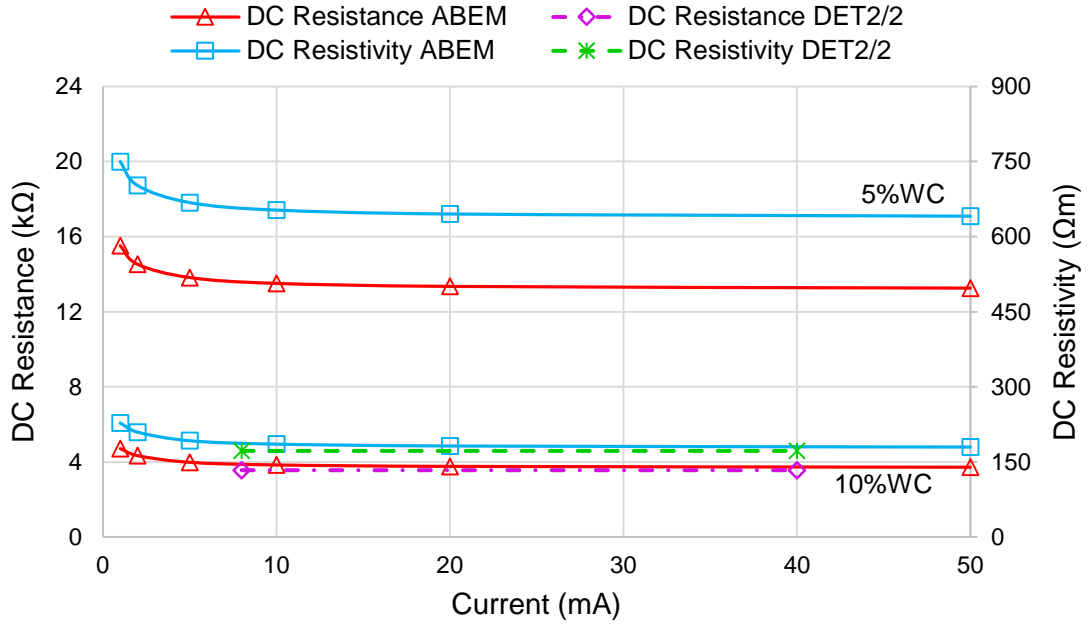
Figure 7.5: Measured DC resistance and resistivity of 20 mm Cotswold buff decorative stone chippings, sample (a).
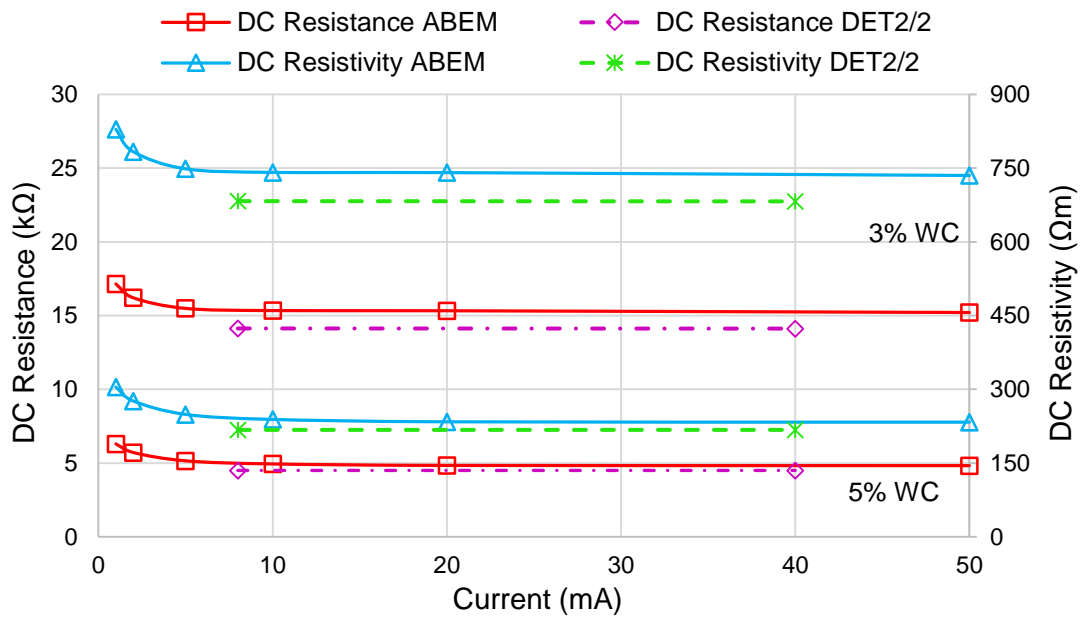
Figure 7.6: Measured DC resistance and resistivity of 20 mm limestone chippings, sample (b).
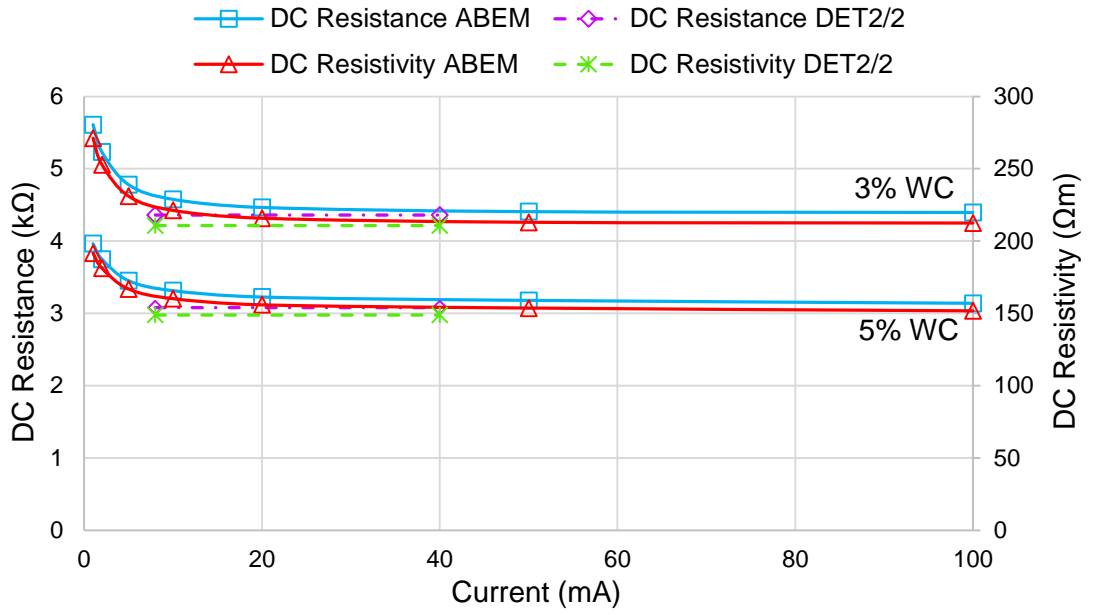
Figure 7.7: Measured DC resistance and resistivity of 20 mm bulk gravel, sample (c).
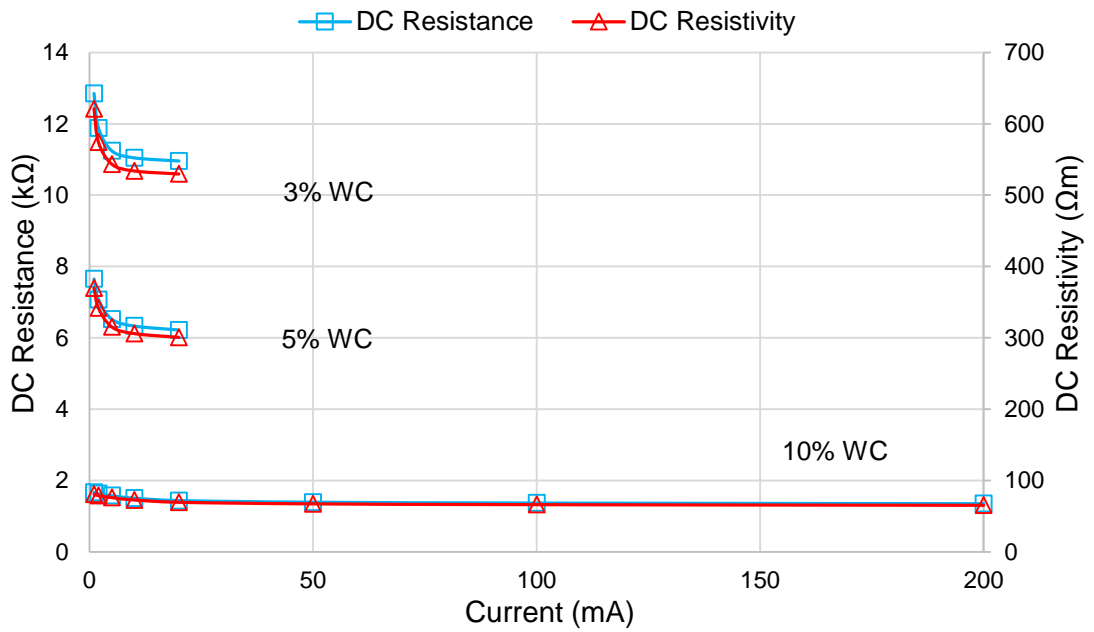
Figure 7.8: Measured DC resistance and resistivity of 10 mm bulk, sample (d).
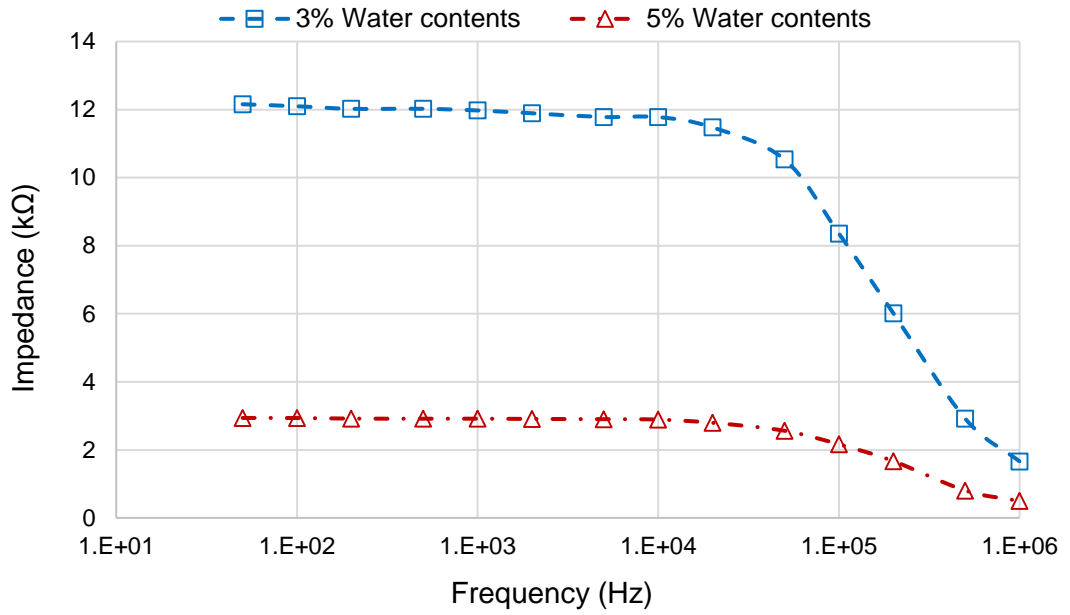
Figure 7.9: The measured impedance of gravel: 20 mm Cotswold buff decorative stone chippings, sample (a) as a function of frequency and water content.
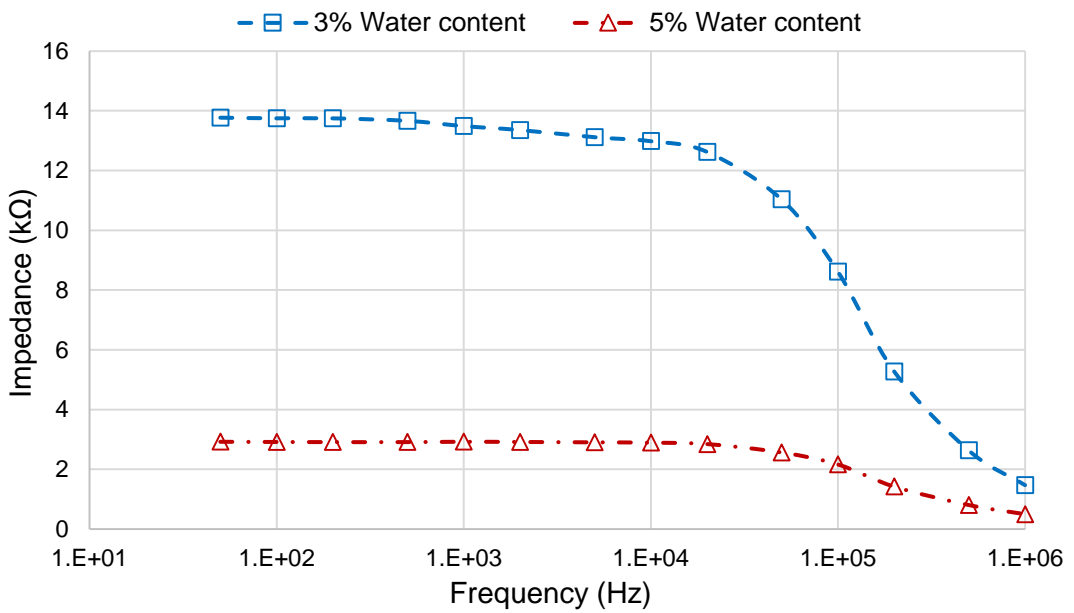
Figure 7.10: The measured impedance of gravel: 20 mm limestone chippings, sample (b) as a function of frequency and water content.
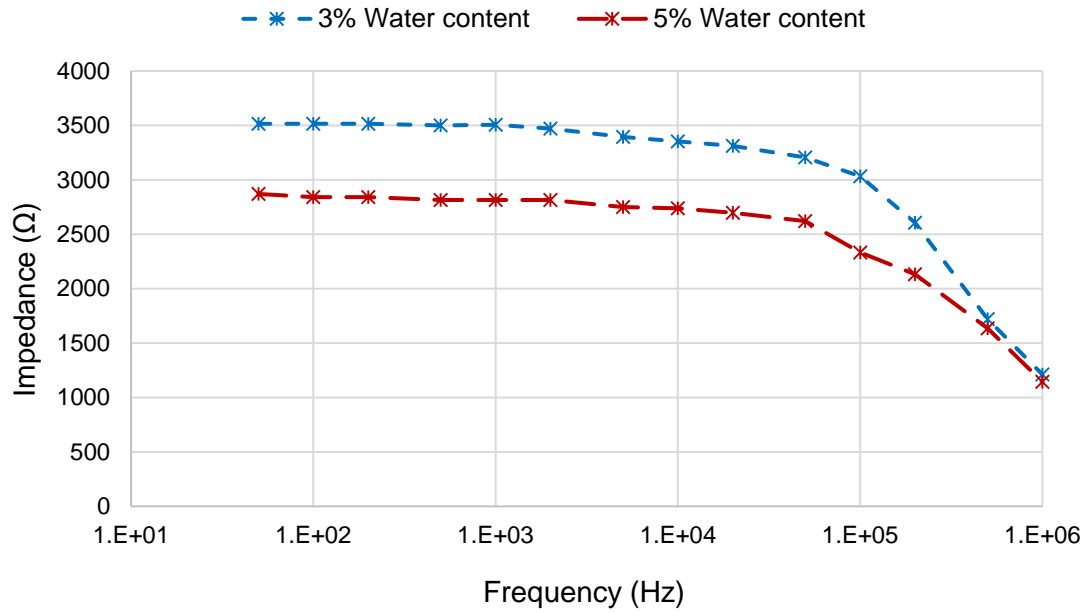
Figure 7.11: The Measured impedance of gravel: 20 mm bulk gravel, sample (c) as a function of frequency and water content.
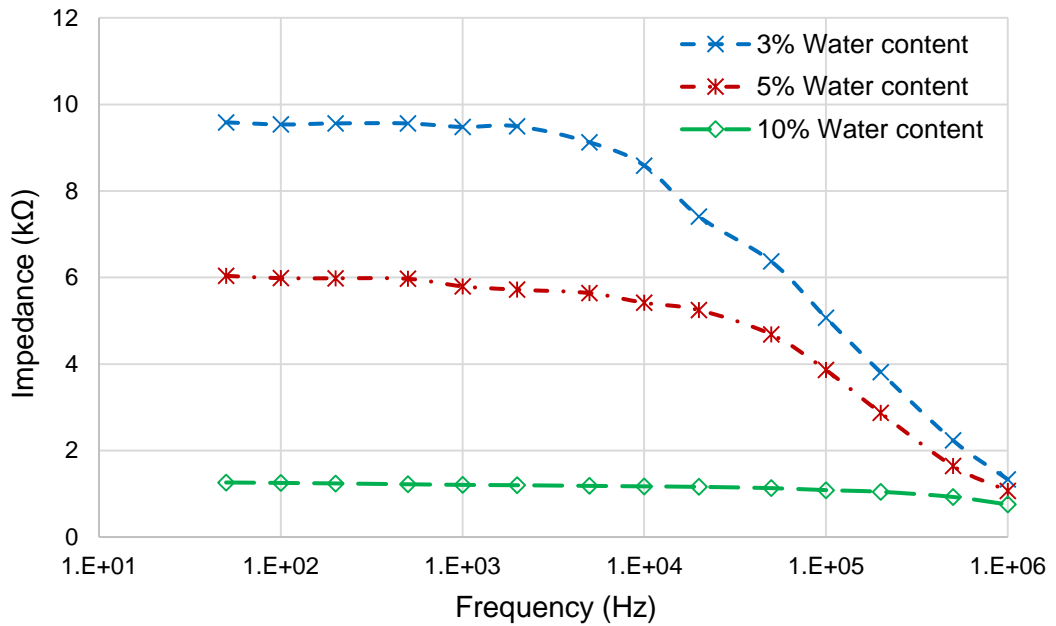
Figure 7.12: The measured impedance of gravel: 10 mm bulk, sample (d) as a function of frequency and water content.

Table 7.1: A comparison of DC resistance and AC impedance for each gravel sample.

Gravel Sample	Water content	DC Resistance (20 mA)	AC Resistance (50 Hz)
a	5%	13.5 kΩ	12.16 kΩ
	10%	3.76 kΩ	2.94 kΩ
b	3%	15.33 kΩ	13.76 kΩ
	5%	4.84 kΩ	2.92 kΩ
c	3%	5.23 kΩ	3.51 kΩ
	5%	3.749 kΩ	2.87 kΩ
d	3%	10.958 kΩ	9.585 kΩ
	5%	6.22 kΩ	6.039 kΩ
	10%	1.438 Ω	1.263 kΩ

From Figure 7.5 to Figure 7.12 and Table 7.1, it was found that the four different types of gravel have high resistivity under both DC and AC tests, and the resistance value at THE highest water content is still high. These resistances were considered as series resistances with the human body resistance, neglecting gloves and work boots. Therefore, and according to IEEE Std 80-2000 [7.1], the tested materials (gravel types) provide high additional resistance and are considered as an important mitigation technique to ensure the safety of workers.

7.4.2 Concrete and shoes

The DC resistance and resistivity of the samples is shown in Figures 7.13 and Figure 7.14. The resistance of the dry concrete was high and, hence, it was measured as an open circuit. The concrete was then immersed in water for 15, 30, 60 minutes, and the resistance was measured and was found to have decreased due to the increasing moisture contents. These intervals of time were chosen to give an example about the effect of water content on the measured resistance; however, the concrete absorbs much water as the immersed time increase. It is clear from the results that the time taken between DET2/2 and ABEM tests

have an effect on the results. For 15 minutes immersing time, the difference between the tests is about 500 Ω, then the difference decrease as the immersing time increase.

For AC, the RMS values for the voltage and current from the CT and differential probe were saved and the impedance calculated. As the frequency increased, the impedance decreased due to the capacitive effect. In addition, the moisture contents having a significant effect on the measured impedance, the higher moisture contents show lower measured impedance magnitude. Further analysis was carried out to calculate the phase angle. The results are given in Figures 7.15. The DC resistance, as compared to the AC tests at 50 Hz, shows close agreement, as shown in Table 7.2.
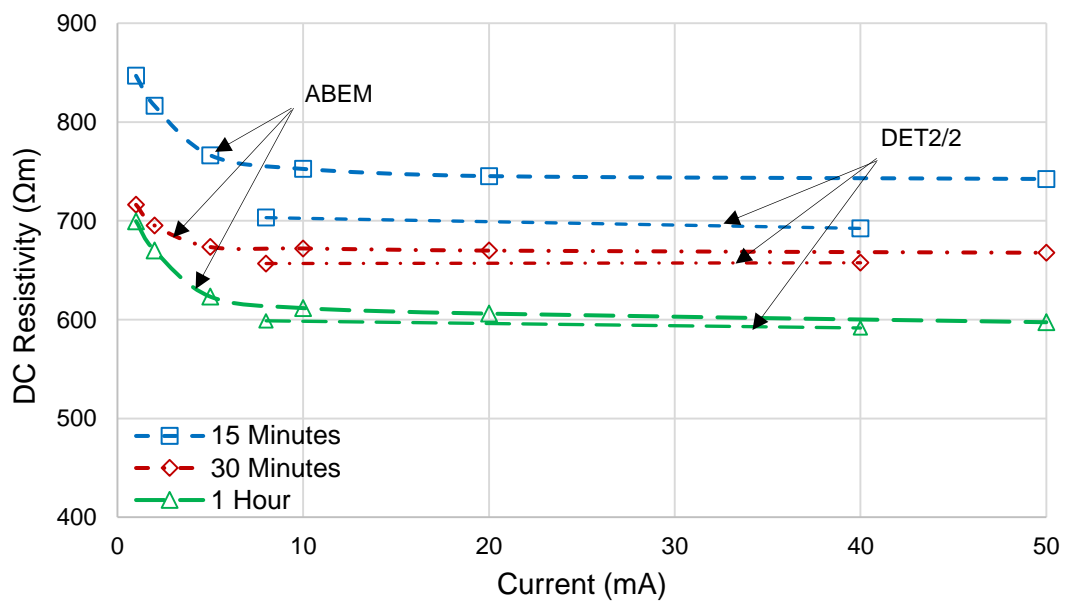
Figure 7.13: The effect of water content on DC resistivity of the concrete.
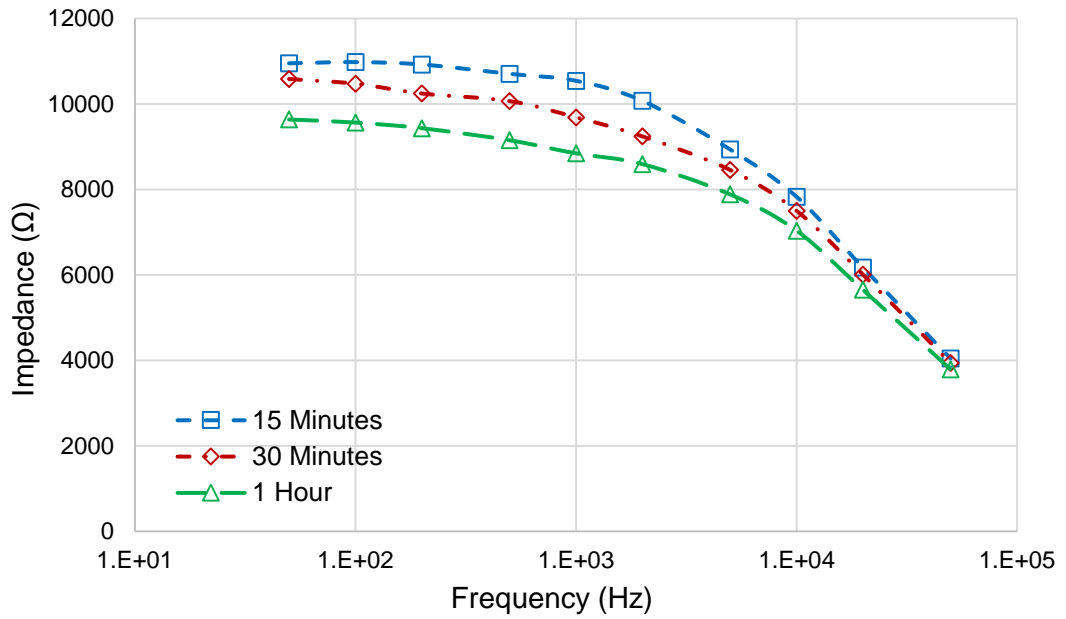
Figure 7.14: The effect of water content and frequency on the impedance of the concrete.
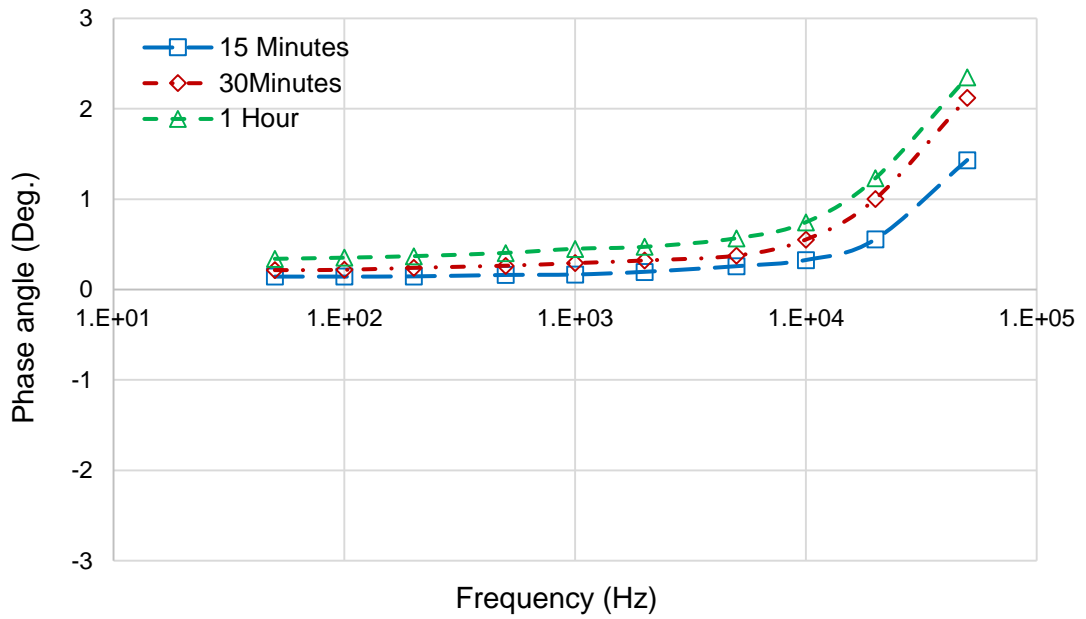
Figure 7.15: The effect of water content and frequency on the phase angle of the concrete

sample.

144

Table 7.2 : A comparison of DC resistance and AC impedance for the concrete.

Concrete	DC Resistance (20 mA)	AC Resistance (50 Hz)
15 Minutes	10.38 kΩ	10.07 kΩ
30 Minutes	9.27 kΩ	9.23 kΩ
1 Hour	8.43kΩ	8.58 kΩ

From the experimental results, it was found that the concrete offer much higher resistivity than the gravel for both DC and AC tests, and less effected by water content. These results may be useful to consider when the earthing system is designed especially for countries with high precipitations.

7.5   Conclusion

Extensive laboratory investigations have been performed for different samples of gravel and concrete. The objective of these investigations is to measure the contact resistance between the earth and the people on the surface and to examine the effect of moisture on the measured resistivity. In addition, the measured resistance is compared with the standard to ensure the safety of the workers in the substation. Different samples of high resistivity materials, such as gravel and concrete, were prepared in a high voltage laboratory for use in this study. The effect of water content in the resistance of concrete used in tower base of overhead lines and at substation have been examined. Their DC resistance shows a reduction in its magnitude as the moisture content is increased. However, the resistivity of the tested materials is still high. This mean that, the high resistivity material layer provide sufficient resistance in series with the resistance of human body which resist the flow of current through the body. Therefore, concrete and substation ballasts is one of the important techniques to ensure safety environment for the workers. As expected, the experiments show a clear and significant dependence of the

resistance and impedance on water content. The implication of this for real grounding systems is that under heavy rain the ground resistance drops significantly but, as the soil dries, it is important to consider its impact on rise of ground potential and safety implications.

CHAPTER EIGHT: GENERAL DISCUSSION AND CONCLUSIONS

8.1 Conclusions

A review of the published work on the behaviour of earth electrode systems under high frequency and transient conditions has been conducted, and it has been identified that the behaviour of earthing electrodes subjected to power frequency is significantly different from the behaviour under impulse currents. In addition, the performance of earthing systems is significantly influenced by the soil resistivity, the arrangement of the electrodes, the frequency and magnitude of the current and the impulse wave shape. Moreover, the literature review has identified frequency dependence of soil parameters and important equivalent circuit work. Different analytical approaches, both experimental tests and computational models, were developed to achieve a more quantified performance. One of the most common numerical models used to simulate the earthing electrodes is based on the method of moments and is commercially available through software such as CDEGS. This numerical model has been used to characterise the behaviour of different earthing electrodes, specifically, vertical and horizontal electrodes. Special studies were carried out to identify the effect of electrode segmentation on the magnitude of the calculated impedance. The study offers the following recommendations: a small number of segments is suggested for vertical electrodes. However, the number of segments should be as big as possible for horizontal electrodes.

The literature search provided useful information, which is considered as guidance for earthing system installations and measurements. Two earthing system facilities were prepared at different locations taking into consideration all safety requirements for the personnel, people in the vicinity and to characterise the electrical parameters to be ready for testing various earth electrodes. Soil resistivity measurements were carried out at the Llanrumney earthing system facility as the first stage of the earthing system installation.

The apparent resistivity and 2D soil resistivity maps were obtained. The 2D resistivity maps helped to develop a two-layer soil model for the facility. According to the resistivity survey, the variations in soil resistivity within the same location were identified. In addition, experimental tests were carried out on the vertical and horizontal electrodes installed at the first facility, which is located at the university's playing fields Llanrumney, Cardiff. DC and AC low voltages, low magnitude impulse voltage and high voltage tests were applied. The obtained results exhibited close agreements with published work and with simulation results, which are considered for the recommendations provided in Chapter 3.

Moreover, the results from the experiments, described in Chapters 4 and 5 and the published studies, clarified how the soil resistivity varies vertically and with depth and how this variation affects the measured impulse resistance. Therefore, the second full-scale earthing facility located at Dinorwig pumped storage substation in North Wales, UK, was prepared. In this facility, the earthing grid was installed in fresh water, which was considered as a uniform medium. The earthing system characteristics were examined under DC, AC low voltage and low and high magnitude impulse energisations. The results showed that the resistive behaviour dominates the performance of the test object and exhibited a reasonable agreement with the published and simulation investigations. These results were used to validate the analytical approaches and numerical simulation techniques developed to clarify the performance of earthing systems.

In addition, there is no previous work available in the literature related to laboratory characterisation of site soils with variable frequency and impulse, and the relation with the electrode tests. Therefore, further investigations were implemented in the high voltage laboratory at Cardiff University to clarify the frequency dependence of soil parameters (conductivity and permittivity). The literature provided different theoretical and

experimental approaches as well as numerical simulation techniques to clarify how conductivity and permittivity of real site materials depend on frequency. These studies resulted in different models to express conductivity and permittivity frequency dependence. However, there is no accurate model to characterise these phenomena. In addition, the conservative model, in which the resistivity is assumed equal to the measured DC resistance and the permittivity varies from 1 to 80 with respect to water content, is still applied. Therefore, extensive laboratory investigations were carried out with soil taken from the test site at Llanrumney, which was brought from the site, prepared and tested in the laboratory with controlled different water contents. Both conductivity and permittivity values were determined under DC and AC variable frequency and impulse energisation conditions. These measured values were compared with the models available in the literature. The results showed that, as the percentage of water increased, both the measured resistivity and permittivity values showed a fall in their values. In addition, the impulse resistance decreased in value at high soil resistivity (low water contents); as the water content increased, the measured impulse resistance decreased and exhibited only a slight variation in its magnitude. This is explained by the soil's non-linear properties.

The measured soil parameters and their variation with frequency were compared with the published frequency dependent models. The results showed reasonable agreements with some models in high resistivity soil. However, a marked divergence was obtained with increases in the water content.

Furthermore, there is no available published work on the characterisation of gravel and concrete using variable frequency. Therefore, laboratory experiments were carried out on high resistivity materials, which were used with different thicknesses to increase the contact resistance between the earth and the workers in substations. Different

commercially available types of gravel and concrete have been investigated with different water contents according to the volume to highlight the resistivity value variations with respect to water content. High resistivity materials were subjected to DC and low voltage AC energisations to measure the resistivity. The results showed that, as expected, the resistivity value decreased as the water content increased up to saturation point, which depends on the nature of the material. After this point, increasing the water content has no effect on the resistivity value. Therefore, gravels and concrete offer additional resistance in series with body resistance and resist the flow of accidental current through the human body. This is mean that high resistivity materials considered as an important mitigation technique to ensure a safety environment for personnel.

8.2   Future work

The following suggestions are proposed for future work:

1. Further experimental investigations with a uniform conducting medium should be conducted. Special emphasis should be given to the behaviour of earthing systems under high voltage and high current energisation conditions. The results should be compared with the developed analytical approaches, the empirical expressions, and the computational models to check their validity and limitations.

2. Further experimental studies could be conducted at the field test site on the frequency-dependent electrical soil parameters to develop a greater understanding of the characteristics of earthing systems under high frequency and low /high current impulse.

References

Chapter One

[1.1] BS 74530:2011, "Code of practice for protective earthing of electrical installations," British Standard Institution, 2011.

[1.2] E.-T. 41-24, "Guidelines for the design, installation, testing and maintenance of main earthing system in substations," Energy Networks Association, no. 1, UK, 1992.

[1.3] "IEEE Guide for Safety in AC Substation Grounding," ANS/IEEE, New York, USA, 2000.

[1.4] N. M. Nor, A. Haddad and H. Griffiths, "Performance of earthing systems of low resistivity soils," in IEEE Transactions on Power Delivery, vol. 21, no. 4, pp. 2039-2047, Oct. 2006.

[1.5] S. Mousa, N. Harid, H. Griffiths, and A. Haddad, "Experimental investigation of high frequency and transient performance of earth rod systems," Electric Power Systems Research, vol. 113, Elsevier B.V., pp. 196–203, 2014.

[1.6] S. Mousa, H. Griffiths, N. Harid, and A. Haddad, "Current distribution under high frequency and transient conditions in earth electrode systems," proccedings of ICHVE 2012 - 2012 International Conference on High Voltage Engineering and Application, 2012, pp. 150–153.

[1.7] N. M. Nor, "Effect of enhancement materials when mixed with sand under high impulse conditions," proceedings of 2006 IEEE 8th International Conference on Properties & applications of Dielectric Materials, Bali, 2006, pp. 916-919.

[1.8] N. M. Nor, "Characteristics of sodium chloride (NaCl) under DC, AC and impulse conditions," proceedings of 2006 IEEE 8th International Conference on Properties & applications of Dielectric Materials, Bali, 2006, pp. 926-931.

[1.9] R.Zeng, J. He, J. Zou, and X. Sheng, "Novel method in decreasing grounding resistance of urban substations by utilizing peripheral geographical conditions," IEEE Publication 0-7803-7420-7, pp. 1113–1119, 2002.

[1.10] Y. Tu, J. He, and R. Zeng, "Lightning impulse performances of grounding devices covered with low-resistivity materials," IEEE Transactions on Power Delivery, vol. 21, no. 3, pp. 1706–1713, 2006.

[1.11] A. Haddad and Warne D., Advances in High Voltage Engineering. 2004.

[1.12] L. Grcev and F. Dawalibi, "An electromagnetic model for transients in grounding systems," IEEE Transactions on Power Delivery, vol. 5, no. 4, pp. 1773–1781, 1990.

[1.13] S. Visacro and A. Soares, "HEM: A model for simulation of lightning-related engineering problems," IEEE Transactions on Power Delivery, vol. 20, no. 2, pp. 1206–1208, 2005.

[1.14] J. C. Salari and C. Portela, "A methodology for electromagnetic transients calculation - An application for the calculation of lightning propagation in transmission lines," IEEE Transactions on Power Delivery, vol. 22, no. 1, pp. 527–536, 2007.

[1.15] R. S. Alípio, M. A. O. Schroeder, M. M. Afonso, and T. A. S. Oliveira, "Electric fields of grounding electrodes : frequency and time domain analysis," Grounding Earthing (GROUND), pp. 379–383, 2009.

[1.16] L. Grcev, "Impulse efficiency of ground electrodes," IEEE Transactions on Power Delivery, vol. 24, no. 1, pp. 441–451, 2009.

[1.17] R. L. Smith-Rose, "Electrical Measurements on Soil with Alternating Currents," Journal of the Institution of Electrical Engineers, vol. 75, no. 452, pp. 221–237, 1933.

[1.18] J. H. Scott, R. D. Carroll, and D. R. Cunningham, "Dielectric constant and electrical conductivity of moist rock from laboratory measurements," Sensor and Simulation Note 116, Kirtland AFB, NM, Aug., 1964.

[1.19] J. Scott, "Electrical and Magnetic Properties of Rock and Soil," Theoretical Notes, Note 18, U.S. Geological Survey, May 1966 [Online]. Available: https://www.ece.unm.edu/summa/notes/Sensor.html.

[1.20] R. Alipio and S. Visacro, "Frequency dependence of soil parameters: Effect on the lightning response of grounding electrodes," IEEE Transactions on Power Delivery, vol. 27, no. 2, pp. 927–935, 2012.

[1.21] M. Akbari, K. Sheshyekani, and M. R. Alemi, "The effect of frequency dependence of soil electrical parameters on the lightning performance of grounding systems," IEEE Transactions on Electromagnetic Compatibility, vol. 55, no. 4, pp. 739–746, 2013.

Chapter Two

[2.1] H. M Towne: 'Impulse Characteristics of Driven Grounds, General Electric Review, Vol. 31, No. 11, pp. 605-609, November, 1928

[2.2] L. Bewley, "The counterpoise," General Electric Review, vol.37, no.2, pp. 73,Feb, 1934

[2.3] P. Bellaschi, ''Impulse and 60-Cycle Characteristics of Driven Grounds'', AIEE Transactions, Vol.60, p.123-128, March 1941

[2.4] P. Bellaschi, P.L., R.E. Armington and A. E. Snowden, ''Impulse and 60-cycle characteristics of driven grounds-II,'' AIEE Transactions, vol.61, pp. 349-363, 1942

[2.5] A. Vainer, ''Impulse characteristics of complex earth grid'', Elektrichestvo, no. 3, pp.107-117, 1965

[2.6] A. Liew and M. Darveniza, ''Dynamic model of impulse characteristics of concentrated earths'', Proc. IEE, vol.121, no.2, p.122, February 1974

[2.7] S. Mousa, "Experimental investigation of enhanced earth electrode systems under high frequency and transient conditions,'' Ph.D. dissertation, Cardiff University, 2014

[2.8] M. Ahmeda, "Earthing performance of transmission line towers,'' Ph.D. dissertation, Cardiff University, 2012

[2.9] D. Lathi, "Impulse measurements in earthing systems,'' Ph.D. dissertation, Cardiff University, 2012

[2.10] L.Bewley, "Theory and tests of the counterpoise," Electrical Engineering, no.53, p 1163, Aug., 1934

[2.11] R. Gupta, and B. Thapar, ''Impulse impedance of grounding grids,'' IEEE Transactions on Power Apparatus and Systems, vol.PAS-99, no.6, p.2357 Nov/Dec 1980

[2.12] R. Gupta,V. Singh,'' Impulse impedance of rectangular grounding grid, Impulse impedance of grounding grids, '' IEEE Transactions on Power Delivery, vol.7, no.1, pp.214-218,Jan. 1991

[2.13] S. Toshio, H. Takesus and S. Sekioka,''Measurement on surge characteristics of grounding resistance of counterpoise for impulse currents, ''International Conference on Lightning Protection (ICLP), Rhodes, Greece, September 2000

[2.14] G. Yanqing, H. Jinliang, Z. Rong and L. Xidong, "Impulse transient characteristic of grounding grids'' Proceedings on 3rd International Electromagnetic compatibility, pp. 276-280, Beijing, China, May 2002

[2.15] S. Brourg and B. Sacepe, "Deep earth electrodes in highly resistive ground frequency behaviour,'' IEEE International Symposium on Electromagnetic Compatibility, pp. 584-589, 1995

[2.16] J. Choi, Y. Ahn, S. Goo, K. Park, J. Yoon and G. Jung, " Direct measurements of frequency domain impedance characteristics of grounding system,'' Proc. International Conference on Power System Technology (Power Con 2002), pp.2218-2221, vol.4, 2002

[2.17] P. Llovera, J. Antonio, A. Quijano and V. Fuster, "High frequency measurements of grounding impedance on resistive soils,'' Proceedings on 28th International Conference on Lightning Protection (ICLP), Kanazawa, Japan, Sep. 2006

[2.18] J. Choi and B. Lee, ''An analysis of the frequency-dependent grounding impedance based on the ground current dissipation of counterpoises in the two-layered soils,'' Electric Power Systems Research, April 2012, Vol. 70, no. 2, pp.184-191

[2.19] P. L. Bellaschi, R. E. Armington, ''Impulse and 60-cycle characteristics of the driven ground -III,'' ALEE Transactions, Vol.62, P.334, 1943

[2.20] R. Davis, J. E. M. Johnson, '' The surge characteristics of tower and tower footing impedance, '' Journal of the IEE, p. 453, October 1941

[2.21] R. Rudenberg, '' Grounding principles and practice I-Fundamental considerations on ground currents,'' Electrical Engineering,Vol.64, No.1, p.1, January 1945

[2.22] R. Rudenberg, ''Electrical shock waves in power systems,'' Harvard University Press, 1968

[2.23] S. S. Devgan and E. R. Whitehead, "Analytical Models for Distributed Grounding Systems," in IEEE Transactions on Power Apparatus and Systems, vol. PAS-92, no. 5, pp. 1763-1770, Sept. 1973.

[2.24] R. Verma and D. Mukhedkar, "Impulse Impedance of Buried Ground Wire," in IEEE Transactions on Power Apparatus and Systems, vol. PAS-99, no. 5, pp. 2003-2007, Sept. 1980.

[2.25] C. Mazetti and G. M Veca, "Impulse behaviour of .grounding electrodes,'' IEEE Trans. Power App. Syst., vol 102, no. PAS-9, 3148-3154, 1983.

[2.26] R. Velazquez and D. Mukhedkar, "Analytical Modelling of Grounding Electrodes Transient Behavior," in IEEE Transactions on Power Apparatus and Systems, vol. PAS-103, no. 6, pp. 1314-1322, June 1984.

[2.27] R. Verma and D. Mukhedkar, "Fundamental Considerations and Impluse Impedance of Grounding Grids," in IEEE Transactions on Power Apparatus and Systems, vol. PAS-100, no. 3, pp. 1023-1030, March 1981.

[2.28] M. Lorentzou and N.D. Hatziargyriou, EMTP Modelling of Grounding Electrodes 32nd UPEC Conference, Manchester, 10–12 September 1997

[2.29] L. Grecev and M. Popov, "On High-frequency circuit equivalents of a vertical ground rod,'' IEEE Transactions on Power Delivery, vol. 20, no.2, April 2005

[2.30] F. Dawalibi, Electromagnetic Fields Generated by Overhead and Buried Conductors. Part 1 - Single Conductor, IEEE Transactions on Power Delivery, Vol PWRD-1, 105-119, October 1986.

[2.31] F. Dawalibi, Electromagnetic Fields Generated by Overhead and Buried Conductors. Part 2 - Ground Networks, IEEE Transactions on Power Delivery, Vol PWRD-1, 105-119, October 1986.

[2.32] L. Grcev and F. Dawalibi, "An electromagnetic model for transients in grounding systems," in IEEE Transactions on Power Delivery, vol. 5, no. 4, pp. 1773-1781, Oct 1990.

[2.33] R. Alipio and S. Visacro, "How the frequency dependence of soil parameters affects the lightning response of grounding electrodes,'' Proceedings on 31st International Conference on Lightning Protection (ICLP), Vienna, Austria, 2012

[2.34] D. Sunde., Earth conduction Effects in Transmission line Systems, Dover Publications Inc., 1968

[2.35] R. L. Smith-Rose, "Electrical measurements on soil with alternating currents," Proc. IEE, vol. AP-75, pp. 221–237, Aug. 1934.

[2.36] J. H. Scott, R. D. Carroll, and D. R. Cunningham, "Dielectric constant and electrical conductivity of moist rock from laboratory measurements," Sensor and Simulation Note 116, Kirtland AFB, NM, Aug. 1964.

[2.37] J. H. Scott. (1966, May). "Electrical and magnetic properties of rock and soil," Theoretical Notes, Note 18, U.S. Geological Survey [Online]. Available: https://www.ece.unm.edu/summa/notes/Theoretical.html

[2.38] J. H. Scott, D. Carroll, and D. R. Cunningham, "Dielectric constant and electrical conductivity measurements of moist rock: A new laboratory method," J. Geophys. Res., vol. 72, no. 20, pp. 5101–5115, 1967.

[2.39] C. L. Longmire and H. J. Longley. (1973). "Time domain treatment of media with frequency dependent parameters," Theoretical Notes 113, Defense Nuclear Agency, Santa Barbara, CA, USA [Online]. Available: https://www.ece.unm.edu/summa/notes/Theoretical.html

[2.40] K. S. Smith and C. L. Longmire, "A universal impedance for soils," Defense Nuclear Agency, Alexandria, VA, USA, Topical Report for Period Jul. 1 1975– Sep. 30 1975, 1975.

[2.41] F. S. Visacro and C. M. Portela, "Soil permittivity and conductivity behavior on frequency range of transient phenomena in electric power systems," presented at the Symp. High Voltage Eng., Braunschweig, Germany, 1987.

[2.42] C. M. Portela, "Measurement and modeling of soil electromagnetic behavior," in Proc. IEEE Int. Symp. Electromagn. Compat., 1999, vol. 2, pp. 1004–1009.

[2.43] S. Visacro and R. Alipio, "Frequency dependence of soil parameters: Experimental results, predicting formula and influence on the lightning response of grounding electrodes," IEEE Trans. Power Del., vol. 27, no. 2, pp. 927–935, Apr. 2012.

[2.44] M. Akbari, K. Shehyekani, and M. R. Alemi, "The Effect of Frequency Dependence of Soil Electrical Parameters on the Lightning Performance of Grounding Systems,'' IEEE Transactions on Electromagnetic Compatibility, Vol. 55, No. 4, 2013

[2.45] S. Visacro, R. Alipio, M. H. M. Vale, and P. Clever, "The Response of Grounding Electrodes to Lightning Currents: The Effect of Frequency-Dependent soil Resistivity and Permittivity,'' IEEE Transactions on Electromagnetic Compatibility, Vol. 53, No. 2, 2011

[2.46] M. Guimaraes N., L. Araujo, R. V. Castro, L. F. D. Santos, M. H. Murta and S. Viscaro, "Impulse response of Grounding Grids: Experimental versus Simulated Results,'' Proceedings on 31st International Conference on Lightning Protection (ICLP), Vienna, Austria, 2012

[2.47] F. H. Silveira, S. Visacro, H. B. Ferreira and A. Conti, "Lightning-Induced Voltages Calculated with The Hybrid Electromagnetic Model Considering Frequency-Dependent Soil Parameters,'' IEEE International Symposium on Lightning Protection (XII SIPDA), Belo Horizonte, Brazil, October 2013, PP. 236-240

Chapter Three

[3.1] SES (Safe Engineering Services), Current distribution electromagnetic grounding analysis software (CDEGS), available: htt://www.sestech.com/products/spftpackages/cdegs.htm

[3.2] BS EN 50522:2010, Earthing of power installations exceeding 1 kV a.c. 2010.

[3.3] IEEE Std 81.2-1991, IEEE Guide for Measurement of Impedance and Safety Characteristics of Large, Extended or Interconnected Grounding Systems. 1992.

[3.4]   H. Griffiths and N. Pilling ", Chap. 8 'Earthing,'" in Advances in high voltage engineering, Hakodate Japan, 2004, pp. 349–413.

[3.5]   D. Clark Handover report ", Exported Potentials and Profiles Around Earth Electrodes and Opposite Side Injection for Large-Area Earthing Systems," Advanced High Voltage Engineering Research Centre, January 2014.

[3.6]   G. F. Tagg, Earth Resistances. London UK: Newnes, 1964.

[3.7]   B. 7430, "Code of practice for earthing," Br. Stand. Inst., 1991.

[3.8]   S. Mousa, "Experimental investigation of enhanced earth electrode systems under high frequency and transient conditions,'' Ph.D. dissertation, Cardiff University, 2014

[3.9]   "Lund Imaging System, Instruction Manual, ABEM Instrumnet AB," Bromma, Sweden.

[3.10] "RES2DINV, Geoelectrical Imaging 2D, Geotomo Software, Nov.," 2011.

[3.11] H. Hasan, H. Hamzehbahmani, S. Robson, H. Griffiths, D. Clark, and A. Haddad, "Characterization of horizontal earth electrodes: Variable frequency and impulse responses," Proc. Univ. Power Eng. Conf., vol. 2015–Novem, 2015.

Chapter four

[4.1] L. Grcev, F. Dawalibi, "An electromagnetic model for transients in grounding systems," IEEE Trans. Power Delivery, Vol. 5, pp. 1773- 1781, Oct. 1990.

[4.2] L. Grcev, "Improved earthing system design practices for reduction of transient voltages," in Proc. 1998 CIGRÉ Session, pp. 1-6

[4.3] L. Grcev, "Improved design of transmission line grounding arrangements for better protection against effects of lightning," in Proc. Int. Symp. On Electromagnetic Compatibility, Roma, Italy, 1998, pp. 100- 103.

[4.4] SES (Safe Engineering Services), Current distribution electromagnetic grounding analysis software (CDEGS), available: htt://www.sestech.com/products/spftpackages/cdegs.htm

[4.5] A.M. Davies: 'High Frequency and Transient Performance of Earthing Systems', PhD Thesis, University of Wales, Cardiff, 1999.

[4.6] A.M. Davies, H. Griffiths, T.E. Charlton: 'High Frequency Performance of a Vertical Earth Electrode', Proceedings of the 24th International Conference on Lightning Protection (ICLP), Birmingham UK, pp. 536-540, 1998.

[4.7] L. Grcev, "Impulse efficiency of simple grounding electrode arrangements," in Proc. Int. Zurich Symp. Electromagn. Compat., Zurich, Switzerland, 2007, pp. 325–328.

[4.8] J. He, Y. Gao, R. Zeng, J. Zou, X. Liang, B. Zhang, J. Lee, and S. Chang, "Effective length of counterpoise wire under lightning current," IEEE Trans. Power Deliv., vol. 20, no. 2 II, pp. 1585–1591, 2005.

[4.9] I. Jurić-Grgić, R. Lucić, and D. Ljubičić, "Effective length of horizontal grounding electrode," SoftCom 2008 16th Int. Conf. Software, Telecommuncations Comput. Networks, no. 3, pp. 47–50, 2008.

[4.10] D. S. Gazzana, A. S. Bretas, G. A. D. Dias, M. Tello, D. W. P. Thomas, and C. Christopoulos, "Effective length study of grounding electrod reached by lightning

based on Transmission Line modelling Method," IEEE Int. Symp. Electromagn. Compat., pp. 777–781, 2012.

[4.11] K. Yamamoto, S. Sumi, S. Sekioka, and J. He, "Derivations of Effective Length Formula of Vertical Grounding Rods and Horizontal Grounding Electrodes Based on Physical Phenomena of Lightning Surge Propagations," IEEE Trans. Ind. Appl., vol. 51, no. 6, pp. 4934–4942, 2015.

[4.12] N. M. Nor, A. Haddad, and H. Griffiths, "Performance of Earthing Systems of Low Resistivity Soils," IEEE Trans. Power Deliv., vol. 21, no. 4, pp. 2039–2047, 2006.

[4.13] Y. Tu, J. He, and R. Zeng, "Lightning impulse performances of grounding devices covered with low-resistivity materials," IEEE Trans. Power Deliv., vol. 21, no. 3, pp. 1706–1713, 2006.

[4.14] E. Al-Ammar, Y. Khan, N. Malik, and N. Wani, "Development of low resistivity material for grounding resistance reduction," 2010 IEEE Int. Energy Conf. Exhib. EnergyCon 2010, vol. 35, pp. 700–703, 2010.

[4.15] Q. Meng, J. He, F. P. Dawalibi, and J. Ma, "A new method to decrease ground resistances of substation grounding systems in high resistivity regions," IEEE Trans. Power Deliv., vol. 14, no. 3, pp. 911–916, 1999.

[4.16] A. Elmghairbi, "Potential rise and safety voltages of wind turbine earthing systems under transient conditions," Electr. Distrib. …, no. 0937, pp. 8–11, 2009.

[4.17] A. A. Al-Arainy, Y. Khan, M. I. Qureshi, N. H. Malik, and F. R. Pazheri, "Optimized pit configuration for efficient grounding of the power system in high

resistivity soils using low resistivity materials," 2011 4th Int. Conf. Model. Simul. Appl. Optim. ICMSAO 2011, pp. 5–8, 2011.

[4.18] S. Mousa, H. Griffiths, N. Harid, and A. Haddad, "Experimental investigation of high frequency and transient performance of earth rod systems," in 2012 International Conference on Lightning Protection (ICLP), pp. 1–5, 2012.

[4.19] T. Bari, "Influence of Conductor Segmentation in Grounding Resistance Calculation Using Boundary Element Method," in Progress in Electromagnetic Research Symposium, pp. 141–144, 2004.

[4.20] T. C. Moratti Cardoso and A. De Conti, "Calculation of return-stroke currents and remote electromagnetic fields using circuit and transmission line theories: Influence of segmentation and excitation function," 2013 Int. Symp. Light. Prot. SIPDA 2013, pp. 151–156, 2013.

Chapter Five

[5.1] S. Mousa, H. Griffiths, N. Harid, and A. Haddad, "Experimental investigation of high frequency and transient performance of earth rod systems," in 2012 International Conference on Lightning Protection (ICLP), 2012, pp. 1–5.

[5.2] L. Grcev and M. Popov, "On high-frequency circuit equivalents of a vertical ground rod," IEEE Trans. Power Deliv., vol. 20, no. 2 II, pp. 1598–1603, 2005.

[5.3] K. Yamamoto, S. Yanagawa, K. Yamabuki, S. Sekioka, and S. Yokoyama, "Analytical surveys of transient and frequency-dependent grounding characteristics of a wind turbine generator system on the basis of field tests," IEEE Trans. Power Deliv., vol. 25, no. 4, pp. 3035–3043, 2010.

[5.4] K. Tanabe and T. Kawamoto, "Impedance with respect to vertical and rotational symmetric grounding electrodes and its computational results from full-wave analysis using FD-TD method," IEEJ Trans. B, vol. 125, no. 2, pp. 165–169, 2005.

[5.5] L. W. Choun, M. Zainal, C. Gomes, and W. F. Wan Ahmed, "Analysis of Earth Resistance of Electrodes and Soil Resistivity at Different Environments," in nternational Conference on Lightning Protection (ICLP), 2012, pp. 1–9.

[5.6] Y. Tu, J. He, and R. Zeng, "Lightning impulse performances of grounding devices covered with low-resistivity materials," IEEE Transactions on Power Delivery, vol. 21, no. 3, pp. 1706–1713, 2006.

[5.7] R. Zeng, J. He, Z. Wang, Y. Gao, W. Sun, and Q. Su, "Analysis on influence of long vertical grounding electrodes on grounding system for substation," PowerCon 2000 - 2000 Int. Conf. Power Syst. Technol. Proc., vol. 3, pp. 1475–1480, 2000.

[5.8] L. Grcev, "Impulse efficiency of ground electrodes," IEEE Transactions on Power Delivery, vol. 24, no. 1, pp. 441–451, 2009.

[5.9] W. Ahmad, M. Hashim, and A. Kadir, "Effects of Homogenous Soil Characteristics to the Transient Responses of a Single Long Horizontal Ground Conductor Model," no. PECon 08, pp. 367–371, 2008.

[5.10] A. El Mghairbi, "A New Method to Increase the Effective Length of Horizontal Earth Electrodes," pp. 3–6, 2010.

[5.11] A. Elmghairbi, M. Ahmeda, N. Harid, H. Griffiths, and A. Haddad, "A technique to increase the effective length of horizontal earth electrodes and its application to a practical earth electrode system," 2011 7th Asia-Pacific Int. Conf. Light. APL2011, pp. 690–693, 2011.

[5.12] L. Greev, "Impulse efficiency of simple grounding electrode arrangements," Proc. 18th Int. Zurich Symp. Electromagn. Compat. EMC, pp. 325–328, 2007.

[5.13] N. Harid, D. Clark, S. Mousa, H. Griffiths, and A. Haddad, "Impulse characterization of ground electrodes," 2014 Int. Conf. Light. Prot. ICLP 2014, no. 3, pp. 1418–1423, 2014.

[5.14] V. Mashayekhi, S. H. H. Sadeghi, R. Moini, H. R. Karami, K. Sheshyekani, S. H. H. Sadeghi, and A. Nasiri, "Frequency-dependent modeling of grounding system for wind turbine lightning transient studies," 3rd Int. Conf. Renew. Energy Res. Appl. ICRERA 2014, pp. 927–931, 2015.

[5.15] G. Visacro, S. Rosado, "Response of Grounding Electrodes to Impulsive Currents : An Experimental Evaluation," IEEE Trans. Electromagn. Compat., vol. 51, no. 1, pp. 161–164.

[5.16] M. Akbari, K. Sheshyekani, and M. R. Alemi, "The effect of frequency dependence of soil electrical parameters on the lightning performance of grounding systems," IEEE Trans. Electromagn. Compat., vol. 55, no. 4, pp. 739–746, 2013.

[5.17] R. Alipio and S. Visacro, "Frequency Dependence of Soil Parameters: Effect on the Lightning Response of Grounding Electrodes," Electromagn. Compat. IEEE Trans., vol. 55, no. 4, pp. 739–746, 2013.

[5.18] C. Portela, "Frequency and transient behavior of grounding systems II - Practical application examples," IEEE 1997, EMC, Austin Style. IEEE 1997 Int. Symp. Electromagn. Compat. Symp. Rec. (Cat. No.97CH36113), pp. 385–390, 1997.

[5.19] R. Alipio and S. Visacro, "Frequency Dependence of Soil Parameters: Experimental Results, Predicting Formula and Influence on the Lightning Response

of Grounding Electrodes," IEEE Transactions on Power Delivery, vol. 27, no. 2, pp. 927–935, 2012.

[5.20] S. Visacro, R. Alipio, M. H. Murta Vale, and C. Pereira, "The response of grounding electrodes to lightning currents: The effect of frequency-dependent soil resistivity and permittivity," IEEE Trans. Electromagn. Compat., vol. 53, no. 2, pp. 401–406, 2011.

[5.21] H. Hasan, H. Hamzehbahmani, H. Griffiths, N. Harid, D. Clark, S. Robson, and A. Haddad, "Characterisation of earth electrodes subjected to impulse and variable frequency currents," in The 19th International Symposium on High Voltage Engineering, Pilsen, Czech Republic, 2015, pp. 23–28.

[5.22] D. Clark, "Exported Potentials and Profiles Around Earth Electrodes and Opposite Side Injection for Large-Area Earthing Systems," 2014.

[5.23] D. Clark, H. Griffiths, N. Harid, A. Haddad, and D. Guo, "Wireless measurement system for a large-scale grounding electrode test facility," Proc. Univ. Power Eng. Conf., pp. 2–5, 2013.

[5.24] H. Griffiths, P. Jones, N. Harid, and A. Haddad, "Proposal for Measurement of Earth Impedance Using Variable Frequency Injection," Meas. Sci. Technol., vol. 21, no. 8, p. 085102 (8pp), 2010.

[5.25] SES (Safe Engineering Services), Current distribution electromagnetic grounding analysis software (CDEGS), available: htt://www.sestech.com/products/spftpackages/cdegs.htm

[5.26] IEEE Std 81.2-1991, IEEE Guide for Measurement of Impedance and Safety Characteristics of Large, Extended or Interconnected Grounding Systems. 1992.

[5.27] H. Griffiths and N. Pilling, "Chap. 8 'Earthing,'" in Advances in high voltage engineering, Hakodate Japan, 2004, pp. 349–413.

[5.28] E. B. Curdts, "Some of the Fundamental Aspects of Ground Resistance Measurements," Trans. Am. Inst. Electr. Eng. Part I Commun. Electron., vol. 77, pp. 760–767, 1958.

[5.29] D. Guo, D. Clark, D. Lathi, N. Harid, H. Griffiths, A. Ainsley, and A. Haddad, "Controlled Large-Scale Tests of Practical Grounding Electrodes Part II: Comparison of Analytical and Numerical Predictions With Experimental Results," IEEE Trans. Power Deliv., vol. 29, no. 3, pp. 1231–1239, 2014.

[5.30] H. Griffiths, N. Harid, and A. Haddad, "Modeling the effective length of earthing systems under variable frequency," CIGRE SC C4 Colloq., p. 6, 2012.

[5.31] N. Harid, H. Griffiths, S. Mousa, D. Clark, S. Robson, and A. Haddad, "On the analysis of impulse test results on grounding systems," IEEE Trans. Ind. Appl., vol. 51, no. 6, pp. 5324–5334, 2015.

[5.32] Committee and I. P. and Energy, "IEEE Guide for Measuring Earth Resistivity, Ground Impedance, and Earth Surface Potentials of a Grounding System IEEE Power and Energy Society," vol. 2012, pp.1-86. December 2012.

[5.33] 1-866-254-0962 by Megger, "'Getting Down to Earth, A Practical Guide to Earth Resistance Testing.'" [Online]. Available: www.megger.com.

[5.34] R. Zeng, J. He, and Z. Guan, "Novel measurement system for grounding impedance of substation," IEEE Trans. Power Deliv., vol. 21, no. 2, pp. 719–725, 2006.

[5.35] W. Li, J. Zou, and H. Sun, "Research on the new clamp-on ground resistance on-line tester based on AC variable frequency," Proc. World Congr. Intell. Control Autom., vol. 2, pp. 5286–5289, 2006.

[5.36] E. D. Sunde, Earth conduction effects in Transmission systems. New York: Van Nostrand, 1949.

[5.37] G. F. Tagg, Earth Resistances. London UK: Newnes, 1964.

[5.38] L. Grcev and F. Dawalibi, "An electromagnetic model for transients in grounding systems," IEEE Transactions on Power Delivery, vol. 5, no. 4, pp. 1773–1781, 1990.

[5.39] I. Colominas, F. Navarrina, and M. Casteleiro, "A boundary element numerical approach for grounding grid computation," Comput. Methods Appl. Mech. Eng., vol. 174, no. 1–2, pp. 73–90, 1999.

[5.40] F. P. Dawalibi, D. Mukhedkar, and D. Bensted, "Measured and Computed Current Densities in Buried Ground Conductors," IEEE Trans. Power Appar. Syst., vol. PAS-100, no. 8, pp. 4083–4092, 1981.

[5.41] W. P. Gorzegno and P. V Guido, "Scale model studies of station grounding grids," IEEE Trans. Power Appar. Syst., vol. PAS-102, no. 3, pp. 548–557, 1983.

[5.42] J. G. Sverak, C. H. Booraem, and D. G. Kasten, ""Post-design analysis and scale model tests for a two grid grounding system serving the 345 kV GIS facilities at Seabrook Power Plant," in CIGRE Symp. High Current Power Syst. under Normal,Emergency Fault Conditions, 1985, pp. 406–410.

[5.43] N. M. Nor, A. Haddad, H. Griffiths, and A. T. Set-up, "Characterization of Ionization Phenomena in Soils Under Fast Impulses," vol. 21, no. 1, pp. 353–361, 2006.

[5.44] N. Mohamad Nor, A. Haddad, and H. Griffiths, "Performance of Earthing Systems of Low Resistivity Soils," IEEE Transactions on Power Deliver, vol. 21, no. 4, pp. 2039–2047, 2006.

[5.45] N. M. Nor, A. Haddad, and H. Griffiths, "Determination of threshold electric field EC of soil under high impulse currents," IEEE Trans. Power Deliv., vol. 20, no. 3, pp. 2108–2113, 2005.

[5.46] D. Guo, D. Clark, D. Lathi, N. Harid, H. Griffiths, A. Ainsley, and A. Haddad, "Controlled large-scale tests of practical grounding electrodes-Part I: Test facility and measurement of site parameters," IEEE Trans. Power Deliv., vol. 29, no. 3, pp. 1231–1239, 2014.

[5.47] N. Harid, A. Zanini, A. Haddad, and H. Griffiths, "Characterisation of tower base earthing system under impulse conditions," in 27th Int. Conf. Light. Protect., 2004, p. 5a2 1-6.

[5.48] Y. Chen and P. Chowdhuri, "Correlation between laboratory and fielf tests on the impulse impedance of rod-type ground electrodes," IEE Proc. Gen. Transm. Distrib., vol. 150, no. 4, pp. 420–426, 2003.

[5.49] M. Bouchard, F. Dawalibi, and D. Mukhedkar, "Survey on ground resistance and earth resistivity measurements," IEEE Trans. Power App. Syst., vol. PAS-96, no. 4, pp. 1067–1067, 1977.

[5.50] H. G. Sarmiento, J. Fortin, and D. Mukhedkar, "Substation Ground Impedance : Comparative Field Measurements with High and Low Current Injection Methods," IEEE Trans. Power App. Syst., vol. 103, no. 7, July, pp. 1677–1683, 1984.

[5.51] P. Lipavsky, "Measurements of ground potential difference at power substations," IEEE Trans. Power Deliv., vol. 6, no. 1, pp. 62–69, 1991.

[5.52] W. C. Boaventura, I. J. S. Lopes, P. S. A. Rocha, R. M. Coutinho, F. Castro, and F. C. Dart, "Testing and evaluating grounding systems of high voltage energized substations: alternative approaches," IEEE Trans. Power Deliv., vol. 14, no. 3, pp. 923–927, 1999.

[5.53] T. Ragheb and L. A. Geddes, "Electrical properties of metallic electrodes," Med. Biol. Eng. Comput., vol. 28, no. 2, pp. 182–186, 1990.

Chapter Six

[6.1] N. Harid, H. Griffiths, S. Mousa, D. Clark, S. Robson, and A. Haddad, "On the analysis of impulse test results on grounding systems," IEEE Trans. Ind. Appl., vol. 51, no. 6, pp. 5324–5334, 2015.

[6.2] P. Yutthagowith, "Transient Characteristics of Grounding Systems," Proc. Int. Electr. Eng. Congr., 2014.

[6.3] G. Karnas, G. Maslowski, R. Ziemba, and S. Wyderka, "Influence of different multilayer soil models on grounding system resistance," 31st Int. Conf. Light. Prot. ICLP 2012, 2012.

[6.4] J. He, R. Zeng, Y. Gao, Y. Tu, W. Sun, J. Zou, and Z. Guan, "Seasonal Influences On Safety Of Substation Grounding System," IEEE Trans. Power Deliv., vol. 18, no. 3, pp. 788–795, 2003.

[6.5] B. R. L. Smith-rose, D. Ph, and A. Member, "Electrical Measurements on Soil with Alternating Currents." IET, vol. 75, no. 452, pp. 221–237, 1934.

[6.6] J. H. Scott, R. D. Carroll, and D. R. Cunningham, "Dielectric constant and electrical conductivity measurements of moist rock: A new laboratory method," U.S. Geol. Surv. Denver, vol. 72, no. 20, pp. 5101–5115, 1967.

[6.7] K. S. L. C. L. Smith, "A Universal Impedance For Soils," Def. Nucl. AGENCY, 1975.

[6.8] C. L. Longmire and H. J. Longley ",Time domain treatment of media with frequency dependent parameters," Theor. Notes 113, March 1971.

[6.9] M. A. Messier, "The propagation of an electromagnetic impulse through soil: Influence of frequency dependent parameters," Mission Res. Corp., St. Barbar. CA, USA, Tech. Rep.MRC-N-415, 1980.

[6.10] F. S.Visacro and C. M. Portela, "Soil permittivity and conductivity behavior on frequency range of transient phenomena in electric power systems," Present. Symp. HighVoltageEng.,Braunschweig,Germany, 1987.

[6.11] C. M. Portela, "Measurement and modeling of soil electromagnetic behavior," Proc. IEEE Int. Symp. Electromagn Compat., vol. vol. 2, pp. 1004–1009, 1999.

[6.12] R. Alipio and S. Visacro, "Frequency dependence of soil parameters: Effect on the lightning response of grounding electrodes," IEEE Trans. Electromagn. Compat., vol. 55, no. 1, pp. 132–139, 2013.

[6.13] D. Lathi, "Impulse Measurements in Earthing Systems," PhD Thesis, Cardiff University of Cardiff, November 2012.

[6.14] H. Griffiths, P. Jones, N. Harid, and A. Haddad, "Proposal for measurement of earth impedance using variable frequency injection," Meas. Sci. Technol., vol. 21, no. 8, p. 085102 (8pp), 2010.

[6.15] D. Guo, D. Clark, D. Lathi, N. Harid, H. Griffiths, A. Ainsley, and A. Haddad, "Controlled Large-Scale Tests of Practical Grounding Electrodes 2014;Part II: Comparison of Analytical and Numerical Predictions With Experimental Results," IEEE Trans. Power Deliv., vol. 29, no. 3, pp. 1231–1239, 2014.

[6.16] H. Hasan, H. Hamzehbahmani, S. Robson, H. Griffiths, D. Clark, and A. Haddad, "Characterization of horizontal earth electrodes: Variable frequency and impulse responses," Proc. Univ. Power Eng. Conf. (UPEC), 2015 50th Int. Univ. Stoke Trent, UK, vol. 2015-Novem, pp. 1–5, 2015.

[6.17] H. Hasan, H. Hamzehbahmani, H. Griffiths, N. Harid, D. Clark, S. Robson, and A. Haddad, "Characterisation of earth electrodes subjected to impulse and variable frequency currents," in The 19th International Symposium on High Voltage Engineering, Pilsen, Czech Republic, 2015, pp. 23–28.

[6.18] F. H. Silveira, S. F. Visacro, R. Alipio, and A. De Conti, "Lightning-induced voltages over lossy ground: The effect of frequency dependence of electrical parameters of soil," IEEE Trans. Electromagn. Compat., vol. 56, no. 5, pp. 1129–1136, 2014.

[6.19] M. Akbari, K. Sheshyekani, and M. R. Alemi, "The effect of frequency dependence of soil electrical parameters on the lightning performance of

grounding systems," IEEE Trans. Electromagn. Compat., vol. 55, no. 4, pp. 739–746, 2013.

[6.20]   linliang H. and B. Z. Li, ZhenZhen Li, "The influence of Frequency Dependent Soil Parameters on Transmission Line," Int. Conf. Light. Prot. (ICLPj, Shanghai, China, pp. 1010–1013, 2014.

Chapter Seven

[7.1] IEEE Std 80-2000, IEEE Guide for Safety in AC Substation Grounding, IEEE, New York, USA.,

[7.2] Colin Bayliss ", Transmission and Distribution Electrical Engineering," Reed educational and professional publishing Ltd, Oxford, 1999, ISBN 0 706 40596.

[7.3] AIEE Committee Report ", Voltage gradients through the ground under fault conditions," American Institute of Electrical Engineers (AIEE), vol. 77, pp.669-1043, 1958.

[7.4] Charles F. Dalziel, Eric Ogden and Curtis E. Abbott, „„„Effect of frequency on let-go- Currents,"" AIEE Transactions on Electrical Engineering, vol. 62, pp. 745-750, December 1943.

[7.5] D. N. Abledu, K. O., and Laird, "Measurement of Substation Rock Resistivity" IEEE Trans. Power Deliv., vol. 7, no. 1, pp. 295–300.

[7.6] M. G. Unde and K. B. E., "Measurement of Resistivity of Surface Layer Material in Laboratory," in Power India International Conference (PIICON).

[7.7] "EPRI TR-100863, Seasonal variations of grounding parameters by field tests, SEI/Georgia Power Research Center, July 1992."

[7.8] P. Thompson, "Resistivity tests on electric station ground coverings," Internal Report, Los Angeles Department of Water and Power."

[7.9] P. Thompson, "'Resistivity tests on soil and concrete,' Internal Report, Los Angeles Department of Water and Power,."

[7.10] T. D. Hammond, E., and Robson, "'Comparison of electrical properties of various cements and concretes,'" Eng., vol. 199, no. 5165, pp. 78–80.

[7.11] D. Guo, D. Clark, D. Lathi, N. Harid, H. Griffiths, A. Ainsley, and A. Haddad, "Controlled Large-Scale Tests of Practical Grounding Electrodes 2014;Part II: Comparison of Analytical and Numerical Predictions With Experimental Results," IEEE Trans. Power Deliv., vol. 29, no. 3, pp. 1231–1239, 2014.

[7.12] H. Hasan, H. Hamzehbahmani, H. Griffiths, N. Harid, D. Clark, S. Robson, and A. Haddad, "Characterisation of Earth Electrodes Subjected To Impulse and variablr frequency currents," in The 19th International Symposium on High Voltage Engineering, 2015, pp. 23–28.